

Doctoral Dissertation

Power System Small-Signal
Dynamic Monitoring and Stability Control
Based on Wide-area Phasor Measurements

広域位相計測に基づく電力システムの動特性監視
と安定化制御

By

李長松

(Student ID: 07586407)

Supervisor: Prof. Yasunori Mitani, PhD.

Department of Electrical and Electronic Engineering
Graduate School of Engineering
Kyushu Institute of Technology

September 2010

Acknowledgements

First and foremost, I would like to express my deepest gratitude to my supervisor, Prof. Dr. Yasunori Mitani, for his constant guidance, valuable advice, and patient support during my entire course of studies at Kyushu Institute of Technology. His profound academic knowledge and illuminating comments about my research were very valuable and helpful, not only to my doctoral study, but also to my future research and work.

I also would like to express my sincere gratitude to my dissertation committee members: Prof. Dr. Hiroyuki Ukai from Nagoya Institute of Technology, Prof. Dr. Masayuki Hikita, Prof. Dr. Mochimitsu Komori and Assoc. Prof. Dr. Masayuki Watanabe for their precious time and valuable suggestions, comments.

In addition, I would like to thank all lab members, staff members, other students of Kyushu Institute of Technology and all my friends for their continuous encouragement and support that always enabled me to persevere with my study during last four years in Japan.

Finally, I would like to express my love and gratitude to my parents and younger sister for their endless support and encouragement, and my wife and my girl for their love and patience.

李長松

September 2010

Contents

Acknowledgements

Abstract

List of Figures

List of Tables

1.	Introduction	1
1.1	Research Motivation	1
1.2	Objective of Research	3
1.3	Outline of the Thesis	4
2.	Phasor Measurement Technology	5
2.1	Phasor Measurement	5
2.2	Features of Phasor Measurement Technology	7
2.3	WAMS in the World	9
2.4	The CampusWAMS	15
3.	Measurement-based Analysis Theory	19
3.1	Power System Small-Signal Stability	19
3.1.1	Nature of Small-Signal Stability	20
3.2	Traditional Model-based Analysis	22
3.3	Measurement-based Analysis	24
3.3.1	Underlying Theory	24
3.3.2	Fundamental Assumptions	26
3.3.3	Analysis Objective	26
3.4	Review of Analysis Techniques	27
3.4.1	Random Signal	27
3.4.2	Digital Signal Processing	28

3.4.3	System Identification	32
3.4.4	Optimization	34
4.	Single-mode-oriented Estimation of Power Oscillation Based on Phasor Measurements and Auto-spectrum-based FFT Filter	37
4.1	Introduction	37
4.1.1	Review of Multi-mode-oriented Methods	38
4.1.2	Shortcoming of Multi-mode-oriented Methods	41
4.2	Single-mode-oriented Estimation Method	44
4.2.1	Center Frequency Estimation Using Auto-spectrum Analysis	45
4.2.2	Oscillation Data Extraction Using FFT Filter	48
4.2.3	Simplified Model Identification for Single Oscillation Mode	50
4.3	Simulation Study	52
4.4	Evaluation Using CampusWAMS Measurements	53
4.5	Summary	55
5.	Participation Weight Estimation in Power Oscillation Based on Phasor Measurements and Auto-spectrum Analysis	57
5.1	Introduction	57
5.2	Participation Factor from Traditional Modal Analysis	58
5.3	Input-Output Relationship for Constant-parameter Linear System	60
5.3.1	System Frequency Response Function	61
5.3.2	Input-Output Relationship	61
5.4	Participation Weight from Phasor Measurements	62
5.4.1	Derivation of Participation Weight	63
5.4.2	Estimation of Participation Weight	63
5.4.3	Comparison with Participation Factor	64
5.5	Simulation Study	65
5.5.1	Western Japan 10-Machine System Study	65
5.5.2	Western Japan 30-Machine System Study	69
5.6	Application to CampusWAMS Measurements	71
5.7	Discussion and Summary	73

6.	Modeling of Two-Area HVDC-Connected-System for Load Frequency Control Based on Application of the CampusWAMS	75
6.1	Introduction	75
6.2	Overview of Kita-Hon HVDC Link	76
6.3	Analysis of Kita-Hon HVDC Link for Load Frequency Control	77
6.4	Modeling of Kita-Hon HVDC Link for Load Frequency Control	79
6.4.1	Simulation Model Construction	79
6.4.2	Unknown Model Parameter Estimation	80
6.4.3	Load Input Identification from CampusWAMS Measurements	81
6.4.4	Model Estimation and Evaluation Results	82
6.5	Summary	85
7.	Controller Design for Power Oscillation Damping Improvement Based on Phasor Measurements	87
7.1	Introduction	87
7.2	Controller Structure and Damping Specification	88
7.3	Design of HVDC Supplementary Damping Controller	89
7.3.1	Extended Oscillation Model	90
7.3.2	Controller Parameter Searching	91
7.3.3	Simulation Study	92
7.4	Online Parameter Self-Tuning Control Strategy	94
7.4.1	Online Oscillation Model Estimation	95
7.4.2	Self-Tuning Control Strategy	96
7.4.3	Simulation Study	97
7.5	Summary	100
8.	Conclusions	101
8.1	Contributions	101
8.2	Considerations for Future Work	102
	References	105

Abstract

At present, modern power systems around the world are more interconnected in nation-wide and even continent-wide scope. These interconnected wide-area systems are faced with a series of challenging issues concerning the stability and control of overall system, which result from the lack of transmission lines expansion, unprecedented increase in electricity demand and tie-line power flow, deregulation of electricity markets, and rapid growth in distributed generations. Under this circumstance, any failure in the planning, operation, protection and control of any part of the entire power system could evolve into the cause of cascading events that may eventually lead to a large area power blackout. Among many expected features of a future "Smart Grid", one is essential: self-healing from various power system disturbances, which requires not only more rapid and coordinated recovery after disturbances but also prevention of large area outages by all means. Therefore, these challenging issues set new demand on the development of more rapid, effective, accurate methods for power system dynamic monitoring and stability control.

Traditionally, all aspects of the analysis of power system dynamic and stability are built on the dependence of the mathematic model of power system components and network. In brief, the traditional approach is model-based - for the purpose of performing any analysis, a mathematic model which is appropriate to the concerned analysis has to be constructed in advance. The model-based approach has following significant deficiencies. Firstly, the information about all components' parameter and network configuration has to be known before the model construction. Secondly, the constructed model always shows limitation and incapability of describing the true characteristic of practical power system. Lastly, many operation or control decisions based on the system model are only applicable to the operation condition when these decisions are made.

The advent and deployment of phasor measurement units (PMUs) enables the measurement-based approach to monitoring and control power system dynamic. For the measurement-based approach, a beforehand prepared mathematic model based on the knowledge of overall system information is not necessary and only the measurements of output (and sometimes, input) of power system are available. In principle, the measurement-based approach constructs an online snapshot-model of power system dynamic using these real system measurements, which can achieve quick, timely and accurate representation of real system dynamic. Compared to the conventional measurement from SCADA (supervisory control and data acquisition) system, phasor

measurement provides the crucial information of phase angle which has close relation with power system dynamic and stability. More importantly, the time synchronization information is embedded in phasor measurement so that phasor data from multiple distant locations in a wide-area power system can be correctly and accurately processed.

Accordingly, under the concept of measurement-based approach, this work studies the applications of wide-area phasor measurements to power system small-signal dynamic monitoring and stability control by utilizing various techniques such as digital signal processing, system identification and optimization. Basically, there are indirect and direct ways to take advantage of phasor data for measurement-based power system dynamic monitoring and stability control. For indirect situation, phasor measurements are used to estimate a traditional dynamic model of power system when the base-line information of the concerned system is no available or to validate an existing system dynamic model when the base-line data is available. In this work, a method of modeling a HVDC-only-interconnected two-area power system for describing the effect of its load frequency control is proposed based on wide-area phasor measurements (Chapter 6). In particular, without knowledge of the detailed base-line data of the studied system, the system model parameters that relates to two-area load frequency control are optimally estimated using phasor measurements during the period of an identifiable system disturbance event.

For most situations, phasor measurements can be directly adopted to realize the power system dynamic monitoring or stability controller design. In this work, the single-mode-oriented oscillation data extraction and eigenvalue estimation method and the method of estimating the participation level of generators in one concerned interarea oscillation mode are proposed based on wide-area phasor measurements and auto-spectrum analysis (Chapter 4 and Chapter 5). The auto-spectrum analysis of phasor measurements is adopted to identify the existence of oscillation modes and further to estimate the dominant frequency of each oscillation mode as well as the relative participation level of generators in one oscillation mode. Based on this information, the oscillation data corresponding to the concerned single mode can be accurately extracted from the original phasor measurements to construct an oscillation model which represents the characteristic of the concerned mode.

Furthermore, the controller design scheme in order for improving the damping of one concerned interarea oscillation mode is proposed based on wide-area phasor measurements (Chapter 7). As one of potential damping improvement channels, a HVDC supplementary damping controller is designed using the proposed scheme. Online controller parameter self-tuning strategy is also discussed in order to maintain the sufficient damping when power system is operating under normal but frequent changing conditions.

Compared with the traditional model-based methods for power oscillation analysis

or damping controller design, all proposed methods in this thesis are output- and measurement-only-based. Evaluation results using CampusWAMS (campus wide area measurement system) and simulation systems are provided to show the effectiveness of the proposed methods, which are potentially feasible and applicable to online practical WAMS applications.

List of Figures

Figure 2-1.	Phasor representation of a sinusoidal waveform	6
Figure 2-2.	Major hardware block of modern PMU	7
Figure 2-3.	Phase angle difference with different time skew	8
Figure 2-4.	Central European WAMS devices [13]	10
Figure 2-5.	PMUs location for the CampusWAMS in Japan	15
Figure 2-6.	Data file recording scheme	17
Figure 2-7.	PMUs location for the CampusWAMS in Thailand	17
Figure 3-1.	Classification of power system stability	19
Figure 3-2.	Concept of measurement-based analysis	25
Figure 3-3.	A dynamic system with inputs, outputs and disturbances	32
Figure 4-1.	General linear model of power system	39
Figure 4-2.	Two-area-four-generator (2A4G) test system	41
Figure 4-3.	Model for exciter and governor in 2A4G system	42
Figure 4-4.	Angle difference between Bus1 and Bus11	43
Figure 4-5.	Estimated auto-spectrum of ideal signal	45
Figure 4-6.	Estimated auto-spectrum of practical signal in Figure 4-4	46
Figure 4-7.	Estimated periodogram of practical signal in Figure 4-4	48
Figure 4-8.	Concept of Welch method for auto-spectrum estimation	48
Figure 4-9.	Principle of FFT filter	49
Figure 4-10.	Complete oscillation data extraction process	50
Figure 4-11.	Flowchart of proposed estimation scheme	51
Figure 4-12.	Extract oscillation data from bus frequency deviation	52
Figure 4-13.	Extracted oscillation data from bus phase difference	54
Figure 4-14.	Extracted oscillation data from bus frequency deviation	54
Figure 4-15.	Extracted oscillation data from bus phase difference	54
Figure 4-16.	Estimated eigenvalues of one day for Western Japan power system	55
Figure 4-17.	Estimated eigenvalues of one week for Thailand power system	56

Figure 5-1.	A black-box system	61
Figure 5-2.	Western Japan 10-machine (West-10) example system	66
Figure 5-3.	Exciter model for West10 system	66
Figure 5-4.	Bus 21 phase angle under random load excitation	66
Figure 5-5.	Auto-spectrum estimation for West-10 system	67
Figure 5-6.	Participation weight for West-10 system	68
Figure 5-7.	Participation factor for West-10 system	69
Figure 5-8.	Auto-spectrum estimation for West-30 system	70
Figure 5-9.	Participation weights for West-30 system	70
Figure 5-10.	Participation factors for West-30 system	70
Figure 5-11.	Auto-spectrum estimation for the CampusWAMS	72
Figure 5-12.	Participation weight for the CampusWAMS	72
Figure 5-13.	Participation weights in Mode 1 for the CampusWAMS	73
Figure 6-1.	Interconnection inside Eastern Japan 50-Hz power system	76
Figure 6-2.	CampusWAMS for Eastern Japan 50-Hz power system	77
Figure 6-3.	Frequency deviation signals of Honshu and Hokkaido	78
Figure 6-4.	Coefficient of determination	78
Figure 6-5.	Simulation model for load frequency control analysis	79
Figure 6-6.	Unknown parameter estimation method	81
Figure 6-7.	Measured frequency deviation due to earthquake	82
Figure 6-8.	Comparison of simulated results and measured results	83
Figure 6-9.	Simulated results using derived load variations	84
Figure 6-10.	Coefficient of determination for simulated results	84
Figure 7-1.	General structure of supplementary damping controller	88
Figure 7-2.	A simplified AC/DC parallel system	89
Figure 7-3.	Two-area-four-generator system with HVDC link	93
Figure 7-4.	Simulation model for rectifier (left) and inverter (right)	93
Figure 7-5.	Responses to small random load changes	94
Figure 7-6.	Online process of oscillation model estimation	95
Figure 7-7.	Estimated eigenvalues using online sliding window technique	98
Figure 7-8.	Comparison of angle difference with and without self-tuning strategy	99

List of Tables

Table 2-1.	PMUs of the CampusWAMS in Japan	16
Table 4-1.	Initial load flow setting of 2A4G system	42
Table 4-2.	Oscillation modes in 2A4G system	42
Table 4-3.	Estimated eigenvalues using 200-seconds data	43
Table 4-4.	Estimated eigenvalues using 300-seconds data	43
Table 4-5.	Estimated results using proposed method	52
Table 5-1.	Interarea modes of West-10 system	68
Table 5-2.	Interarea modes of West-30 system	69
Table 5-3.	Interarea modes of western Japan 60-Hz power system	71
Table 6-1.	All Model Parameters	80
Table 6-2.	Parameter estimation result	82
Table 7-1.	BSA Searched controller parameters	93
Table 7-2.	Initial load flow setting of 2A4G system	97
Table 7-3.	Initial parameter for PSS	98

Chapter 1.

Introduction

1.1 Research Motivation

It has been recognized that power systems are the largest, most complicated dynamic systems created by the human. What's more important is that since the beginning, power systems never stop the development and growth of their size, scale and complexity. Interconnecting several relatively small power systems in adjacent areas into one huge, wide-area power system used to be one remarkable step in the history of power system evolvement. On one hand, the interconnection of power systems brought benefits in some aspects such as the reinforcement of overall system security, the improvement in the economics of generator units operation, and the enhancement of power supply reliability, etc. On the other hand, however, with the interconnection of these systems by tie-lines of limited capacity, the problems in the stability and control, especially those involving multiple interconnected areas, concurred.

Especially in last two decades, modern power systems around the world, which are more interconnected in nation-wide and even continent-wide scope than before, are faced with a series of challenging issues concerning the stability and control of overall system, which result from the lack of transmission lines expansion, unprecedented increase in electricity demand and tie-line power flow, deregulation of electricity markets, and rapid growth in distributed generations. Under this circumstance, any failure in the planning, operation, protection and control of any part of the entire power system could evolve into the cause of cascading events that may eventually lead to a large area power blackout. Several recently-happened major widespread blackouts, e.g. August 2003 US-Canada blackout [1], September 2003 Italy blackout [2], September 2003 Sweden-Denmark blackout [3], July 2004 Greece blackout [4], are testimonies to these serious issues. Therefore, these challenging issues set new demands on the development of more rapid,

effective, accurate methods for power system dynamic monitoring and stability control [1][5].

Traditionally, all aspects of the analysis of power system dynamic and stability are built on the dependence of the mathematic model of power system components and network [6][7]. In short, the traditional approach is model-based – for the purpose of performing any analysis, a mathematic model which is appropriate to the concerned analysis has to be constructed in advance. The model-based approach has following significant deficiencies. Firstly, the mathematic model of power system is generally represented by differential-algebraic equations (DAEs). These DAE models are based on approximate system representation and data, therefore, the information about all system components' parameter and network configuration has to be known before the model construction. For a system with e.g. several thousand buses, this process is rather cumbersome. Secondly, the constructed model always shows limitation and incapability of describing the true characteristic of practical power system due to model approximation and system uncertainty. Lastly, many operation or control decisions that are made based on the system model are sometimes only applicable to the operation condition when these decisions are made because the real power system is always experiencing frequent changes while the model mathematic used is slow-updated.

The advent and deployment of phasor measurement units (PMUs) opens new vision for truly online and realtime monitoring and control of power system dynamic using the measurement-based approach [8][9]. Compared to conventional measurement from supervisory control and data acquisition (SCADA) system, modern phasor measurement provides the crucial information of bus phase angle which has close relation with power system dynamic and stability. More importantly, the time synchronization information is embedded in phasor measurement so that phasor data from multiple distant locations in a wide-area power system can be correctly and accurately processed. Thanks to this unique feature, a wide-area measurement and monitoring system (WAMS) based on multiple PMUs can be constructed to enhance the ability of the power system operator for monitoring and control of power system dynamic. Owing to these unique advantages of phasor measurement, the measurement-based approach becomes feasible and applicable to power system. For the measurement-based approach, a beforehand prepared mathematic model based on the knowledge of overall system information is not necessary and only the measurements of outputs and/or inputs of power system are assumed to be available. In principle, the measurement-based approach constructs an online and realtime snapshot-model of power system dynamic using these real system measurements, which can achieve quick, timely and accurate representation of real system dynamic.

Furthermore, synchronized phasor measurement technology is anticipated to play an indispensable role in the near future power system with "Smart Grid" concept. Power

system operators have always wanted to monitor grid operations in real time. Therefore, Smart Grid needs to be designed to combine the existing grid with a wide-area measurement and a communications infrastructure and that supports the real-time ability to integrate and coordinate the production, transmission and distribution of electricity from the generator to the consumer in response to dynamic supply and demand conditions. Among many expected features of a Smart Grid, one is essential: self-healing from various power system disturbances, which requires not only more rapid and coordinated recovery after disturbances but also prevention of large area outages by all means. By making full use of the synchronized phasor data in real time, power system operators can use WAMS as an early warning system – one that can provide timely snapshot of deteriorating system conditions so that operators have enough time to take the kind of corrective action needed to first limit the scope and impact of system disturbances and then prevent major blackouts from occurring.

Hence, based on wide-area synchronized phasor measurements, this thesis studies various issues regarding monitoring and control of small-signal dynamic behavior of a power system using the concept of measurement-based approach. These issues include the participation level and eigen-properties estimation of the dominant interarea oscillation mode from online measurements; the controller design scheme in order for improving the damping of one concerned interarea oscillation mode; and the traditional dynamic model identification and parameter estimation based on phasor measurements.

1.2 Objective of Research

The following topics of interest will be studied in this thesis, concentrating mostly on the use of various analysis techniques, such as digital signal processing, system identification and optimization algorithms, for monitoring and control of power system small-signal dynamic and stability problem:

- 1) Propose a concept straightforward, online applicable, single-mode-oriented identification method to estimate the eigen-properties of dominant interarea oscillation mode in a power system without requiring any extra disturbances.
- 2) Propose a simple, online measure for indicating the relative participation level of generators in one oscillation mode based on phasor measurements.
- 3) Practice a hybrid-simulation technique to construct a traditional dynamic model based on the practical phasor measurements.
- 4) Develop a scheme to design damping improvement controller and an online parameter self-tuning strategy based only on phasor measurements when power system is operated under normal but frequently changing conditions.

1.3 Outline of the Thesis

This thesis is structured as follows:

Chapter 2 introduces the concept of phasor measurement and the unique features of phasor measurement technology. Then it describes the recent development of PMU-based WAMS projects in major world economies. The CampusWAMS (campus wide-area measurement system) used throughout this thesis in order to demonstrate the feasibility of the proposed methods is also presented in this chapter.

Chapter 3 first presents the basic theory of power system small-signal problem and a brief review of traditional model-based analysis method. Then the underlying theory and fundamental assumptions of the measurement-based analysis approach are explained. Various techniques to enable the measurement-based approach are also reviewed in this chapter.

Chapter 4 describes the development of the single-mode-oriented eigenvalue estimation method after reviewing the multi-mode-oriented time-series models and their associated shortcomings. In specific, the auto-spectrum analysis of phasor measurements is adopted to automatically and correctly estimate the center frequency of the concerned dominant oscillation mode and FFT filter is used to extract the oscillation data from the corresponding mode. The evaluation results based on phasor measurements from the CampusWAMS are presented.

Chapter 5 describes the derivation of a proposed participation level measure used to indicate the relative participation of generators in one oscillation mode. The results for simulation system as well as the CampusWAMS are presented.

Chapter 6 presents the modeling technique for a two-area HVDC-connected-system based on the practical phasor measurements from the CampusWAMS. In particular, without knowledge of detailed base-line data of Kita-Hon HVDC Link, the unknown model parameters that relate to two-area load frequency control are estimated using phasor measurements during the period of an identifiable system disturbance event.

Chapter 7 first presents a design scheme for the damping controller based on phasor measurements. As one of potential damping provider, the proposed scheme is demonstratively applied to design a HVDC supplementary damping controller. Then it discusses several strategies for online controller parameter self-tuning in order to maintain sufficient damping when power system is assumed to operate under normal but frequently changing conditions. .

Finally, Chapter 8 summarizes the main contributions of this thesis, and provides some considerations for possible future research work.

Chapter 2.

Phasor Measurement Technology

2.1 Phasor Measurement

A phasor is a mathematical representation of a sinusoidal waveform (Figure 2-1). The magnitude is either a peak or RMS value of the sinusoid. The phase angle is determined by the given sinusoidal frequency and a time reference. This reference is arbitrary and is generally chosen to be convenient for the particular situation; however, the reference frequency and time scale can be fixed for a class of measurements. Time-synchronized phasors – already given an exclusive term as "synchrophasor" – are phasor values that represent power system sinusoidal waveforms referenced to the nominal power system frequency and coordinated universal (UTC) time, the international time standard. The phase angle of a synchrophasor is uniquely determined by the waveform, the system frequency, and the time of measurement. Thus, with a universal precise time reference, power system phase angles can be accurately measured throughout a power system. The advent of global positioning system (GPS) technology has made this economically and practically feasible. This simple but powerful extension of the basic phasor concept has opened a whole era of power system grid management.

For a pure sinusoid, the instantaneous phasor value can be directly stated from the formula for that waveform. In practice, however, a waveform is often corrupted with other signals of different frequencies. It then becomes necessary to extract a single frequency component of the signal (usually the principal frequency of interest in an analysis) and then represent it as a phasor. A series of sample points of the waveform taken at appropriate intervals and over a sufficient time span are required to determine a phasor. This indicates a phasor – more accurately, a phasor of the fundamental frequency positive sequence component of a practical waveform – has to be estimated from sampled measurements [10]. The most commonly used algorithm for phasor estimation is the

discrete Fourier transform (DFT). This technique uses the standard Fourier estimate applied over one or more cycle's sample at the nominal system frequency. With a sufficient sample rate and accurate synchronization with UTC, it produces an accurate and very usable phasor value for most system conditions.

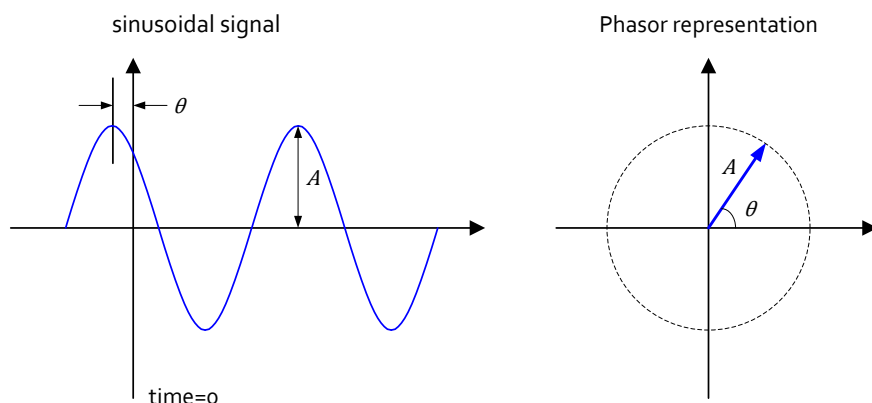


Figure 2-1. Phasor representation of a sinusoidal waveform

A phasor measurement unit (PMU) is such an electronic device that can sample the practical ac waveforms (voltages and currents), estimate their phasors (voltage phasors and current phasors, respectively) synchronously and output phasor data with time synchronization [8][9]. Figure 2-2 illustrates major hardware block of a modern PMU. The analog current and voltage inputs are converted to voltages signals with appropriate instrument transformers in order to match with the requirements of the analog-to-digital (A/D) converters. The sampling clock is phase-locked with the GPS clock pulse. Sampling rates have been going up to as high as 96 or 128 samples per cycle in latest modern types, accompanied by the application of faster A/D converters and advanced digital signal processors (DSP). DSP implements the most important task of estimating a phasor as well as other necessary algorithms. Basically, PMU hardware is same as that of a digital fault recorder or digital relay, except for GSP-time-tag processing indicated by dotted line in Figure 2-2. In PMU, the time-tag is created from the signals derived from GPS receiver and embedded into each estimated phasor, which gives each phasor a unique time identity. As a result, the principal output of the PMU is the time-stamped measurement to be transferred over the communication links through suitable modems to a higher level measurement system.

The structure specification of output phasor measurements and the industry standard for modern PMU can be found in [11].

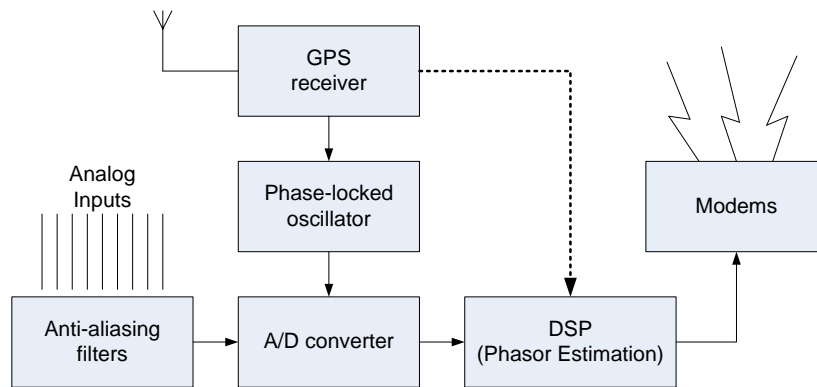


Figure 2-2. Major hardware block of modern PMU

2.2 Features of Phasor Measurement Technology

The phasor measurement technology features in following three aspects:

- Phasor data

Before phasor measurement technology, all necessary power measurements in order for operation and control of power system come from supervisory control and data acquisition (SCADA) system. Various power system applications are running based on SCADA data, such as system monitoring, state estimation, fault location, disturbance analysis, etc. For SCADA data, only the magnitude of voltage and current as well as real power and reactive power are measured. The angle of voltage at all buses or current on all lines have to estimated based on available SCADA data using state estimation algorithms which could contain unpredictable errors. It is well known to power system engineers that the voltage phase angle – more accurately, phase angle difference between any two buses – plays a crucial role in the analysis, monitoring and control of power system stability. Therefore, the availability of bus voltage angle information due to phasor measurement technology can thoroughly open a new vision to operators for real-time observation and operation of a large power system.

- Time-synchronization

Another essential distinction between phasor data and SCADA data is time-synchronization. With no insertion of precise time-stamp, traditional SCADA data could be useless for some power applications such as post-disturbance analysis. Furthermore, it is meaningless to compare or process data from multiple locations without universal and precise time-stamp. The time skew between two signals could lead to undesirable consequence.

The importance of time-synchronization can be easily found from Figure 2-3. It shows the phase angle difference, which is computed using phasor data of two locations inside a practical power system. Figure 2-3(a) is result when time-tag is well synchronized, while (b), (c), (d) are results when time skew is assumed to be 10 cycles, 30 cycles and 60 cycles, respectively. It can be easily observed that the time skews in the measurement can induce errors in the phase angle difference computations. In Figure 2-3(a), the true value of phase angle difference between two sets of measurements was approximately -0.76 degrees. However, when one of these two phase angle signals was skewed by different time, and then the phase angle difference was computed, then the resulting answer incorrectly indicated a phase angle difference of as much as approximately $+15$ degrees between those two data sets.

Therefore, the time-synchronization among multiple phasors is indispensable in order to obtain correct phase angle difference. Through the use of GPS receiver, PMUs sample synchronously at selected locations throughout the overall power system. This provides a system-wide snapshot of the electrical system. The GPS not only provides time tagging for all the measurements but also ensures that all phase angle measurements are synchronized to the same time as well. Without time-synchronization, phasor data could be worthless.

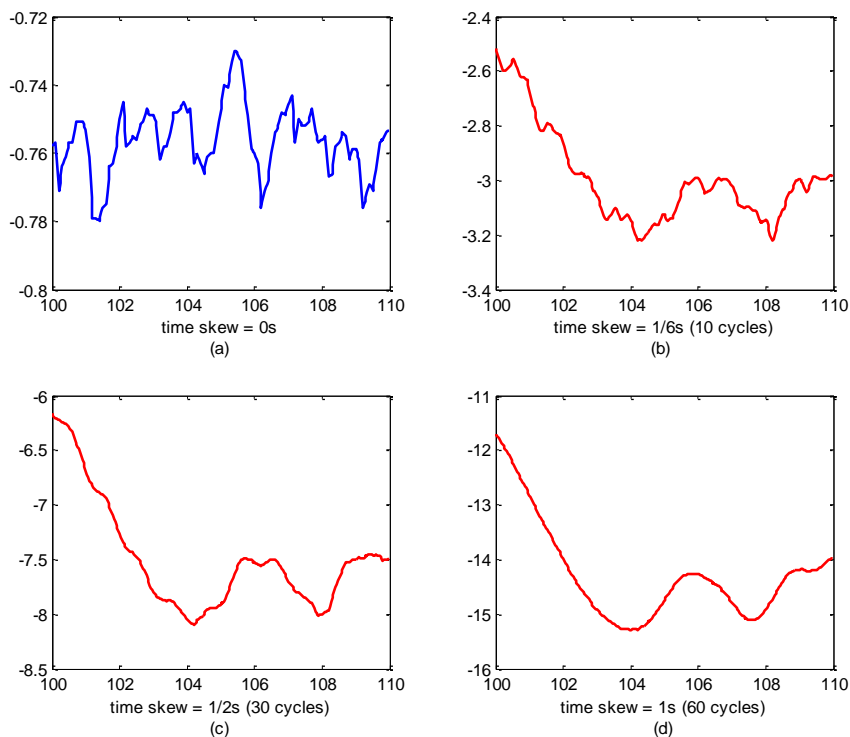


Figure 2-3. Phase angle difference with different time skew

- Networking

Most stability events involve oscillations and control interactions between neighboring utilities and geographic operating regions. This dictates the need for multiple recording devices at key locations throughout the interconnection. Since PMU provides measurement with precise time-synchronization, phasor data measured by PMUs from multiple locations can be collected, integrated and processed together even these locations are very distant geographically with each other. Consequently, by deploying multiple PMUs at key substations in a large interconnected power system and collecting phasor data from all locations to a data center or control center, a wide-area measurement system (WAMS) can be constructed. Furthermore, depending on what applications are running based on collected phasor data, a higher level wide-area measurement and control system (WAMCS) or wide-area protection and control system (WAPCS) can be implemented. Base on networking phasor data, existing power applications can be significantly enhanced and new applications can be developed. In short, the power of phasor measurement technology relies on a network of multiple PMUs rather than a single PMU.

2.3 WAMS in the World

Phasor measurements were introduced as a specialized power system measurement in 1986. Following a paper published in 1983 describing the technique [10], Virginia Tech produced prototype phasor measurement units (PMUs) that were supplied to American Electric Power (AEP) and the Bonneville Power Administration (BPA). These units were tested and used by these utilities for several years before the first commercial unit, the Macrodyne 1690, was introduced in 1991. Using the original PMUs, AEP and BPA built phasor measurement systems that only provided recorded data for analysis with basic plotting tools. BPA redesigned the measurement system in 1997 into a true real-time, wide area measurement system using commercial PMUs and a custom phasor data concentrator (PDC). Since then, many phasor data systems have been developed and deployed throughout the world.

In recent years, the interest in phasor measurement technology has reached a peak. In most countries installing the PMUs and getting to know the PMU system behavior through continuous observations of system events has been the first step. All installations are reaching for a hierarchical WAMS so that the measurements obtained from various substations on the system can be collected at central locations from which various monitoring, protection, and control applications can be developed. In this section, the current state and recent activities in WAMS development in major world economies are summarized based on the reports in [12][13][14].

1) North America

In the Western part of the United States, starting in 2002, the research and prototype testing efforts were combined with a real-time dynamic monitoring system (RTDMS) workstation for offline analysis by the California Independent System Operator (CAISO). In parallel, the deployment of real-time PMU data analysis, voltage, and dynamic stability assessment and data visualization applications were further enhanced by deploying the latest technology at BPA and several relevant utilities. For Eastern part of the United States, the establishment of the Eastern Interconnection Phasor Project (EIPP) was also started in 2003 and gained momentum as a result of the Northeast North America blackout of August 2003. Since early 2007, two projects have been combined to become the North American Synchrophasor Initiative (NASPI) that also covers Canada and Mexico. As of 2009, in excess of 200 PMUs are in service across the North America, and approximately 20 systems are being installed and implemented for various power applications.

In addition, the frequency monitoring network (FNET) which obtains GPS-synchronized wide-area measurements in a low-cost, easily deployable manner has been implemented in Virginia Tech. Over 40 Frequency Disturbance Recorders units have been deployed covering the three major interconnections of North America power grid to detect and analyze power system disturbances in near-real time.

2) UCTE (Central European)

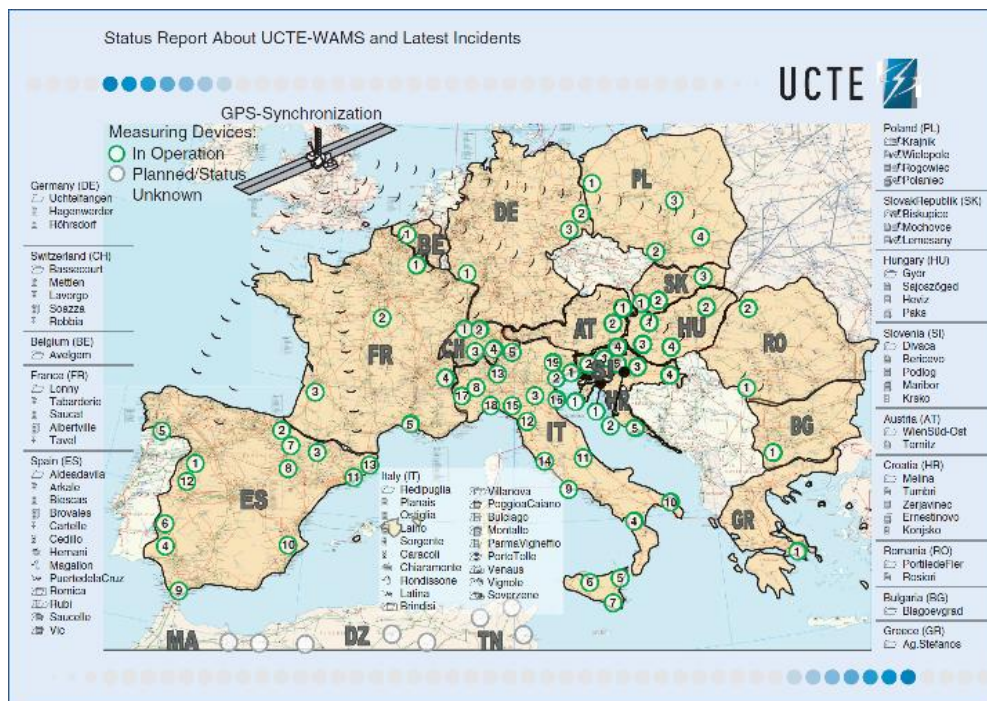


Figure 2-4. Central European WAMS devices [13]

Within the highly meshed power system of central Europe a multitude of WAMS are currently in operation (Figure 2-4). Inside the UCTE, wide-area phasor measurements are exchanged between the transmission system operators (TSOs) in order to calibrate the system dynamic models or for postmortem analysis. One major focus currently is the monitoring of the occasional appearance of poorly damped interarea oscillations. In the center of the system and the southeast part, activities of exchanging online measurements between several data concentrators have already started and are in the phase of further extensions. The additional basic functions of these online devices include voltage phase angle difference monitoring, line thermal monitoring between two substations, voltage stability monitoring, and online monitoring of system damping.

3) Nordic (Northern European)

The PMU activities in Norway started around the year 2000. The TSO Statnett has built several projects. The PMU data are integrated with the Statnett SCADA system and recently a visualization tool based on LabVIEW was developed to combine PMU data and digital fault recorder data. In the very near future a project on phasor-based damping control of SVC and HVDC devices will be launched.

In Finland, the TSO Fingrid has installed a considerable number of PMUs. They are currently used for disturbance monitoring. A near-term goal is to present damping information in real-time, which may be extended to feedback control of an HVDC link or SVC to improve damping of interarea oscillation.

Since 2005, streaming PMUs have been installed by the TSO Energinet.dk in Denmark. In order to monitor the ac interconnection with Germany, one of these is actually located in Germany. The main application so far is disturbance analysis, but future applications include monitoring of power plant operation, thermal line monitoring, and stability indicators.

In Sweden the TSO Svenska Kraftnat installs PMUs in their main stations as these are upgraded, which is done with a pace of about two stations a year. The plan is to integrate phasor data with the SCADA system to realize disturbance. Future use includes real-time monitoring of oscillations in the control center and improved state estimation.

Since Iceland is isolated from the other countries in the Nordel system, the transmission system is relatively weak and electromechanical oscillations are an important issue to the TSO Landsnet. The system is therefore monitored using seven PMUs sending data to the national control center, where damping of oscillatory modes is presented in real time. The monitoring system has also been used for tuning of power system stabilizers with good results.

4) Russia

Synchronous interconnection of the 14 national power systems of Eastern Europe,

Central Asia, and Siberia from the western borders of the Ukraine to Baikal and from Tajikistan to Kola Peninsula has been achieved. Interconnection consists of the unified power system (UPS) of Russia and Kazakhstan; the interconnected power system (IPS) of other 12 nations. It is the most geographically extended power system in the world, spanning eight time zones. Dynamic behavior investigation of such an extended power system needs information on electromechanical transient parameters with high resolution and synchronized by GPS time tags. Such information is provided by IPS/UPS WAMSs. Development of this system started in 2005. Currently 26 PMU s are located in the major power plants and substations from the east to the west and from the south to the north of this immense interconnected power grid.

Phasor measurements in the IPS/UPS are currently used primarily for system performance monitoring and analysis. One of the important phasor measurements applications is the reference dynamic model validation. Another application considered is low-frequency oscillation monitoring, including assessment of amplitudes and decrements of oscillations with a frequency range of 0.02-0.2 Hz.

5) China

China owns one of the largest power networks in the world. Currently, the national power system is organized into two huge power grids, i.e. China State Grid and China Southern Grid, as well as several separated provincial power grids (e.g., Xinjiang, Tibet). Two grids are interconnected by HVDC links. Inside each grid, there are also HVDC links connecting sub-grids. To securely and efficiently operate such a complex system is a real challenging problem. To meet the new challenges and at the same time to utilize the most up-to-date information and communication technologies in the power industry, numerous efforts have been made to develop PMU/WAMS applications in China since the middle 1990s.

The installation of PMUs in the China power grid began in 1995. By the end of 2002, Chinese manufacturers began to provide their own commercial PMUs, which have been commissioned in the China power grid since 2003. By the end of March 2007, about 400 PMUs had been commissioned. These are installed at the substations and power plants of 500-kV and 330-kV voltage levels. Furthermore, it is reported in [14] that by the June of 2009, over 1000 PMUs have been commissioned in China power grid and all the 500-kV and above substations and 100-MW and above power plants have PMUs. With more than one manufacturer of PMUs, a Chinese standard on PMUs and WAMS was drafted by the State Grid Company and manufacturers in 2003 and issued in 2005. The standard defines the transmission protocol of historical data, provides technical specification for manufacturers and allows interchange of data between a wide variety of users of both real-time and offline phasor measurements.

The functions of China WAMS include visualization of dynamic processes and

available transmission capacity, wide-area data recording and playback, and online low-frequency oscillation analysis, etc. Due to the long transmission distances and weak interconnections, interarea low-frequency oscillations are a severe problem in China. As the only tool capable of capturing the oscillation data, the WAMS plays an important role in low-frequency oscillation identification and control in China. The closed-loop low-frequency identification and damping control system has passed the field test. Other PMU applications, such as state estimator, security assessment, adaptive protection, and emergency control are also currently undergoing development.

6) India

In India, large generation addition is taking place, and continuous expansion of the grid through increasing grid connectivity is leading to the geographical spread of the grid. Power flow is taking place in multiple directions coupled daily/seasonal basis. Under this situation, it becomes important to know the dynamic state of the grid and this issue calls for development of an intelligent grid on the basis of WAMS. Toward achieving this objective, the POWERGRID, the central transmission utility, initiated the work for development of an intelligent grid comprising WAMS, remedial action scheme (RAS) and system integrated protection scheme (SIPS), etc., for dynamic state estimation and control purposes. For this, the following staged approach is adopted: In the first stage, a few PMU s (four to five in each region) are to be installed at critical buses in all the regional grids. Output of these PMUs can be used to validate the offline simulation models, especially exciter and governor characteristics of large generators. Based on the output of these PMUs, a common state estimator is to be developed by combining regional state estimators. Based on the success of stage 1, more PMU s are to be installed at various buses. All the PMU data are to be stored in different PDCs. Further, data from a number of PDCs will be collected at a central location. After installing PMUs, many phenomena hitherto unknown, such as poorly damped oscillations, can be detected. In the final step, RAS and SIPS for regulation and control purpose are to be developed.

7) Australia

The major power system in Australia encompasses the states of Queensland, New South Wales, Victoria, South Australia and Tasmania, with voltage levels ranging from 500kV down to 110kV. This interconnected system represents a power system that stretches for 5000 km with a maximum demand of about 30 GW. The long, thin nature of this system, which hugs the coast of eastern and southern Australia, has long presented unique problems in terms of oscillatory stability, both in design and operation. . With new phasor measurement technology, it is possible to monitor system damping and ensure that the system is operated within its technical envelope. The TSO, NEMMCO, employs both short term and long term model-estimators to achieve this. NEMMCO, together with PowerLink, the transmission network service provider in Queensland, have

installed a Psymetrix Power Dynamics Management (PDM) system with a number of measurement nodes in various locations around the power system. The Psymetrix PDM employs advanced signal processing techniques to continually assess system damping by monitoring the oscillations in steady state power transfers.

8) Brazil

The Brazilian National Interconnect Power System (SIN) is characterized with a dominant hydroelectric power generation and long-distance power transfers from generation parks to load centers. Studies for phasor measurement applications in Brazil were started in the early 1990s. Since late 2000, the Brazilian independent system operator ONS has launched two WAMS-related projects which aim to implement a large-scale synchronized phasor measurement system (SPMS) for both offline and real-time applications. One project is "Deployment of a Phasor Recording System". The main goal of this project is to specify and deploy a SPMS to record SIN system dynamics during long duration wide-area disturbances, envisioning the most probable future real-time applications. Another project is "Application of Phasor Measurement Data for Real-Time System Operation Decision Making". The main goal of this project is to extend the initial SPMS for control center real-time applications, such as phasor visualization, modal frequency alarming, and state estimator improvement for supporting system dispatcher real-time decisions.

During 2007, ONS investigated the effective use of phasor measurement technology to improve real-time system operation. The following four were chosen for a proof-of-concept pilot implementation: a tool to monitor system oscillations in SIN and alarm dispatchers for oscillations with poor damping; a tool to monitor the stresses of the electric power transmission system based on the angle differences; a tool to assist the dispatchers to resynchronize islands using angle differences information; A tool to assist the dispatchers to close loops in parts of the SIN using angle differences information.

Based on above introductions, it can be seen that a wide variety of application of wide-area phasor measurements from WAMS in monitoring and control of power system can be expected. These applications include:

- Dynamic angle and frequency monitoring and analysis;
- Phasor-based state estimation;
- Interarea oscillation detection and monitoring;
- System performance and post-disturbance analysis;
- Model estimation and validation;
- Phasor-based controller design;
- etc.

2.4 The CampusWAMS

In this thesis, the CampusWAMS, which is the written abbreviation of “Campus Wide-Area Measurement System”, is used to specially represent the phasor measurement system that was initially proposed and started to construct since 2002 by one research group under the leadership of Prof. Mitani of Kyushu Institute of Technology [15]. Since the multiple phasor measurements from the CampusWAMS will be used many times in the following chapters of the thesis, some necessary information of the CampusWAMS, such as its cover range and technical specification, is given in this subsection.

Until now, the CampusWAMS has been developed to cover the typical power supply areas of the entire Japan nation-wide power grid. In specific, the CampusWAMS presently encompasses 12 PMUs: 9 of them are installed in the supply area of Western Japan 60-Hz system and another 3 in the supply area of Eastern Japan 50-Hz system. The locations of these 12 PMUs are marked with red-filled circle associated with respective city name in Figure 2-5. All PMU are the same model – NCT2000 Type-A – manufactured by Toshiba [16].



Figure 2-5. PMUs location for the CampusWAMS in Japan

In Japan, there are ten independent power companies which individually operate their own power network as well as the tie-lines that link them to the adjacent companies. Because each power company is independent operating entity, there is no way to collect synchronized phasor measurements of transmission high voltage level from all power companies at present. For the CampusWAMS, however, at least one PMU is installed in

the supply network of each power company; therefore, the CampusWAMS is in fact a unique wide-area monitoring system which spreads over the overall power supply area of ten companies and continuously provides synchronized phasor measurements of practical systems.

For reference and latter use, 12 PMUs in the CampusWAMS of Japan are numbered and grouped as Table 2-1.

Table 2-1. PMUs of the CampusWAMS in Japan

No.	Area	Installed City	Group
1	Western 60-Hz	Miyazaki	Lower-end
2		Kumamoto	
3		Kitakyushu	
4		Hiroshima	Center
5		Tokushima	
6		Osaka	
7		Fukui	Upper-end
8		Nagoya	
9		Okinawa	
10	Eastern 50-Hz	Yokohama	
11		Hachinohe	
12		Sapporo	

In reality, each PMU is placed in the laboratory of university in each city. Every PMU measures the single phase voltage phasor of 100V outlet on the wall of laboratory with GPS-synchronized time-tag. In specific, 30 (for Western 60-Hz area) or 25 (for Eastern 50-Hz area) voltage phasor data are computed and recorded in the PMU per second – each voltage phasor data is estimated using 96 sample data per voltage sine-wave cycle. Afterwards, for every 20 minutes, the voltage phasor data saved in each PMU are automatically transmitted and collected into multiple data servers and saved as one single data file for future offline analysis. That is to say, each data file contains the 1,200s measurements of single phase voltage waveform – 36,000 phasor data in case of Western 60-Hz area or 30,000 phasor data in case of Eastern 50-Hz area. Such data sample frequency is sufficient for power system small-signal analysis. The developed analysis applications run in other computers and read data from these servers to process. Thus, a wide-area measuring and monitoring system is constructed.

Moreover, the start time-point of above-mentioned 20 minutes setting can be specified as required. Currently, as illustrated in Figure 2-6, three data files are generated for the time sections from 50-min to 10-min, 10-min to 30-min and 30-min to 50-min respectively in the period of one hour.

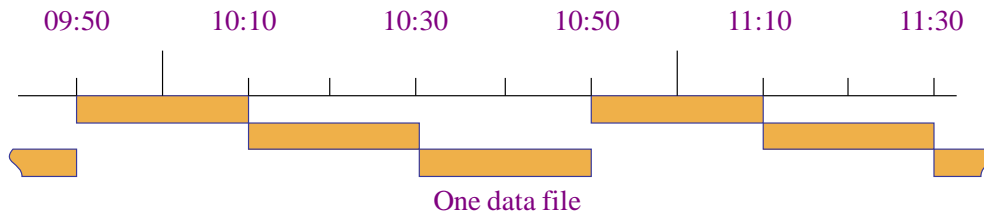


Figure 2-6. Data file recording scheme

From 2004, the project of CampusWAMS was extended to install PMU in the power grid of several countries in Southeast Asia such as Thailand, Singapore and Malaysia. The CampusWAMS of Thailand power system, as shown in Figure 2-6, consists of three PMUs which are placed at three universities respectively. Three PMUs cover the typical power supply area of north part (Chiang Mai), center part (Bangkok), and south part (Songkla) of Thailand power network.

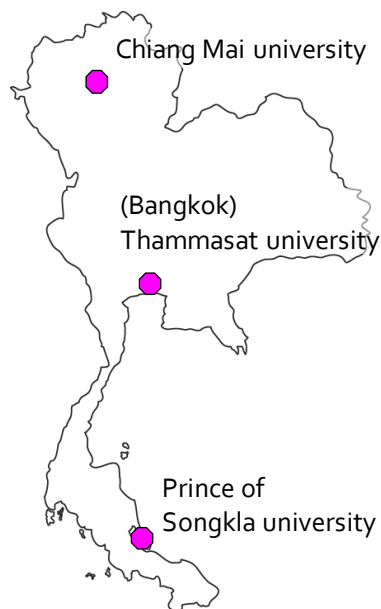


Figure 2-7. PMUs location for the CampusWAMS in Thailand

Similarly, these PMUs measure the single phase voltage phasor of 220V wall outlet in the laboratory with GPS-synchronized time-tag. Because the nominal frequency of Thailand power system is 50Hz, 25 phasor data are computed and recorded in the PMU per second. The phasor measurements of every 20 minutes are transmitted and saved into data servers as one single data file.

Based on the phasor measurements of the CampusWAMS, two important signals can be readily calculated using Equation (2.1) and (2.2). They are the voltage phase difference between any two locations, and the frequency deviation of any one location. From Chapter 4, these two signals will be adopted to analyze the characteristic of power system dynamic.

$$\theta_{ij} = \theta_i - \theta_j \text{ (deg.)} \quad (2.1)$$

$$\Delta f_i = \frac{\theta_i}{\Delta t} \cdot \frac{1}{360^\circ} \text{ (Hz)} \quad (2.2)$$

where θ_i , θ_j are the voltage phase angle of i-th and j-th location respectively and Δt is the time interval of the recorded phasor data in a data file.

Chapter 3.

Measurement-based Analysis Theory

3.1 Power System Small-Signal Stability

According to [17], power system stability is the ability of the grid to return to a normal operating condition after being subjected to a disturbance. As illustrated in Figure 3-1, power system stability can be generally classified in terms of the main system variables: generator rotor angles, bus voltage magnitudes, and system frequency [6][17]. In particular, the rotor angle stability refers to the ability of the system's synchronous machines to remain in synchronism after large or small disturbances. In principle, this angle stability problem is directly associated with maintaining or restoring the equilibrium between electromagnetic torque and mechanical torque at each synchronous machine in the system.

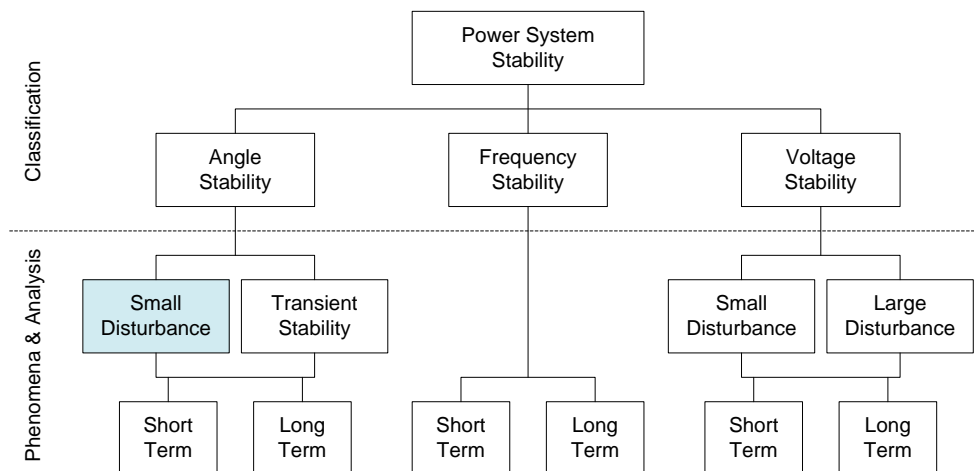


Figure 3-1. Classification of power system stability

The further classification of angle stability shown in Figure 3-1 has to do with the characteristics of the physical phenomena as well as the techniques used for their analysis. Thus, small-signal (also referred to small-disturbance or oscillatory) rotor angle stability is associated with the ability of generators to maintain synchronism after small disturbances, with "small" meaning that the perturbations should be of a magnitude such that the phenomenon can be studied through a linearization of system model equations. This problem is usually associated with the appearance of low-damped or un-damped oscillations in the system due to lack of sufficient damping torque. On the other hand, large-disturbance rotor angle stability, more commonly referred to as transient stability, corresponds to the ability of generators to maintain synchronism when subjected to severe disturbances such as a short circuits or outages of major transmission lines. In this case, the system nonlinearities govern the system response; hence, equation linearization does not work, requiring short-term analysis tools that fully account for the main nonlinear system characteristics. On the basis of nonlinear system theory, this analysis can be viewed as determining whether the system fault trajectory at the "clearance" point is outside or inside of the stability region associated with the post-contingency stable equilibrium point.

3.1.1 Nature of Small-Signal Stability

As mentioned above, small-signal (or small-disturbance) stability is the ability of the power system to maintain synchronism under small disturbances. Such disturbances occur continually on the system in the form of small variations in loads and generation. It should be noted that the disturbances are considered sufficiently small as long as under such disturbances, the system equations are permissible for linearization for purposes of analysis. In practice, the force maintaining the synchronism of a generator at equilibrium comes from the balance between electromagnetic torque and mechanical torque. Under the assumption of 'small disturbance', the mechanical torque can be considered as unchanged for the analysis of small-signal stability. Therefore, only the electromagnetic torque is concerned. By linearization around equilibrium, the change in electromagnetic torque of a synchronous machine following a disturbance can be resolved into two components [6][7]:

$$\Delta T_e = T_S \Delta \delta + T_D \Delta \omega \quad (3.1)$$

where

- $T_S \Delta \delta$ is the component of torque change in phase with the rotor angle variation $\Delta \delta$ and is referred to as the synchronizing torque component; accordingly, T_S is the synchronizing torque coefficient.

- $T_D\Delta\omega$ is the component of torque in phase with the speed deviation $\Delta\omega$ and is referred to as the damping torque component; accordingly, T_D is the damping torque coefficient.

Small-signal stability depends on the existence of both components of torque for each of the synchronous machines. On one hand, lack of sufficient synchronizing torque results in instability through a non-periodic drift in rotor angle. On the other hand, lack of sufficient damping torque results in oscillatory instability. Therefore, small-signal angle instability may develop in following two forms: (i) steady increase in rotor angle due to lack of sufficient synchronizing torque, or (ii) rotor oscillations of increasing amplitude due to lack of sufficient damping torque.

The nature of system response to small disturbances depends on a number of factors including the initial operating, the transmission system strength, and the type of generator excitation controls used. For a generator connected radially to a large power system, in the absence of automatic voltage regulators (i.e., with constant field voltage) the small-signal instability is due to lack of sufficient synchronizing torque. This results in small-signal instability through a non-oscillatory mode. With continuously acting voltage regulators, the small-disturbance stability problem is one of ensuring sufficient damping of system oscillations. Instability is normally through angle or power oscillations of increasing amplitude.

In today's practical power system, small-signal stability problem is largely caused by insufficient damping of oscillations. Furthermore, it has been recognized that such oscillations could occur in different range and lead to following classification of different mode of power system oscillation [7]:

- *Local modes* or *machine-system modes* are associated with the swinging of units at a generating station with respect to the rest of the power system. The term local is used because the oscillations are localized at one station or a small part of the power system.
- *Interarea modes* are associated with the swinging of many machines in one part of the system against machines in other parts. They are caused by two or more groups of closely coupled machines being interconnected by weak ties.
- *Control modes* are associated with generating units and other controls. Poorly tuned exciters, speed governors, HVDC converters and static var compensators are the usual causes of instability or these modes.
- *Torsional modes* are associated with the turbine-generator shaft system rotational components. Instability of torsional modes may be caused by interaction with excitation controls, speed governors, HVDC controls, and

series-capacitor-compensated lines.

With the spreading interconnection of multiple power grids over distant geographic area and its operation near transmission limits of inter-ties, the problem of interarea oscillation is becoming more serious and is producing more threats on the safety and stability of entire power system. This thesis studies the issues of power system interarea oscillations based on wide-area phasor measurements using various analysis techniques.

3.2 Traditional Model-based Analysis

Taking power system small-signal stability analysis as an example, the principle and disadvantages of traditional model-based approach is described in this subsection.

Here, “model” actually means a set of mathematic equations which are derived to describe the dynamic of generators and their associated control devices like exciter and automation voltage regulator (AVR), the dynamic of other control devices like power system stabilizer (PSS), as well as the interaction between generators and power network and loads. In order to construct such a mathematic model for either a simple system or a large interconnected system, all information about the studied system – from grid topology to component parameters, from loads profile to control settings – must be collected prior to starting any analysis. Obviously, it is a tedious process, especially for a relatively large system to be analyzed. This is first disadvantage of traditional model-based small-signal stability analysis.

Generally, part of these model equations is a group of nonlinear differential equations and the remaining part is a group of nonlinear algebraic equations, since the physical nature of these dynamics is nonlinear. Therefore, the entire system model is finally constructed in the following form:

$$\begin{cases} \dot{x} = f(x, u, t) \\ y = g(x, u, t) \end{cases} \quad (3.2)$$

where x , y , u and t are the state vector, output vector, input vector and time vector respectively. $f(\dots)$ and $g(\dots)$ represent the differential functions and algebraic functions respectively. If the system is autonomous, time t can be eliminated from above equations.

With all necessary information known, next step is to specify multiple normal operating conditions and linearize the system model for each normal operating condition to obtain a linearized system small-signal model. Hence, each small-signal model just corresponds to a specific normal operating condition. Because each normal operating condition differs in the generation and load setting, the final analysis result of every small-signal model is also just applicable to the corresponding operating condition. One

has to repeat the same analysis process when the operating condition changes. This is second disadvantage of model-based traditional small-signal stability analysis.

The linearized system small-signal model is usually in the state-space form as follows:

$$\begin{cases} \Delta\dot{x} = A\Delta x + B\Delta u \\ \Delta y = C\Delta x + D\Delta u \end{cases} \quad (3.3)$$

where A , B , C and D are the state matrix, input matrix, output matrix and feed-forward matrix respectively.

Then all subsequent analysis focuses on the state matrix of the linearized model. From the stability analysis principle of a dynamic system, it is known that the eigenvalues of the state matrix A have close relation with the characteristic of the small-signal stability under the considered operating condition. In particular,

- A *real eigenvalue* corresponds to a non-oscillatory mode. A negative real eigenvalue represents a decaying mode. The larger its magnitude, the faster the decay. A positive real eigenvalue represents non-periodic instability.
- *Complex eigenvalues* occur in conjugate pairs, and each pair corresponds to an oscillatory mode. The real part of the eigenvalues gives the damping, and the imaginary part gives the frequency of oscillation. A negative real part represents a damped oscillation whereas a positive real part represents oscillation of increasing amplitude. That is to say, for a given pair of complex eigenvalues:

$$\lambda = \sigma \pm j\omega \quad (3.4)$$

The frequency of oscillation in Hz, i.e. the actual or damped frequency, is

$$f = \frac{\omega}{2\pi} \quad (3.5)$$

The damping ratio, which determines the rate of decay of the amplitude of the oscillation, is given by

$$\xi = -\frac{\sigma}{\sqrt{\sigma^2 + \omega^2}} \quad (3.6)$$

For a large power system, the dimension of state matrix of its linearized small-signal model is usually very high, for example, up to several hundred, which is a very serious problem when the eigenvalues are computed. This can be said as third inconvenience of model-based traditional small-signal stability analysis. On the other hand, however, by observing the eigenvalues, it is easy to identify all modes

simultaneously: stable and unstable, non-oscillatory or oscillatory, as well as the associated mode parameters. This is one merit of model-based traditional small-signal stability analysis.

Further analysis can be performed based on the computed eigenvalues to get more insight into each identified mode, especially for those oscillatory modes, such as mode shape and mode participation.

Of course, all model-based analysis is generally performed by utilizing a set of computer programs, which can easily memory system parameters, carry on repetitive computation for different operating conditions, save computation time and improve computation accuracy. However, the inconveniences of using these programs still exist. Moreover, one of the most obvious problems is that the operator find it very difficult to match a model-based analysis result to a scenario of real power system because the real power system is always in the changing operating conditions. In one word, the model-based analysis method cannot reflect the real dynamic and its characteristic of a practical power system.

3.3 Measurement-based Analysis

After the introduction of wide-area time-synchronized phasor measurements, measurement-based analysis becomes possible. Owing to the high-speed, high accuracy and time-synchronization sample technology of modern PMU, the variables that tightly relate to the dynamic of small-signal stability, such as bus voltage angle, bus frequency or tie-line active power, are readily available. Even the measurements of these dynamic variables come from distant, wide-spread multiple locations of a large power system, it is safe to compare or process them together due to time-synchronization among all measurement locations. Based on these realtime phasor measurements, new methods can be developed to perform online or near-realtime small-signal stability analysis.

3.3.1 Underlying Theory

First of all, phasor measurement-based methods have no dependence on a complex system mathematical model which can only be formed by knowing all information about the system in advance. Secondly, it is assumed that only the measurement of system output variables (and/or input variables) is available. From the point of this view, the measurement-based method is more like the concept of system identification – to identify an approximate model or estimate an quantity that can describe the system dynamic or its characteristics, given that the output (and/or the input) of a system is measurable.

In this concept, the system to be analyzed is assumed to behave like a 'black-box', i.e. no detail information about the inside of the system is known; only the output and/or input of the system are measured. The object is to find a model – parametric or non-parametric model – that can reproduce the same output with measured data when the same input is applied. Under most situations which are actually more common for a practical power system, only the output of the system is available and the input to the system is either unidentifiable or unmeasurable. Figure 3-2 can be used to explain the underlying theory that the phasor measurements can be used to analyze the small-signal stability (e.g. power system oscillations).

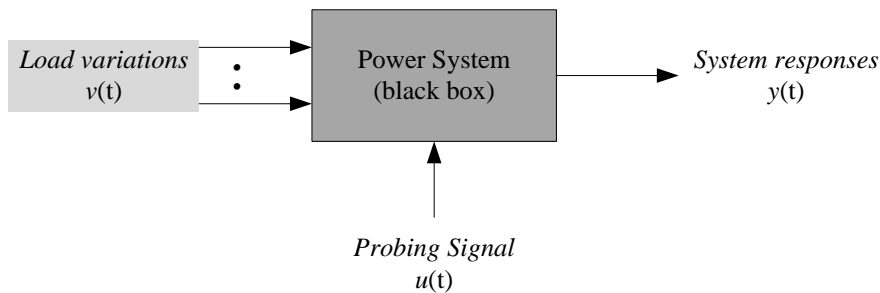


Figure 3-2. Concept of measurement-based analysis

Suppose we don't know too much about the detail of the power system to be studied so that it is basically regarded as a black-box. But one thing we do know is that the power system is constantly subjected to the small-disturbances, i.e. some load variations. The feature of load variations in a practical power system is that they are neither predictable nor measurable, which indicates the randomness of the small load variations. Consequently, these random small load variations can be considered as noise inputs (i.e. excitations) to the power system and then the power system will respond to these excitations. Unlike unmeasurable noise inputs, the power system responses to random load variations can be easily measured from various power variables such as bus voltage or line current. Therefore, the key point of underlying theory of measurement-based method is: the output signal must contain the effects of both the input signal and the system dynamics. In other words, from the output signal measurements, the characteristic of the dynamics or modes which the system contains can be observed and discovered. Moreover, since the input noise is unknown in this case, the developed method is only based on the measurements of the output signals.

Another way to excite the studied power system is to use probing signal. A well-designed probing signal is usually imposed into the system through some control devices such as AVR, dc converter and the system responses corresponding to this special signal

are measured. Similarly, the output signal must contain the effects of both the probing signal and the system dynamic characteristic. In this case, the developed method can be based on the measurements of both signals because the input probing signal is known.

Either way, the final output measurements contain measurement noise produced by instruments, communication channels, recording systems, and similar devices. It is hard to separate the real responses to input signals from these measurement noises which are basically unpredictable and unmeasurable. Therefore, the developed methods must consider pre-processing the final output measurements before they are used for small-signal analysis.

3.3.2 Fundamental Assumptions

Another important point of the measurement-based method illustrated in Figure 3-2 is that the following two fundamental assumptions must be made for the small-signal analysis:

- Firstly, the input noise is assumed to be a stationary, random white noise signal. White noise is a random signal (or process) with a flat power spectral density. In other words, the signal contains equal power within a fixed bandwidth at any center frequency. For a real power system, it is reasonable to regard the small variations in loads under normal operating condition as a white noise signal.
- Secondly, the concerned power system is assumed to be a linear system with constant parameters. For a constant-parameters linear system, it does not cause any frequency translation but only modify the amplitude and/or phase of the applied input. For a large power system, as long as the load variations are sufficiently small, it can be linearized around every equilibrium operation point and regarded as having constant parameters during the period of small-signal analysis.

3.3.3 Analysis Objective

Although the phasor measurement-based method and traditional model-based method for small-signal analysis differ in the concept and analyzing techniques, the objective of oscillation analysis is same – to identify the existence of power oscillation modes and estimate the associated characteristics for each mode. The characteristic information about a power oscillation mode includes:

- Mode parameters(eigenvalues), usually represented in terms of frequency and

damping;

- Mode shape, usually represented by the relative strength and phasing of generators swing for each mode;
- Mode participation, usually a factor or a weight representing the relative participating level of generators for each mode.

Moreover, the power variables whose measurements can be used for small-signal analysis are usually selected to be bus voltage angle, bus frequency or active power flow on tie-lines.

3.4 Review of Analysis Techniques

As explained above, the core principle of measurement-based method is to estimate the parameter or the characteristic of unknown system from the measurements of system outputs and inputs. In order to realize this principle, various analysis techniques must be adopted to process and analyze the available measurements. In this section, the analysis techniques and pertinent concepts that are to be applied in the work are briefly reviewed. More details will be introduced in the following chapters where necessary.

3.4.1 Random Signal

A random signal represents a random phenomenon that cannot be described by an explicitly mathematical relationship because each of observation of the phenomenon is unique. In other words, any given observation can only represent one of many possible results which might occurs. Load variation in a power system is a typical random signal – load demand at different locations or at same location but different time produces a different and unpredictable load variation time history record.

Furthermore, a single time history representing a random phenomenon is called a *sample function* (or a *sample record* when observed over a finite time period). The collection of all possible sample functions (also called the *ensemble*) which the random phenomenon might have produced is called a *random process* or a *stochastic process*. Hence, a sample record of data for a random physical phenomenon may be thought of as one physical realization of a random process.

- Stationary Random Processes

When a physical phenomenon is considered in terms of a random process, its properties can hypothetically be described by computing average values at any instant of time over the collection of sample functions which describe the random process, or by

computing a correlation between the values of the random process at two different times. If these two properties do not vary as time varies, the random process is said to be *weakly stationary*. Therefore, for a weakly stationary random process, the mean value is a constant. Moreover, the similar definition is applicable to a single time history record, i.e. a sample record.

- Ergodic Random Processes

The stationary property of a random process is determined by computer ensemble averages at specific instants of time. In most cases, however, it is also possible to describe the properties of a stationary random process by computing time averages over specific sample functions in the ensemble. In definition, if the random process is stationary, and the mean value and the autocorrelation function of any sample function do not differ when computed over different sample functions, the random process is said to be *ergodic*. In other words, the ergodicity of a random process implies that the time average of all possible single sample function are equal to the same constant, i.e. the ensemble average of the random process.

Ergodic random processes are a very important class of random processes because all properties of ergodic random processes can be determined by performing time averages over a single sample function. Fortunately, in practice, random data representing stationary physical phenomenon are generally ergodic. It is for this reason that the properties of stationary random phenomenon can be measured properly, in most cases, from a single observed time history record.

3.4.2 Digital Signal Processing

Digital signal represents the measurement data of a real life signal in the form of discrete digital number. Most signals in real life are continuous in amplitude and time – that is, *analog* – but after sampling and conversion by digital system, they become series of discrete sample data which can be read and processed by digital electronic computer using either hardware or software. The task of digital signal processing is to observe and analyze the measurement data of one signal so that the concerned properties of signal itself as well as the concerned properties of the system that produces this signal can be estimated. For measurement-based methods of power system small-signal dynamic monitoring and stability control, various digital signal processing are indispensable.

- Least Squares Approximation

Suppose having a measurement data vector of one signal with N elements, $x = [x_1, x_2, x_3, \dots, x_N]$ and the objective is to find a function $\hat{F}(c, x, y, nT)$ to approximate the measurement data vector. Define the total squared error (TSE) as

$$\text{TSE} = \sum_{n=1}^N (x_n - \hat{F}(c, x, y, nT))^2 \quad (3.7)$$

where x_n is nth element of x , y is other relevant measurement data vectors, and T is the time interval between measurement data. If unknown function parameter c is selected to make TSE as small as possible, then the approximation function $\hat{F}(c, x, y, nT)$ is called as least squares approximation (LSA) to the corresponding measurement data vector x .

- Discrete Fourier Transform

The discrete Fourier transform (DFT) transforms measured data in time domain into representation in frequency domain. In particular, the DFT is widely employed in digital signal processing to analyze the frequency contents contained in a sampled signal.

For a measurement data vector of one signal $x = [x_0, x_1, x_2, \dots, x_{N-1}]$, the N-point DFT of x can be computed by

$$X_m = \sum_{n=0}^{N-1} x_n e^{-\frac{j2\pi mn}{N}} ; m = 0, 1, \dots, N-1 \quad (3.8)$$

It is to say that the N-point DFT of an N-element data vector is still an N-element vector. It is to be noticed that each element of DFT result is a complex value. Hence, the absolute and the angle of each DFT component can be computed to obtain the amplitude and phase of the different sinusoidal components as follows:

$$\begin{aligned} \text{Amplitude spectrum} &= \text{abs}(X) = [|X_0|, |X_1|, \dots, |X_{N-1}|] \\ \text{Phase spectrum} &= \text{angle}(X) = [\angle X_0, \angle X_1, \dots, \angle X_{N-1}] \end{aligned} \quad (3.9)$$

On the other hand, the DFT result can be transformed reversely to obtain the original time-domain data by performing the inverse DFT (IDFT) on the X_m frequency-domain values using the following formula:

$$x_n = \frac{1}{N} \sum_{m=0}^{N-1} X_m e^{\frac{j2\pi mn}{N}} ; n = 0, 1, \dots, N-1 \quad (3.10)$$

In practice, the DFT or IDFT can be computed efficiently using a fast Fourier transform (FFT) algorithm. Therefore, for the rest of the thesis, the short term FFT and DFT, IDFT and IFFT will be used interchangeably.

- Correlation

Basically, correlation is a quantitative measure we use in the field of digital signal processing to identify how much two signals are like each other. In this situation, it is usually called cross-correlation. The auto-correlation, on the other hand, is used to tell how much a signal at one time is like itself at some other time.

For two sampled signals, $x[n]$ and $y[n]$, the cross-correlation function of $x[n]$ and $y[n]$ is

$$\varphi_{xy}(k) = E\{x_n \cdot y_{n+k}\}; k \geq 0 \quad (3.11)$$

where k is the sample shift and $E\{\cdot\}$ represents the expectation value operator. If $\varphi_{xy}(k) = 0$ for all k , two signals are said to be uncorrelated.

Similarly, the auto-correlation function of $x(n)$ is

$$\varphi_{xx}(k) = E\{x_n \cdot x_{n+k}\}; k \geq 0 \quad (3.12)$$

Obviously, $\varphi_{xy}(k)$ has maximum value for $k = 0$. The auto-correlation function is a very powerful mathematical tool for finding repeating patterns, such as the presence of a periodic signal which has been buried under noise, or identifying the missing fundamental frequency in a signal implied by its harmonic frequencies.

- Power Spectrum Density

In some literatures, it is also called power spectral density. Both are abbreviated as PSD. PSD is a measure of signal power in frequency domain – it represents amount of power per unit (density) of frequency (spectral) as a function of the frequency. The plot of PSD against a range of frequency can describes how the power of a signal or time series is distributed with frequency.

If $x[n]$ is a vector consisting of N samples of one signal $x(t)$, the average power in signal $x(t)$ is

$$\text{Average power} = \frac{1}{N} \sum_{n=0}^{N-1} x_n^2 \approx \frac{1}{NT} \int_0^{NT} x^2(t) dt \quad (3.13)$$

Substituting x_n in (3.13) with its IDFT formula (3.10), it becomes

$$\text{Average power} = \frac{1}{N} \sum_{n=0}^{N-1} \left(\frac{1}{N} \sum_{m=0}^{N-1} X_m e^{\frac{j2\pi mn}{N}} \right)^2 \quad (3.14)$$

Using the properties of DFT and after some mathematical management, the average power expression becomes

$$\text{Average power} = \frac{1}{N^2} \sum_{m=0}^{N-1} |X_m|^2 \quad (3.15)$$

Thus, in combination with (3.13), it can be seen that

$$\frac{1}{N} \sum_{n=0}^{N-1} x_n^2 = \frac{1}{N^2} \sum_{m=0}^{N-1} |X_m|^2 \quad (3.16)$$

This result presents average signal power in terms of power spectrum. Known as Parseval's Theorem, it reveals an important insight and link between the time and frequency domains.

Furthermore, the periodogram can be defined as

$$\text{Periodogram: } P_{xx}(m) = \frac{1}{N} |X_m|^2 = \frac{1}{N} \left| \sum_{n=0}^{N-1} x_n e^{-\frac{j2\pi mn}{N}} \right|^2 \quad (3.17)$$

Using the definition of periodogram, (3.16) can be rewritten as

$$\text{Average power} = \frac{1}{N} \sum_{n=0}^{N-1} x_n^2 = \frac{1}{N} \sum_{m=0}^{N-1} P_{xx}(m) \quad (3.18)$$

Consequently, in the same way that x_n^2 gives a measure of signal power at a point in the time domain, $P_{xx}(m)$ gives a measure of signal power at a point in the frequency domain. Therefore, the vector $P_{xx} = [P_{xx}(m)]$ is said to be a measure of the *power spectrum density* of $x(t)$, because its average value in (3.18) is another expression of the average power estimate.

From above derivation, it can be found that the periodogram is actually the counterpart in the frequency domain of correlation which is defined in the time domain. It can be proved that the periodogram $P_{xx}(m)$ is the DFT of $\varphi_{xx}(k)$.

$$P_{xx}(m) = \text{DFT}(\varphi_{xx}(k)) = \sum_{n=0}^{N-1} \varphi_{xx}(n) e^{-\frac{j2\pi mn}{N}} \quad (3.19)$$

- White Noise Signal

A white noise signal is a zero-mean random signal with constant (flat) PSD within a fixed bandwidth at any center frequency. An infinite-bandwidth white noise signal is merely theoretically possible. By having power at all frequencies, the total power of such a signal is infinite and therefore impossible to generate. In practice, however, a signal can be "white" with a flat spectrum over a defined frequency band.

3.4.3 System Identification

A *system* is an object in which variables or different kinds interact and produce observable signals. The observable signals that are of interest to us are usually called *outputs*. The system is also affected by external drive force. External signals that can be manipulated by the observer are called *inputs*; for example, the probing signal in Figure 3-2 is in the scope of such input signals. Others external signals that cannot be manipulated by the observer are called *disturbances* and can be divided into two types: *measurable disturbances* which represents any deterministic input, and *unmeasurable disturbances* which represent stochastic inputs to the system. For example, the load variations in Figure 3-2 belong to the scope of the *unmeasurable disturbances*. In some situations the inputs may be missing. The output signals are important source which provide useful information about the system. Figure 3-3 shows a schematic diagram of a dynamic system with inputs, outputs and disturbances.

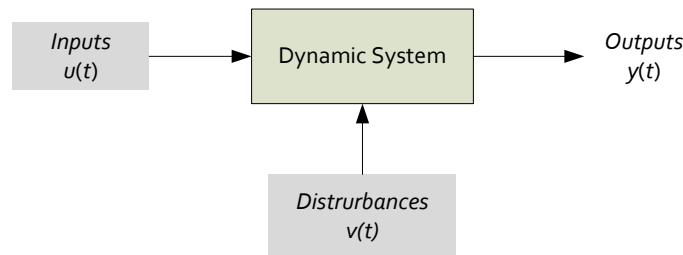


Figure 3-3. A dynamic system with inputs, outputs and disturbances

System identification represents mathematical tools and algorithms that build dynamical models of the studied system from measured data of system inputs and outputs. Hence, the problem of system identification is specified by three elements [22]:

- A data set obtained from measurements of outputs and/or inputs.
- A model set or a model structure, containing candidate models.
- A criterion to select the best model(s), or a rule to evaluate candidate models,

based on the data.

The inputs-outputs data are usually collected through experiment. In this case, the experiment must be designed to decide input (or test) signals, output signals to be measured, the sampling interval, etc., thereby systems characteristics are well reflected in the observed data. Thus, to obtain useful data for system identification, some a priori information or some physical knowledge about the system are necessary. Also, there are cases, e.g. for a real power system, where such designed experiments cannot be performed due to such as safety, technical and/or economic reasons, so that only measured data under normal operating conditions can be used.

A choice of model set is a difficult issue in system identification. A model in this context is a mathematical description of the dynamic behavior of the system in either the time or frequency domain. Dynamical models could be transfer functions, state space models, time-series models, which are parameterized in terms of finite number of parameters. Thus these dynamic models are referred to as parametric models. Also used are non-parametric models such as impulse responses, and frequency responses, power spectral density functions, etc.

On the other hand, depending on how much the knowledge about the system is known and how the model is used after identification, two types of model can be chosen. For one type, several classes of discrete-time linear time-invariant (LTI) models can be selected to model the characteristic of system inputs-outputs as well as the relationship between system inputs and outputs. Since these models do not necessarily reflect the knowledge about the structure of the system, they are referred to as black-box models. Such models include Prony model, auto regressive (AR) model and auto regressive moving average (ARMA) model, etc. One of the most difficult problems of using this type model is to find a good model structure, or to determine the order of the models based on the given inputs-outputs data. For another type, by using some physical principles and priori information about a system, so-called gray-box models can be constructed to describe the dynamics of a system. The problems of using this type model are to estimate unknown parameters.

The next step of system identification is to determine the final model or its unknown parameter which the experiment data is best explained. A criterion that can measure the distance between a model and a real system must be set for selecting the best model. Subsequently, the identification problem in narrow sense reduces to an optimization problem minimizing criterion.

After finding the best model, it has to be validated. In particular, model validation is to determine whether or not an identified model should be accepted as a suitable description that explains the dynamics of a system. Thus, model validation is based on the way in which the model is used, a priori information on the system, the fitness of the

model to real data, etc. For example, if we identify the transfer function of a system, the quality of an identified model is evaluated based on the step response and/or the pole-zero configurations. If the performance is not satisfactory, the same process of system identification must be repeated, including the selection of model structure, or experiment design, etc.

3.4.4 Optimization

It can be found that many engineering problems, such as power spectrum density estimation, system identification, parameter estimation, and controller design, etc, will eventually become to an optimization problem. Therefore, the optimization problems and algorithms play a significant role in the measurement-based methods for power system small-signal dynamic analysis and stability control.

Mathematically speaking, optimization is the minimization or maximization of a function subject to constraints on its variables. Generally, three elements are involved with an optimization problem:

- x : the vector of variables, also called unknowns or parameters;
- f : the objective function, a (scalar) function of x that needs to be maximized or minimized;
- c_i : constraint functions, which are scalar functions of x that define certain equations and inequalities that the unknown vector x must satisfy.

With three elements, an optimization problem can be written as follows:

$$\min_{x \in R^n} f(x) \quad \text{subject to} \quad \begin{array}{l} c_i(x) = 0, \quad i \in \mathcal{E} \\ c_i(x) \geq 0, \quad i \in \mathcal{J} \end{array} \quad (3.20)$$

where \mathcal{E} and \mathcal{J} are sets of indices for equality and inequality constraints, respectively.

According to the different forms that three elements may have, optimization problems can be categorized in many different ways, such as continuous and discrete optimization, linear and non-linear optimization, constrained and unconstrained optimization, global and local optimization, stochastic and deterministic optimization, etc. Usually, there are special optimization algorithms for solving each category of optimization problems. Each algorithm may differ in the principle, implementation and performance, but they generally are iterative. In the beginning an initial guess of the variable x is determined and a sequence of improved estimates (called "iterates") is generated until a solution is achieved based on the objective function.

Many optimization problems in power system engineering, such as optimal power flow, available transfer capacity, PMU placement, system model estimation, controller parameter determination and multiple controller coordination are all non-linear. Moreover, there is usually more than one objective function for these problems and every objective function is usually very complex and sometimes has no explicit mathematical expression. Consequently, most traditional gradient-based optimization algorithms often fail to find a solution or can merely find a local solution which is not the real global solution. In order to find a global solution, many global optimization algorithms based on random and heuristic searching concept has been proposed and applied to power system optimization problems. These algorithms include evolutionary programming (EP), genetic algorithms (GA), simulated annealing (SA), particle swarm optimization (PSO), ant colony search (ACS), tabu search (TS), bacterial foraging algorithm (BSA), and so on.

More detailed and thorough introduction of above analysis techniques can be referred to many textbooks, such as [17] for random data analysis, [19], [20], [21] for digital signal processing and spectrum analysis, [22] and [23] for system identification, [24] and [25] for traditional optimization and global optimization.

Chapter 4.

Single-mode-oriented Estimation of Power Oscillation Based on Phasor Measurements and Auto-spectrum-based FFT Filter

4.1 Introduction

Experiences from recent blackouts occurring in the North America and Europe have revealed that partial or complete blackouts can arise from sustaining small disturbance angle instability. Therefore, online estimating and monitoring of the characteristic of interarea power oscillation caused by various disturbances such as frequent load changes or unexpected line tripping is of great importance for power system stable operation and preventive control. Over past decade, the wide area monitoring system (WAMS) based on multiple Phasor Measurement Units (PMUs) has been put into commission in some large interconnected power system [42]-[46]. In these WAMS projects, the multiple synchronized phasor measurements, which contain rich and precise information of system wide dynamics of transmission high voltage level, are utilized to implement online monitoring and estimation of interarea low-frequency oscillation mode.

With increasing application of WAMS, the measurement-based approach to estimate the low-frequency oscillation parameters became prevailing. Without knowledge of generator and line parameters, the measurement-based approach primarily employs statistical signal processing technique and system identification theory to discover the characteristic of low-frequency oscillation mode which usually buries in the bus voltage phase angle or tie line power variations due to random and constant load variations.

4.1.1 Review of Multi-mode-oriented Methods

As reviewed in Section 3.4, several analysis techniques for digital signal processing and system identification can be applied to realize measurement-based approach to estimate the low-frequency oscillation. Among these techniques, Prony method and a family of autoregressive (AR) methods have been most often used in many previous publications.

- Prony Method

Prony method is a signal processing technique for extracting the sinusoid or exponential signals from a uniformly sampled signal by solving a set of linear equations for the coefficients of the recurrence equation that the signals satisfy. It extends Fourier analysis by directly estimating the frequency, damping, strength, and relative phase of modal components presenting in a given signal. Therefore, Prony method belongs to the type of parametric analysis, which is defined as any tool that estimates the modal (eigen) properties of oscillation modes based upon finite measurements of output signals.

The Prony analysis directly estimates the parameters of the eigen-properties by fitting a sum of complex damped sinusoids to evenly spaced sample (in time) values of the output as:

$$\hat{y}(t) = \sum_{i=1}^L A_i e^{(\sigma_i t)} \cos(2\pi f_i t + \phi_i) \quad (4.1)$$

where A_i , σ_i , ϕ_i and f_i is the amplitude, damping coefficient, phase and frequency of component i respectively; L is the total number of damped exponential components; $\hat{y}(t)$ is the estimate of the observed data for $y(t)$ consisting of N samples $y(t_k) = y[k]$, $k = 0, 1, 2, \dots, N - 1$ that are evenly spaced.

Prony analysis for power system applications was first introduced in [26] with a large number of additional publications since then [27]-[32]. Typically, Prony analysis operates upon a few or more cycles of a strong oscillation, which is initiated by a sudden disturbance like a relatively big load change within a short period or network switching, to estimate modal properties. Usually, such a strong oscillation is in a free ringdown form and its oscillating amplitude is much bigger than that of a normal oscillation. It turned out that Prony method is only a good tool for such ringdown signal.

- AR-family Models

The family of AR methods is also a type of parametric mode-estimation approach. But it differs from Prony method. It is more applicable to the estimation of modal properties using measurements under normal operating conditions with constant small load variations. The key point of Prony method is that it assumes the analyzed signal is

the sum of multiple complex-exponential. From this point, this is actually a priori determination of signal model which can simplify the estimation. However, on the other hand, this point also limits the applicability of Prony method only to specific such as ringdown signals. In other words, applying Prony method to the signal with small signal-to-noise ratio would fail to produce satisfactory estimation results due to no obvious sign of complex exponential components. In this situation, a general linear model of signal without any component assumption has to be considered.

For the family of AR methods, as illustrated in Figure 4-1, the power system response output $y(t)$ can be regarded as the result of an approximately stationary white noise input $u(t)$, i.e. constantly varying loads, in the frequency band of interest over an analysis window. From this angle, the characteristic of the studied power system can be represented by a discrete transfer function $G(z)$ as follows:

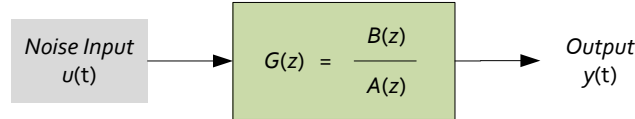


Figure 4-1. General linear model of power system

$$y(t) = \frac{1 + b_1 z^{-1} + b_2 z^{-2} + \dots + b_q z^{-q}}{1 + a_1 z^{-1} + a_2 z^{-2} + \dots + a_p z^{-p}} \cdot u(t) \quad (4.2)$$

In Equation (4.2), p and q are the order of the denominator and numerator polynomial, respectively. It should be noted that the order p and q are the estimation parameters which are needed to be determined for each different case in practice in order to obtain a correct and satisfactory result.

When the order of the denominator p is selected to be zero, the model (4.2) becomes (4.3) which is known as moving average (MA) process of order q . When the order of the denominator q is selected to be zero, the model (4.2) becomes (4.4) which is known as autoregressive (AR) process of order p . Accordingly, the model (4.2) is an autoregressive moving average (ARMA) process of order (p, q) as it contains both AR and MA components.

$$y(t) = (1 + b_1 z^{-1} + b_2 z^{-2} + \dots + b_q z^{-q})u(t) \quad (4.3)$$

$$y(t) = \frac{1}{(1 + a_1 z^{-1} + a_2 z^{-2} + \dots + a_p z^{-p})} u(t) \quad (4.4)$$

The denominator polynomial in model (4.2) or (4.4) is actually the characteristic polynomial of transfer function $G(z)$. The roots of characteristic polynomial are the system poles that describe the system eigen-properties of oscillation modes. Hence, as long as the coefficients $a_1 \dots a_p$ of the characteristic polynomial $A(z)$ can be estimated, then the polynomial is rooted and the system poles can be found as the dominant roots in the frequency band of interest. This is the fundamental theory of AR-family models can be used for power system small-signal analysis. Various algorithms have been proposed to calculate the coefficients $a_1 \dots a_p$ of the characteristic polynomial $A(z)$ from either time-domain or frequency-domain [20][21].

There are two basic ways of utilizing AR-family model: block processing and recursive. With block-processing algorithms, the modes are estimated from a window of data. For each new window of data, a new estimate is calculated. The first application of block processing is contained in [33] where the Yule-Walker (YW) algorithm is used to estimate modes using an AR model. The method is extended to the over-determined modified Yule-Walker method to estimate an ARMA model in [34]. The approach is further extended to multiple signals in [35], which can improve the performance. A variation of the YW approach that estimates the autocorrelation function using a frequency domain calculation is introduced in [40]; this method is termed the Yule-Walker-Spectrum (YWS) method.

For recursive methods, the estimated modes are updated for each new sample of the data. The new estimate is obtained using a combination of the new data point and the previous mode estimate. A forgetting factor is usually employed to discount information based on previous data; therefore, new data is weighted more in each calculation. Similar to the block-processing methods, all recursive methods tested to date require many minutes of data to converge to a steady-state solution. Some results can be found in [36] which uses the Least-Mean Squares (LMS) method and [37]-[38] which use the Regularized Robust Recursive Least Squares (R3LS) method.

- Subspace Method

Apart from using AR-family model to estimate the transfer function model of a power system, the power system shown Figure 4-1 in can also be represented using a state space model as follows:

$$\begin{cases} x(k+1) = Ax(k) + Ku(k) \\ y(k) = Cx(k) \end{cases} \quad (4.5)$$

where A is state matrix whose eigenvalues describe the characteristic of small-signal stability. Similarly, the eigenvalues can be readily calculated provided the state matrix A can be estimated from the measured data of system responses.

Subspace method, which is a new approach to system identification based on the QR decomposition and the SVD is capable of estimating a state space model based on the measurements of system input and output. The initial results using subspace method N4SID (Numerical algorithm for Subspace State-Space System Identification) for estimating the eigen-properties of power oscillations were first introduced in [39].

4.1.2 Shortcoming of Multi-mode-oriented Methods

All methods reviewed in Section 4.1.1 are capable of estimating parameters of several oscillation modes at the same time. However, the obvious shortcomings are also from this capability. In order to estimate the eigen-properties of multiple oscillation modes simultaneously, the suitable model order, e.g. L in model (4.1) or p in model (4.2) and model (4.4), must be carefully and correctly selected for obtaining a satisfactory estimated result. Unfortunately, the determination of this suitable model order has no consistent rules or universal formulas to follow, which means it will meet some difficulties when these methods are applied to various online automatic-mode applications. A simulation example is given to show this point.

The test system is well-known two-area-four-generator (2A4G) system as shown in Figure 4-2. For the following simulations, each generator is represented using a fourth-order transient model with a first order governor and first order exciter with high gain as shown in Figure 4-3. The system parameters shown in Table 4-1 are the same with example 12.6 in [7] and the initial load flow setting has a little difference. Under the selected initial operating condition, the traditional small-signal analysis results shown in Table 4-2 indicate that there is an interarea oscillation mode (Mode 1) between Area 1 (G1 and G2) and Area 2 (G3 and G4) around 0.6Hz. Another two oscillation modes around 1.0 Hz are apparently local modes which only involve the generators in each area.

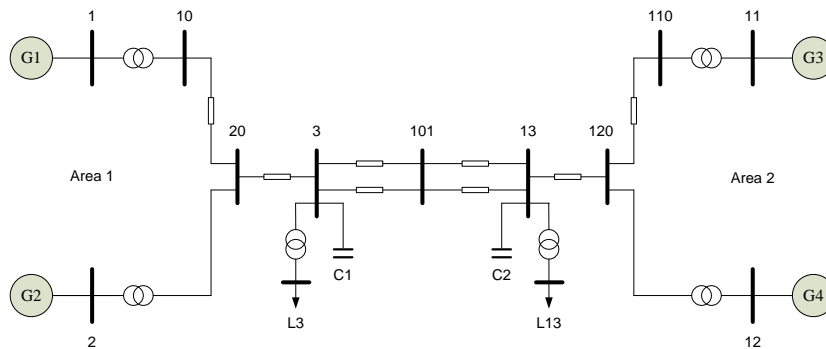


Figure 4-2. Two-area-four-generator (2A4G) test system

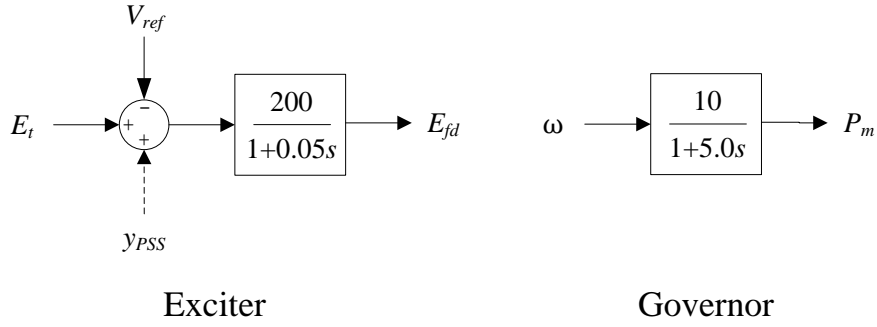


Figure 4-3. Model for exciter and governor in 2A4G system

Table 4-1. Initial load flow setting of 2A4G system

Component	P (MW)	Q (MVA _r)	V (p.u.)	θ (degree)
G1	700	-	1.03	-
G2	700	-	1.01	-
G3	-	-	1.03	-6.8
G4	700	-	1.01	-
L3	800	100	-	-
L13	1200	100	-	-

Table 4-2. Oscillation modes in 2A4G system

Mode	Eigenvalue	Frequency (Hz)	Damping Ratio	Participating Generator
1	- 0.1413 ± j3.7028	0.5897	0.0381	G1,G2,G3,G4
2	- 0.8110 ± j6.5500	1.0504	0.1229	G1,G2
3	- 1.0736 ± j6.2362	1.0071	0.1696	G3,G4

The test system is simulated by injecting at Bus2 small load variations to excite its internal oscillation mode. For the following analysis, the angle difference between Bus1 and Bus 11 for 600-seconds as shown in Figure 4-4 is used to estimate the eigen-properties of the concerned interarea oscillation Mode 1.

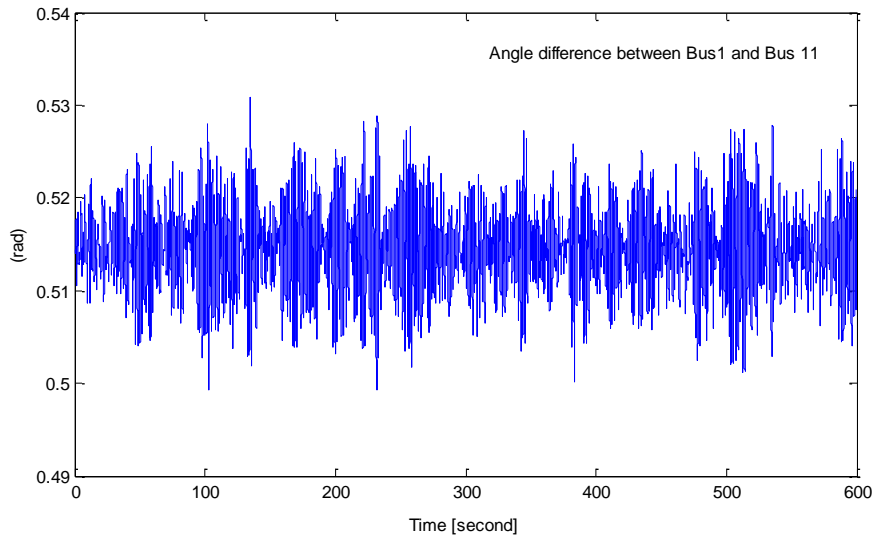


Figure 4-4. Angle difference between Bus1 and Bus11

Table 4-3. Estimated eigenvalues using 200-seconds data

Mode Order	Data Window		
	0s ~ 200s	200s ~ 400s	400s ~ 600s
38	- 0.2136 ± 3.8494i	- 0.2101 ± 3.8485i	- 0.2329 ± 3.8469i
40	- 0.1518 ± 3.8380i	- 0.1489 ± 3.8371i	- 0.1660 ± 3.8347i
42	- 0.2249 ± 3.8633i	- 0.2045 ± 3.8556i	- 0.2215 ± 3.8527i

Table 4-4. Estimated eigenvalues using 300-seconds data

Mode Order	Data Window		
	0s ~ 300s	200s ~ 500s	300s ~ 600s
38	- 0.1968 ± 3.8411i	- 0.2323 ± 3.8726i	- 0.2441 ± 3.8571i
40	- 0.1398 ± 3.8304i	- 0.1648 ± 3.8602i	- 0.1734 ± 3.8444i
42	- 0.2061 ± 3.8534i	- 0.2202 ± 3.8784i	- 0.2291 ± 3.8623i

For the purpose of comparison, different estimation parameters are chose for AR model and the eigenvalue estimation results are summarized in the following tables. It can be found that the accuracy of estimation results has strong dependence on such parameters as data length, data window, and especially the selection of the model order. Too low a guess for model order results in a highly smoothed curve fitting. Too high an order increases the resolution and introduces spurious components into the estimation. Consequently, the optimal combination of all estimation parameters has to be determined case by case because there are no straightforward rules or formulas for this purpose. It is usually necessary in practice to postulate several model orders and then compute some estimation error criterion that can help to indicate which order to choose. Furthermore, subjective judgment, rather than science, is still required in the final analysis to select an order for data from actual signals of an unknown process.

4.2 Single-mode-oriented Estimation Method

Generally, according to power system network structure and generators distribution, only one or two oscillation modes are joined together to dominate overall system dynamics. Furthermore, it is more common that for a studied system there is only one dominant oscillation mode which significantly influences overall system dynamics. Provided that oscillation shape of dominant mode is understood and oscillation data of these modes can be separated from original measurements, the remaining problem turns to be parameter estimation of single oscillation mode.

The main objective of this section is to present a monitoring and estimation scheme of power system interarea oscillation based on wide-area phasor measurements from the CampusWAMS. This scheme only focuses on the estimation of single dominant interarea oscillation mode and includes following steps: estimating the center frequency of single mode of interest, extracting the oscillation data from original phasor measurements, analyzing the oscillation shape, identifying the oscillation model, and estimating the oscillation parameters. Without any additional disturbance intentionally imposed to system, a second-order simplified oscillation model can be derived and identified based on the extracted oscillation data which just corresponds to the aimed single oscillation mode. The FFT filter technique is employed to separate the aimed single oscillation mode from other modes. More importantly, the auto-spectrum analysis is adopted to automatically and correctly determine the center frequency of targeted single oscillation mode, which is the key parameter in order for applying the FFT filter.

4.2.1 Center Frequency Estimation Using Auto-spectrum Analysis

Here, the center frequency means the real oscillation frequency of the aimed interarea mode. The auto-spectrum (i.e. PSD) analysis technique introduced in Section 3.4.2 is adopted to determine this center frequency from original phasor measurements of power system output variables.

The auto-spectrum is a frequency-domain measure of power contained in a signal over a range of frequencies. For a white noise signal, its theoretical auto-spectrum must be constant over entire frequency range because in theory a white noise signal is defined as having same power at any frequency. On the other hand, for a deterministic sinusoidal signal, its theoretical auto-spectrum must be zero over entire frequency range, but with one exception of having non-zero value at the frequency of that sinusoidal signal. Figure 4-5 illustrates these two ideal situations: the left column is a 0.5-Hz sinusoidal signal and its estimated auto-spectrum; the right column is a white noise signal and its estimated auto-spectrum. From this illustration, it can be noticed that the auto-spectrum of one signal containing one deterministic oscillation component must exhibit a steep peak at its oscillation frequency, whereas the auto-spectrum of signal containing no oscillation components obviously shows no clear peak.

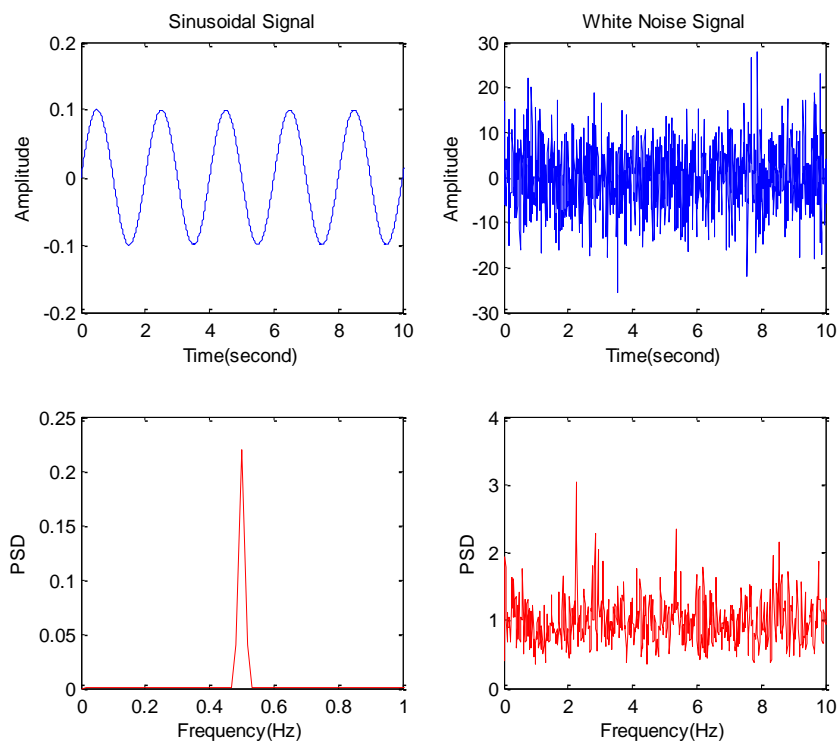


Figure 4-5. Estimated auto-spectrum of ideal signal

For a practical signal which contains both an oscillation component and many noise components, it can be inferred based on above observation that the estimated auto-spectrum of such a signal should be a mixture of auto-spectrum of its sub-components. As an example, Figure 4-6 displays the estimated auto-spectrum of the signal shown in Figure 4-4 (with dc component excluded). The single peak in the estimated auto-spectrum clearly indicates that there is one oscillation component buried in the original signal. The most important point is that the frequency at which the peak occurs in the auto-spectrum plot is exactly the center frequency of this oscillation component.

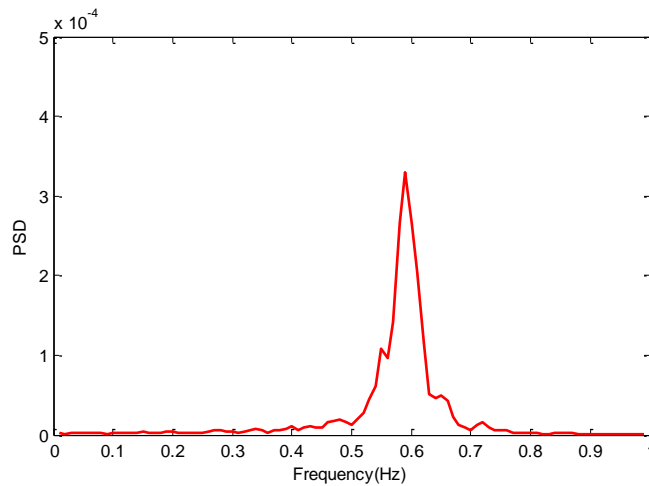


Figure 4-6. Estimated auto-spectrum of practical signal in Figure 4-4

Therefore, for a real power system, as long as the auto-spectrum of power variables can be estimated from phasor measurements, the center frequency of the concerned oscillation mode can be readily determined – the frequency location of the auto-spectrum peak is taken as the center frequency. (In point of fact, only the measurements of system output variables are available for the most cases in a real power system. The system outputs are apparently the results of the system inputs passing the system. Hence, the peak in the auto-spectrum of these output measurements is actually an indication of system inherent mode when two basic assumptions made in Section 3.3.2 are considered. (More detail will be explained in Section 5.3.)

- Estimation of Auto-spectrum

The true auto-spectrum of a deterministic signal can be theoretically derived using explicit mathematical expression. For a random signal, this is impossible. All output signals in a real power system are substantially random signals because they are responses to stochastic input signals, i.e. load variations to power system. What we have

are only measurement data for these output signals, such as bus voltage amplitude and angle, line current amplitude and angle, active power and reactive power, bus frequency and so on. Consequently, the auto-spectrum of a random signal has to be estimated from finite measurement data of this signal. The accuracy of estimation as well as the performance of various methods that are used for auto-spectrum estimation has to be evaluated in terms of statistics too.

Generally, various auto-spectrum estimation methods can be divided into two categories: non-parametric methods and parametric methods. Non-parametric methods, also called classical methods, make use of the transform relationship between auto-spectrum and autocorrelation function of a random process and directly estimate auto-spectrum using the definition in formula (3.17) or (3.19) from measurement data. Parametric methods, also called modern methods, firstly estimate a parametric time-series model which can describes the second-order statistics of the random process from measurement data and then obtain the auto-spectrum estimation from the model parameters. The introduction of each estimation method is not in the scope of the thesis and can be found in [20]-[21]. The method employed to estimate the auto-spectrum in the thesis is called Welch method, which is one of non-parametric methods.

Another name for Welch method is "modified average periodogram" method. The periodogram is defined in (3.17) as square-magnitude of DFT of a signal. It can be used to obtain the true auto-spectrum for a deterministic signal such as sinusoidal. For a random signal representing a random process, the periodogram is actually just a sample spectrum because it only processes a sample record of a random process. It has been proven that the periodogram (sample spectrum) is an inconsistent estimator of the true auto-spectrum. In specific, from the view of the statistical evaluation, although the mean of the sample spectrum will tend to the true auto-spectrum in the limit, the variance will not tend to zero in the limit of infinite data [20]. Figure 4-7 shows the estimated periodogram of the signal shown in Figure 4-4 (with dc component excluded). It is not as smooth as compared to the estimate auto-spectrum shown in Figure 4-6, and the peak that indicates the oscillation component is quite ambiguous.

The Welch method reduces the variance of the periodogram method by using averaging technique to obtain a smoother, consistent estimate of true auto-spectrum from a sample record of a random signal. This method first partitions a sample record of a random signal into successive equal-length segments and then averaging the periodogram of each segment. Each segment can be overlapped with adjacent one in order to get more segments from a finite-length sample record. Moreover, each segment can be windowed to reduce the spectrum leakage when DFT is performed on each segment. Figure 4-8 depicts the modified averaging concept of Welch method.

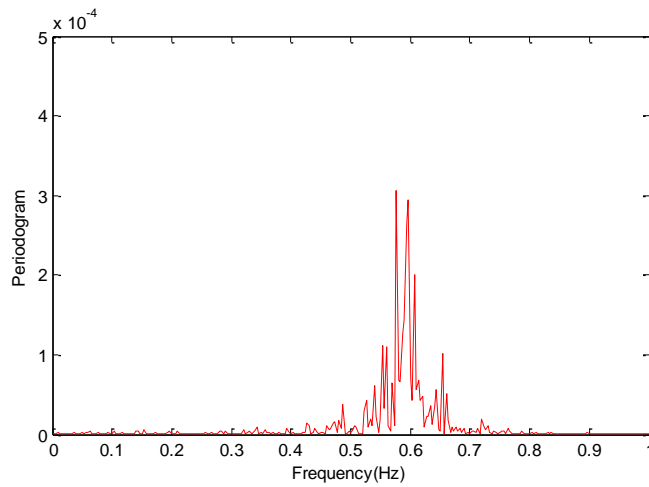


Figure 4-7. Estimated periodogram of practical signal in Figure 4-4

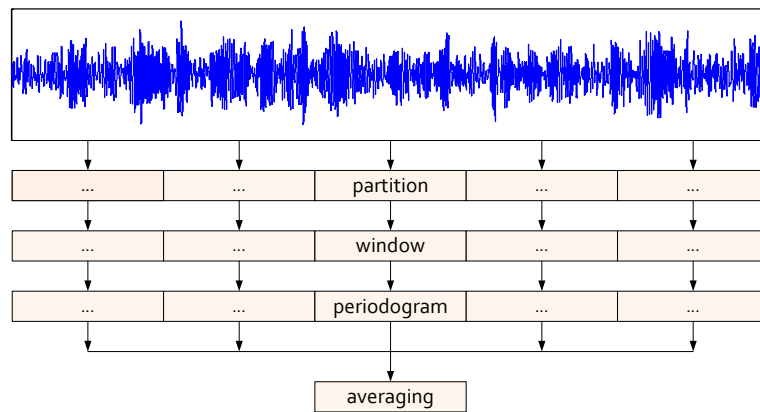


Figure 4-8. Concept of Welch method for auto-spectrum estimation

4.2.2 Oscillation Data Extraction Using FFT Filter

Many tools can be used to extract the oscillation data corresponding to the concerned interarea mode from original phasor measurements. These tools include general digital filter, discrete Wavelet transform (DWT) and fast Fourier transform (FFT). This work adopts FFT-based filter as data extracting tool.

Basically FFT filter is a kind of data filtering technique in pure frequency domain. Figure 4-9 illustrates the principle and process flow of FFT Filter: (a) compute the FFT of original data; (b) set to zero those components of the FFT which are beyond the designated frequency band; (c) compute the Inverse FFT of the remaining data. Thus the

extracted data only contains components within interested frequency range. One advantage of FFT filter is that the frequency range of extracted data can be easily controlled and adjusted.

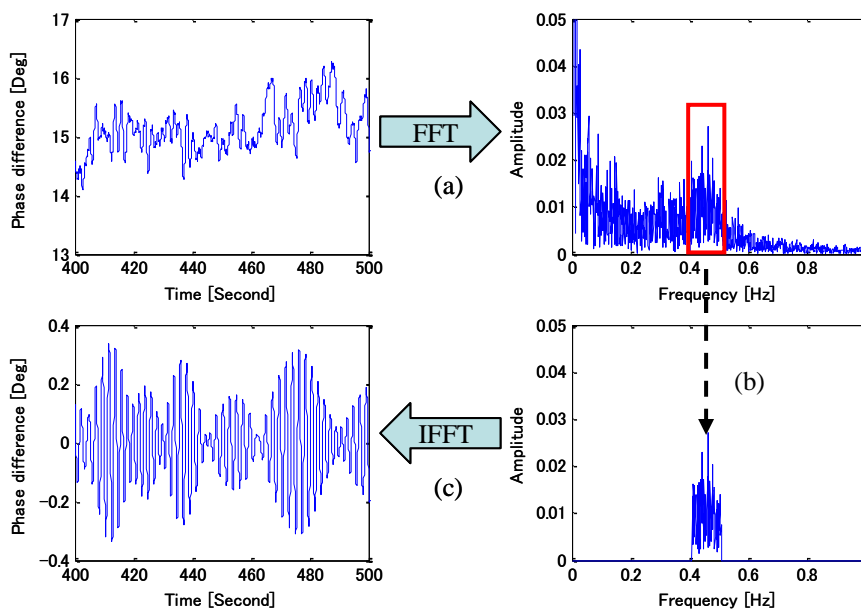


Figure 4-9. Principle of FFT filter

For FFT filter the frequency band of wanted data is one essential parameter to be designated. In order to correctly determine this frequency range for the concerned oscillation mode, the center frequency of the mode is firstly determined. As proposed in Section 4.2.1, it is reasonable to consider the frequency value corresponding to the peak in auto-spectrum plot as the center frequency of the concerned oscillation mode. After getting f_0 , the frequency band of FFT filter is set equal to $f_0 \pm \Delta f$, where Δf is a small value such as 0.05Hz. The suitable value of Δf for different system can be determined by trial and error. Too big Δf should be avoided in order not to accidentally include the oscillation data of the neighboring modes. Based on tests, the value of Δf ranging from 0.05 to 0.1 is appropriate and suggested in this work when there are no too-close neighboring modes. It should be pointed that FFT filter here is utilized to extract oscillation data corresponding to one oscillation mode which is extractable. Under some special circumstances e.g. when two oscillation modes are too close in auto-spectrum results to be difficult to separate, FFT filter may produce unsatisfactory extracting results or cause unexpected error.

Figure 4-10 lists the complete oscillation data extraction process based on the FFT filter and auto-spectrum analysis.

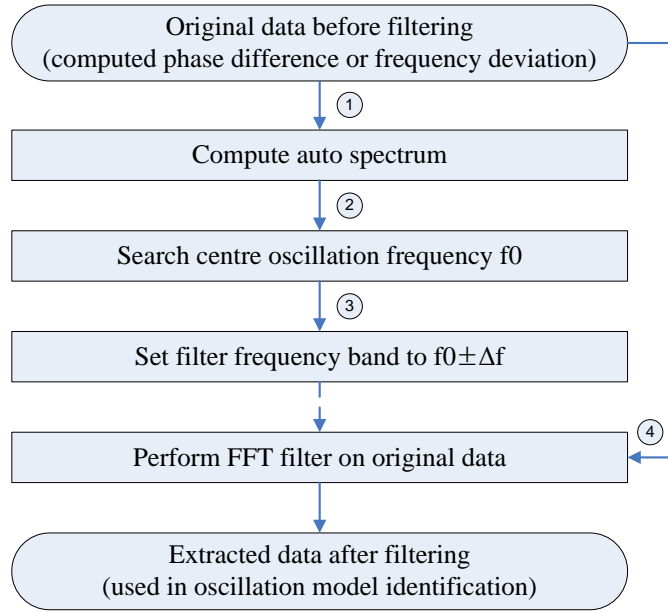


Figure 4-10. Complete oscillation data extraction process

4.2.3 Simplified Model Identification for Single Oscillation Mode

Unlike Prony method or AR-family models for which all oscillation modes and noise components have to be modeled at the same time by a high-order model, a second-order model is enough to describe the dynamic when only single oscillation mode is concerned.

Firstly, the linearized equations for small-signal stability analysis based on swing equation for a single machine infinite bus (SMIB) system can be obtained as follows:

$$\begin{cases} \dot{\delta} = \Delta\omega \\ \dot{\omega} = \alpha_1 \Delta\delta + \alpha_2 \Delta\omega \end{cases} \quad (4.6)$$

Then a second order oscillation model using two locations data for one oscillation mode can be represented in the following form:

$$\begin{bmatrix} \Delta\dot{\delta}_{12} \\ \Delta\dot{\omega}_{12} \end{bmatrix} = \begin{bmatrix} 0 & 1 \\ \alpha_1 & \alpha_2 \end{bmatrix} \begin{bmatrix} \Delta\delta_{12} \\ \Delta\omega_{12} \end{bmatrix} = A \cdot \begin{bmatrix} \Delta\delta_{12} \\ \Delta\omega_{12} \end{bmatrix} \quad (4.7)$$

In model (4.7), $\Delta\delta_{12}$ is oscillation data extracted by FFT filter from phase difference signals between two selected locations. $\Delta\omega_{12}$ is differential of $\Delta\delta_{12}$. All these

data can be computed and then extracted from phasor measurements of power system.

The state matrix A of model (4.7) can be estimated using linear least square approximation method introduced in Section 3.4.2. The quantitative characteristic of extracted oscillation mode can then be fully described by a pair of conjugate eigenvalues of state matrix A . The real part and imaginary part of eigenvalues represent the damping coefficient and oscillation frequency respectively.

Since power system electromechanical oscillation mode primarily involves the dynamics of generator rotor angle, the simplified oscillation model derived from rotor swing equation is capable of clearly describing the dynamics of power oscillation. Moreover, the proposed model is a kind of output-only-based model without any stimulating input signal to power system.

The proposed estimation scheme can be summarized as Figure 4-11.

For the proposed method only the phasor measurements of the system outputs are necessary and all calculation steps can be performed in an automatic manner. It means the proposed method would be applicable to both off-line analysis and online application.

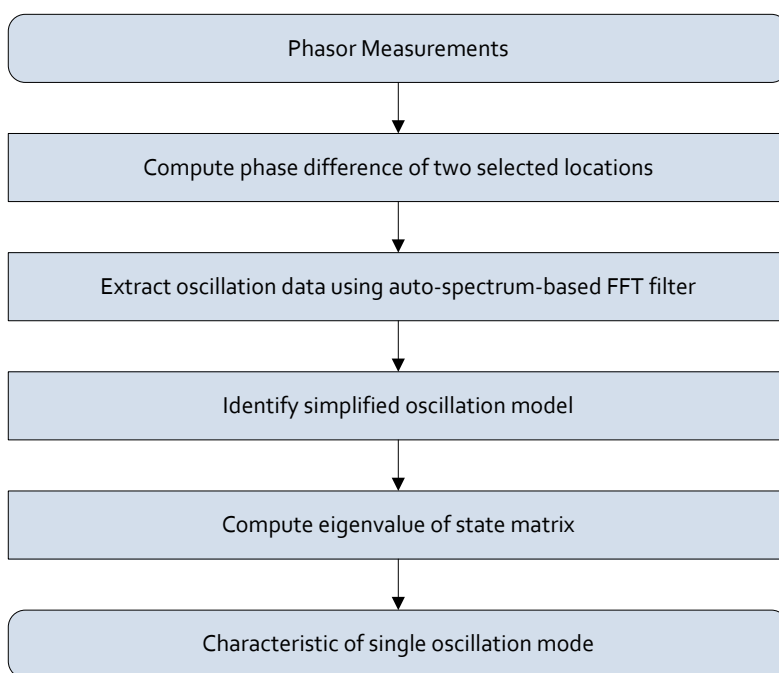


Figure 4-11. Flowchart of proposed estimation scheme

4.3 Simulation Study

In this section, the angle difference between Bus1 and Bus 11 for 600-seconds shown in Figure 4-4 is used to estimate the eigen-properties of the concerned interarea oscillation Mode 1 (in Table 4-2). For comparison, 200 seconds and 300 seconds data within different window are respectively used for center frequency and eigenvalue estimation. The estimated results are summarized in Table 4-5. Compared with the estimated results in Table 4-3 and Table 4-4 using AR method, it is obvious that the proposed method produces better and very good estimation of true eigen-properties for the concerned interarea mode. The auto-spectrum analysis successfully estimates the center frequency of oscillation mode from original phasor measurements.

Table 4-5. Estimated results using proposed method

Data Window	Eigenvalue	Center Frequency	
200s	0s ~ 200s	$-0.1381 \pm 3.7094i$	0.61 Hz
	200s ~ 400s	$-0.1366 \pm 3.6890i$	0.59 Hz
	400s ~ 600s	$-0.1366 \pm 3.6888i$	0.59 Hz
300s	0s ~ 300s	$-0.1375 \pm 3.7011i$	0.59 Hz
	200s ~ 500s	$-0.1374 \pm 3.6990i$	0.59 Hz
	300s ~ 600s	$-0.1372 \pm 3.6954i$	0.59 Hz

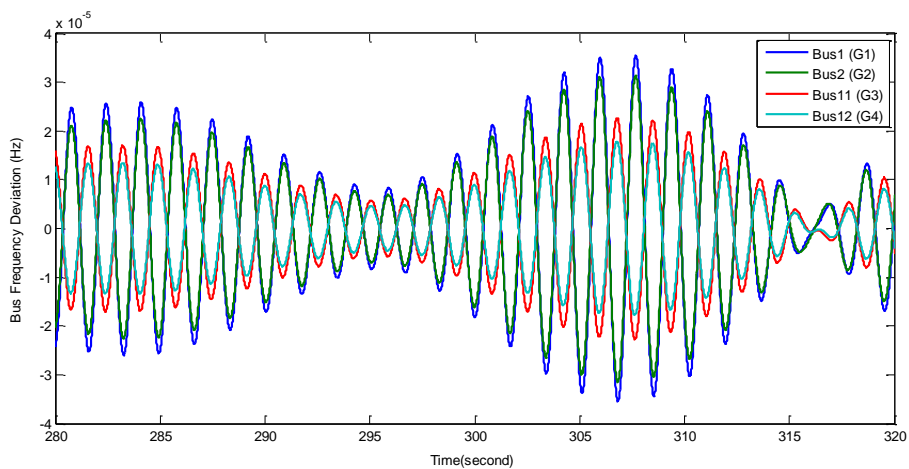


Figure 4-12. Extract oscillation data from bus frequency deviation

Moreover, Figure 4-12 shows waveform of oscillation data corresponding to the dominant interarea oscillation Mode 1 around 0.6-Hz for 2A4G test system, which are extracted from frequency deviation signals of four generators' terminal buses by the auto-spectrum-based FFT filter. Based on this plot of extracted oscillation data, it can be concluded that for 2A4G test system, the shape of dominant interarea Mode 1 is that the generators in Area 1 (G1&G2) oscillates against the generators in Area 2 (G3&G4) in anti-phase manner, while the generators in each area oscillates in phase together.

4.4 Evaluation Using CampusWAMS Measurements

Based on phasor measurements from the CampusWAMS, some estimation results for Western Japan 60-Hz power system and Thailand power system by using the proposed estimation scheme are shown in this section. For the following analysis, 200 seconds phasor data from 50min in every hour is used. The frequency band of FFT filter is set to $f_0 \pm 0.05$ Hz.

Figure 4-13 shows waveform of oscillation data corresponding to dominant interarea mode of Western Japan 60-Hz power system around 0.4-Hz, which are extracted from phase difference signals between Miyazaki and Tokushima (i.e. lower-end group vs. center group), and between Nagoya and Tokushima (i.e. upper-end group vs. center group). For PMU group information, see Table 2-1. Figure 4-14 shows waveform of oscillation data corresponding to about 0.4-Hz dominant interarea mode, which are extracted from frequency deviation signals of Miyazaki, Tokushima and Nagoya (lower-end group, center group, and upper-end group).

Based on these plots of extracted oscillation data, it can be concluded that for Western Japan 60-Hz power system, the shape of dominant interarea mode is that the generators of two end groups oscillate against each other in anti-phase manner with the generators of center group as center oscillation point.

Figure 4-15 shows waveform of oscillation data corresponding to dominant interarea mode of Thailand power system around 0.5-Hz, which are extracted from phase difference signals between Songkla and Chiang Mai (center part vs. north part), and between Bangkok and Chiang Mai (south part vs. north part). These plots indicate that for Thailand power system, the shape of dominant oscillation mode is that the generators of south part oscillate against the generators of center part and north part in anti-phase manner.

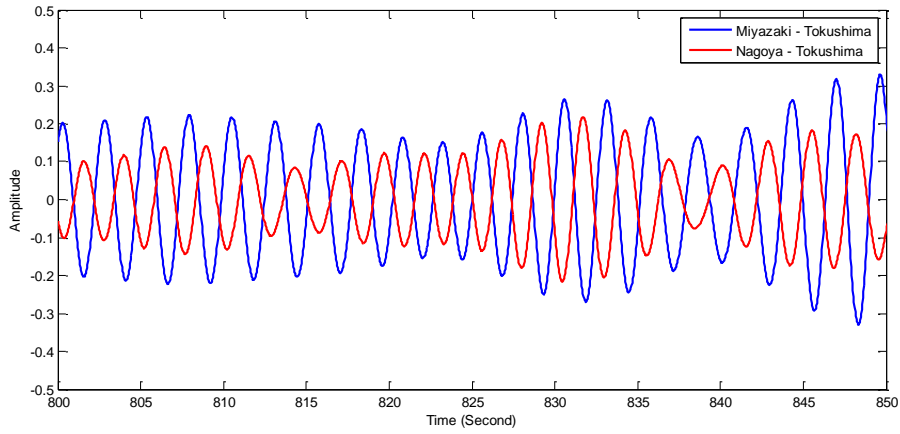


Figure 4-13. Extracted oscillation data from bus phase difference

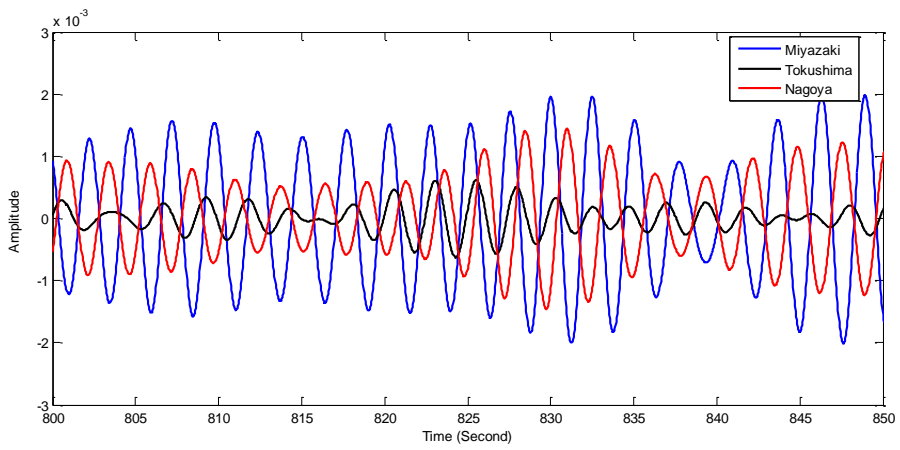


Figure 4-14. Extracted oscillation data from bus frequency deviation

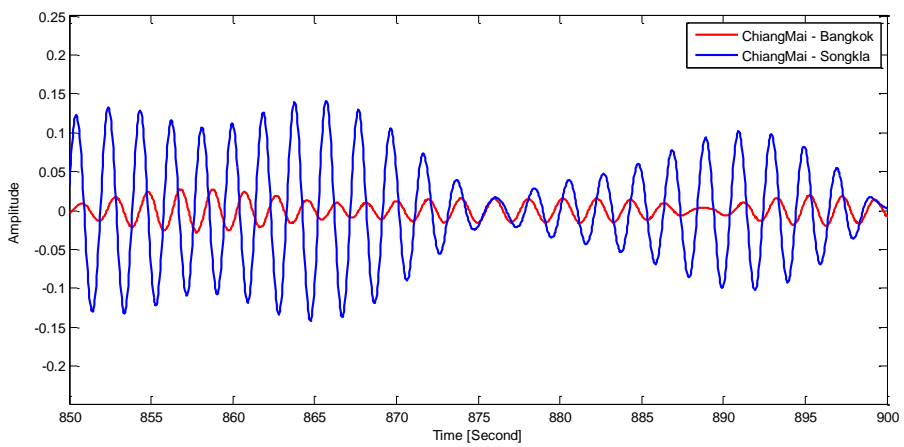


Figure 4-15. Extracted oscillation data from bus phase difference

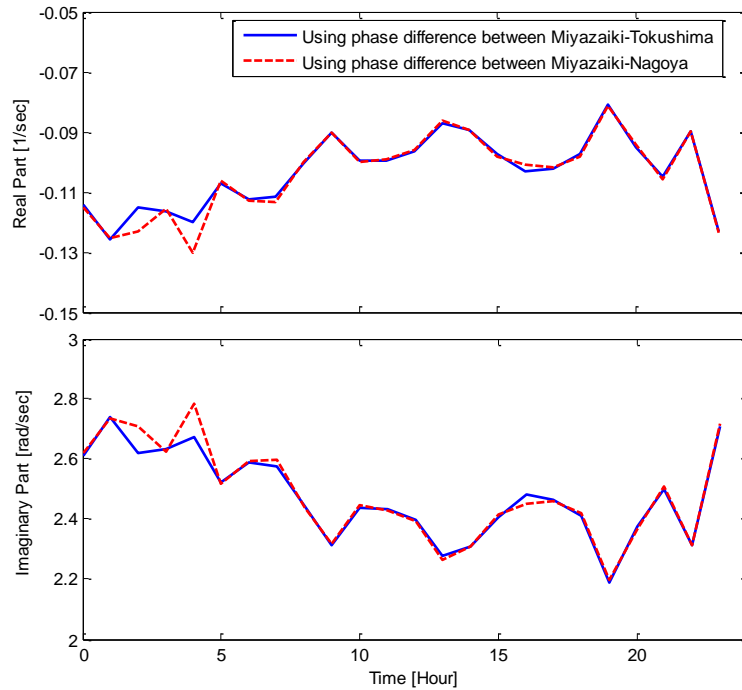


Figure 4-16. Estimated eigenvalues of one day for Western Japan power system

Figure 4-16 shows the estimated eigenvalues of dominant oscillation mode of Western Japan 60-Hz power system in 2007/8/18. The change of eigenvalues in the whole day shows that the system small-signal stability is changing with the load demand variation, e.g. from afternoon to evening when load demand gets increasing the system is tending to become unstable.

Figure 4-17 shows the eigenvalues of dominant oscillation mode of Thailand power system estimated from phase difference between Songkla-Bangkok for one hot week (2006/03/27 to 2007/04/02) and one moderate week (2005/10/31 to 2005/11/06). According to these figures, the change trend of system small-signal stability in the difference season can be easily observed. For example, during hot season power system is tending to become unstable because of increasing load demand.

4.5 Summary

A single-mode-oriented estimation scheme of interarea oscillation mode is proposed based on wide-area phasor measurements. The scheme includes center frequency determination using auto-spectrum analysis, oscillation data extraction using FFT filter, oscillation model identification based on swing equations, and oscillation parameters estimation by linear least squares.

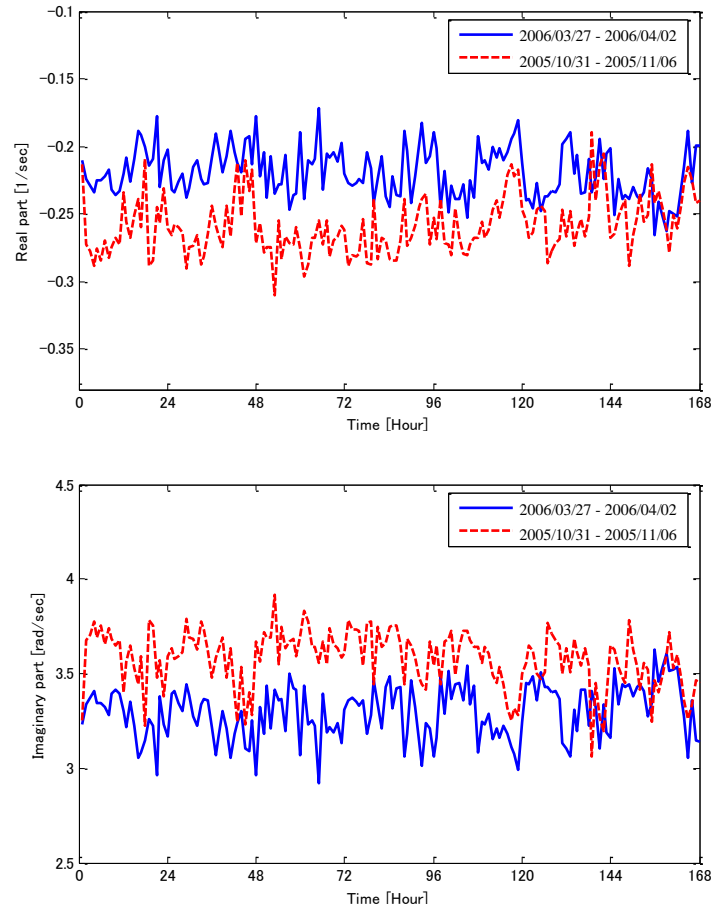


Figure 4-17. Estimated eigenvalues of one week for Thailand power system

Single-mode-oriented estimation allows focusing on single oscillation mode that dominates the system dynamics. The key point of applying this scheme is to determine the center frequency of dominant mode. Based on the random signal processing theory, auto-spectrum analysis is successfully employed to accurately and automatically determine the center frequency. Moreover, the auto-spectrum-based FFT filter can correctly extract oscillation data that corresponds to a single mode of interest. Simulation results compared to multi-mode-oriented methods show the effectiveness of the proposed method.

The proposed scheme is also evaluated by using phasor measurement from the CampusWAMS for Western Japan 60-Hz power system and Thailand power system.

Chapter 5.

Participation Weight Estimation in Power Oscillation Based on Phasor Measurements and Auto-spectrum Analysis

5.1 Introduction

Currently, one key application resulting from SPM is related to analyzing the interarea power oscillations. For example, without any a priori knowledge of the power system, an FFT (fast Fourier transform) analysis of the real-time SPM data stream can quickly discover the interarea oscillations that are not well-damped [47].

In order to achieve proper monitoring and effective control on the interarea power oscillations, the following properties must be estimated after discovering the oscillation modes:

- the relative participation of the generators in each mode;
- the distribution of each mode among the generators;
- and the frequency and damping of each mode.

In a traditional SCADA data-based EMS (energy management system) application, these properties are calculated by conducting an eigen-analysis of a small-signal system model. An important advantage of this model-based approach is that all properties of the concerned modes, such as the participation factors, the mode shapes, the frequencies and dampings, can be obtained at the same time. The main disadvantages consist of the complexity of model construction and the difficulty in eigenvalue calculation. Moreover, entire process has to be repeated when the operating condition is changed.

On the other hand, these properties can be estimated using a measurement-based approach, for example, by directly processing the SPM data without dependence on a complex system model. Such measurement-based approaches can produce fast, timely and dynamic estimate of the real-time characteristics of interarea modes. Some SPM-based methods have been proposed in recent publications for estimating the frequencies and dampings of interarea oscillation modes [40][41] and designing an optimal PSS (power system stabilizer) [49]. Ref. [50] proposed a signal-processing method to estimate mode-shape properties of interarea oscillation modes using SPM. In this chapter, an approach to estimate the relative participation of a generator in one interarea oscillation mode based on SPM and auto-spectrum analysis is proposed.

In a large power system, it is important to quantify the role of each generator in each mode. Traditionally, this is represented using a dimensionless quantity called participation factor which is calculated by combining the right and left eigenvector. The participation factor was initially proposed in [48] and used as a effective measure to select relevant states for selective modal analysis. Subsequently, it became a useful tool for PSS placement and design. For example, the generators with high participation factors are normally candidates for PSS placement [51]. The state variable with the highest participation factor can be an appropriate choice for the feedback signal of PSS.

In this chapter, a quantity called *participation weight* is estimated based on SPM to indicate the relative participation of a generator in each mode of interest. It is defined and calculated based on the auto-spectrum analysis of system response signal, assuming power system is continuously subjected to small random load variations under normal operating condition. For a large power system, load variations in a short period are unpredictable and can be assumed as random excitation signal to power system. Consequently, the response signals of generator, such as generator angle and speed, are also random. Based on this underlying assumption, correlation analysis of input-output measurements in time domain, or spectral analysis in frequency domain, can be conducted to estimate the characteristics of power system.

5.2 Participation Factor from Traditional Modal Analysis

For traditional modal analysis, the power system dynamic model is firstly linearized around a normal operating point to obtain a small-signal model [7]. As introduced in Section 3.2, a small-signal model is usually in the state-space form as:

$$\begin{cases} \Delta \dot{x} = A\Delta x + B\Delta u \\ \Delta y = C\Delta x + D\Delta u \end{cases} \quad (5.1)$$

where A , B , C and D are the state matrix, input matrix, output matrix and feed-forward matrix respectively. Modal analysis, also called eigen-analysis, focuses on the state matrix A and its eigen-properties. For example, a pair of conjugate complex eigenvalues of state matrix A represents an oscillatory mode. The real part of eigenvalue gives the damping, and the imaginary part gives the frequency of oscillation. A negative real part represents a damped oscillation whereas a positive real part represents oscillation of increasing amplitude. In addition to the damping and frequency of each oscillation mode, power system operators still concern which generators and to what extent they are involved in each oscillation mode, and how these involved generators oscillate in the corresponding mode. All the information can be found by computing mode shape and participation factor based on the eigenvectors.

For a state matrix, like A in Equation (5.1), an eigenvector is defined as any vector that corresponds to i_{th} complex eigenvalue, like λ_i , in such a way that:

$$Av_i = \lambda_i v_i \quad \text{or} \quad w_i A = \lambda_i w_i \quad (5.2)$$

Here, the vector v_i is the right eigenvector of state matrix A , which corresponds to the eigenvalue λ_i ; and the vector w_i is the left eigenvector of state matrix A . All the right eigenvectors and left eigenvectors corresponding to all distinct eigenvalues of matrix A constitute two modal matrixes V and W as Equation (5.3). The significance of modal matrixes is that, with the help of modal matrixes, the original physical state variables Δx can be transformed into modal variables Δz , and vice versa.

$$\Delta x = V \Delta z \quad \text{or} \quad \Delta z = W \Delta x \quad (5.3)$$

Thus, the response of each state (Δx_i) is given by a linear combination of all modes (Δz) corresponding to all eigenvalues of the state matrix. By (5.3), it can be found that right eigenvector gives the mode shape, i.e., the relative activity of state variables when a particular mode is excited. The components of the right eigenvectors measure the contribution of the state variables to the corresponding modes:

$$\Delta x_j = \sum_j v_{ji} \alpha_i e^{\lambda_i t} \quad (5.4)$$

The magnitudes of the elements of v_{ji} gives the extents of the activities of the j_{th} state variables in the i_{th} mode, and the angles of the elements gives phase displacements of the state variables with regard to the mode.

On the other hand, the left eigenvector weigh the initial conditions on the corresponding modes:

$$\Delta\alpha_i = [w_i^T \Delta x(0)] \quad (5.5)$$

However, the right eigenvectors are not really appropriate for measuring the participation of a state variable in a mode, since they are dimension dependent. A non-dimensional measure of the participation of the i_{th} mode in the j_{th} state variables can be given by the product of the j_{th} component of right and left eigenvectors corresponding to the i_{th} mode, which is known as the *participation factor* [7]:

$$p_{ji} = w_{ji} v_{ji} \quad (5.6)$$

The mode shape and participation factor provide very useful information for damping controller design. For example, the participation factor is an important index in control design as it is used in identifying the participation of key generator in an interarea oscillation mode of interest. The generators with high participation factor are normally candidates for damping controller. The state variables with the highest participation factor can be an appropriate choice for the feedback signal of designed controller.

5.3 Input-Output Relationship for Constant-parameter Linear System

As introduced in Section 3.3.1, for any measurement-based approach used to estimate the unknown system characteristics, it is assumed that only input and output variables to the system are known while no other information about system itself is available. This implies that the system characteristics have to be estimated by studying the input, the output, as well as the relationship between them. In order to discover a quantity from measurements of the output and/or input variables to represent the relative participation of a generator in one oscillation mode, the spectrum-based input-output relationship for a constant-parameter linear system when subjected to a random input is developed in this section [17].

Figure 5-1 illustrates a black-box system with noise input signal $u(t)$ and output signal $y(t)$. It is important to recall two fundamental assumptions that are made in Section 3.3.2: the applied input is assumed to be a stationary random white noise signal; and the considered system is assumed to be a constant-parameter linear system. It is worth noting that a constant-parameter linear system does not cause any frequency translation but only modify the amplitude and/or phase of the applied input.

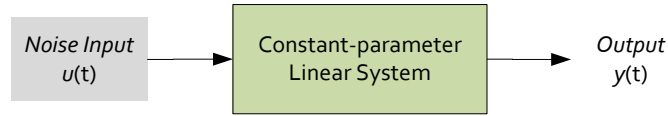


Figure 5-1. A black-box system

5.3.1 System Frequency Response Function

The frequency response function $H(f)$ of a system is defined as the Fourier transform of $h(t)$ which is the system time response function to a unit impulse input. Let $U(f)$ be the Fourier transform of an arbitrary input $u(t)$, then the Fourier transform of resulting output $y(t)$ will be

$$Y(f) = H(f) \cdot U(f) \quad (5.7)$$

Generally, $H(f)$ is a complex function of frequency and can be written in complex polar notation as follows:

$$H(f) = |H(f)| \cdot e^{-j\phi(f)} \quad (5.8)$$

where the norm value $|H(f)|$ is called the system gain factor and the associated phase angle $\phi(f)$ is called the system phase factor.

One remarkable characteristic of gain factor $|H(f)|$ is that it shows peaks at some frequencies. These peaks actually represent the oscillation modes that the system contains. There are two important properties associated with each peak: the frequency where it happens and the amplitude it reaches. Specifically, the frequency of each peak indicates the oscillating frequency of each corresponding mode. This property has been utilized to help in determining the center frequency of the dominant interarea mode for extracting oscillation data by FFT filter in Section 4.2.1. The amplitude of each peak quantifies the system's ability to amplify each corresponding mode. In theory, these peaks as well as their properties can be identified and estimated by analyzing the measurements of input and output even if the knowledge of the system is not available.

5.3.2 Input-Output Relationship

Now the input-output relationship in Figure 5-1 can be derived in terms of system frequency response function and auto-spectrum function of input and output.

The output $y(t)$ is given by

$$y(t) = \int_0^{\infty} h(\tau)u(t - \tau) d\tau \quad (5.9)$$

The autocorrelation function of $y(t)$ is given by

$$R_{yy}(t) = \iint_0^{\infty} h(\xi)h(\eta)R_{uu}(\tau + \xi - \eta) d\xi d\eta \quad (5.10)$$

Taking Fourier transformation on both side of Equation (5.10) yields

$$S_{yy}(f) = |H(f)|^2 \cdot S_{uu}(f) \quad (5.11)$$

where $S_{yy}(f)$ and $S_{uu}(f)$ are the auto-spectrum of output and input respectively.

From Equation (5.11) and the characteristic of $|H(f)|$ stated in previous subsection, the following important conclusions can be drawn.

- The gain factor $|H(f)|$ can be explicitly estimated only if both input $u(t)$ and output $y(t)$ are measureable.
- $S_{uu}(f)$ is actually a constant auto-spectrum over all frequencies because input $u(t)$ is a stationary white noise signal. Suppose $S_{uu}(f) = W$, then Equation (5.11) becomes

$$S_{yy}(f) = |H(f)|^2 \cdot W \quad (5.12)$$

Equation (5.12) indicates that $S_{yy}(f)$ must have the same number of peaks at the same frequencies as of $|H(f)|$. The amplitude of each peak in $S_{yy}(f)$ is the scaled square of the amplitude of corresponding peak in $|H(f)|$.

5.4 Participation Weight from Phasor Measurements

A large power system is substantially a complex non-linear dynamical system, especially under heavy load condition. Under normal operating condition, the system is continuously subjected to small variations in loads. All running generators in the system make responses to these variations based on various control devices to maintain synchronism. From this point of view, the small load variations can be regarded as input signal and the variations in a generator's response, such as generator angle or speed, can be regarded as output signal.

For a large power system, as long as the load variations are sufficiently small, it

can be linearized around every equilibrium operation point. In addition, these small variations in loads are unpredictable and can be reasonably regarded as stationary white noise. Consequently, the conclusions drawn in Section 5.3.2 can be applied to a real power system.

5.4.1 Derivation of Participation Weight

Multiple generators which have the same mode at one frequency and are subjected to the same white noise load variations are considered. Equation (5.12) holds for each generator, which means that for all generators a peak in the auto-spectrum of the output measurement can be observed at same frequency but probably with different amplitude. Accordingly, it is reasonable to regard the amplitude of this peak, for each generator, as a measure of participation level in the corresponding mode.

The remaining issue is that the input signal, i.e. the small load variations, is not measurable. The constant auto-spectrum of the input, W , is never known. However, a relative comparison of the peak amplitude can be made among multiple generators through normalization so that the effect of the unmeasurable input can be eliminated.

Based on preceding analysis, the amplitude of the peak that occurs in the auto-spectrum function of one generator's output measurements is directly defined as *participation weight*, a measure which can be employed to indicate the relative participation of multiple generators in one oscillation mode.

5.4.2 Estimation of Participation Weight

The procedure for estimating participation weights of multiple generators based on SPM is described as follows:

- 1) Select appropriate measured power quantity.

In theory, the measurements of generator angle or speed should be used; but, for most PMUs (phasor measurement units), these signals cannot be directly measured. In practical, the generator bus frequency, which can be calculated from the bus voltage phasor, is a satisfactory approximation to generator speed signal. A SPM of the bus voltage can be easily obtained from a PMU.

- 2) Determine the data length of measurements.

Two requirements have to be considered for the data length determination. On the one hand, enough data points are required to obtain a good estimate of the auto-spectrum. The number of data points is practically determined by the data length of

original measurements and the re-sampling frequency. Typically, several minutes of data with appropriate re-sampling are required. On the other hand, the data length should not be too long; otherwise, the assumption of stationarity of white noise input may not be valid.

- 3) Estimate the auto-spectrum for all generators.

There are two categories of spectrum estimation algorithms: non-parametric and parametric methods. In this thesis, one of non-parametric methods, i.e. the modified average periodogram method introduced in Section 4.2.1 is selected to estimate auto-spectrum. An implementation of this method is included in Matlab Signal Processing Toolbox as function *pwelch* [66]. Moreover, in light of a general knowledge that most of interarea oscillation modes are less than 1-Hz, it is preferable to conduct a pre-filtering before the spectrum estimation to filter out unnecessary frequency components higher than, for example, 2-Hz to reduce some computation burden.

- 4) Identify interarea oscillation modes and the frequency of each mode.
- 5) Obtain the amplitudes of the peak corresponding to each single mode of interest for all generators and normalize them.

5.4.3 Comparison with Participation Factor

Technically, there are some apparent differences between participation factor and participation weight.

The participation factor is computed from model-based modal analysis, which has great dependence on a complex system model; whereas the participation weight is directly defined based on measurements and estimated from synchronized phasor measurements. The participation weight is not a direct estimate of the traditional participator factor but serve as a similar measure as the traditional participation factor to estimate the relative participation level of generators in one concerned oscillation mode. As an indispensable property of any oscillation mode, it is significant to extract the information about mode participation from SPM and subsequently integrate it into other existing SPM-based applications.

More importantly, the participation weight is not only a measurement-only-based quantity, but also an output-only-based quantity. Without knowledge of load variations, the participation weight is estimated by only processing the measurements of the system output signal.

In practice, the participation weight estimation can be online updated manually at the specified time or automatically by the specified period using latest measurements.

From this point of view, the participation weight can be seen as an online dynamic index which can quickly adapt to the change of system operating condition.

5.5 Simulation Study

To demonstrate the estimation of participation weight using the proposed method and to verify the effectiveness of participation weight, two simulation example systems are employed in this section. The simulation tool used is Dymola 6.1 with power system component library called ObjectStab [68].

5.5.1 Western Japan 10-Machine System Study

The diagram of western Japan 10-machine test system is shown in Figure 5-2. It is developed as a standard model of western Japan 60-Hz power system. Detailed information is presented in [52]. The system consists of 10 equivalent generators that connected from bus 21 to 30 respectively, and 17 load buses. In simulation, each generator is represented using a 5-th order transient model with an exciter and a turbine governor. The block diagram of the exciter is shown in Figure 5-3. PMU is assumed to be installed at the terminal bus of every generator.

The loads setting for daytime operation is simulated for this system [52]. In order to excite the system in simulation, one scenario that two hypothetical small variations in active loads are added to Bus 1 and Bus 9 is simulated. Two signals are both stationary white noise but uncorrelated with each other. The system's responses can be observed from measurements at buses where PMUs are installed.

As explained in Section 5.4.2, the bus frequency signal for each generator, which is directly calculated from the bus voltage phasor measurements, is selected for estimating participation weight. As for the data length of measurements, 5 minutes is used. Based on the simulation experiments, it is found that 5-min measurements with 0.02s resampling interval can give satisfactory estimation of auto-spectrum. Figure 5-4 shows the resulting random variation in phase angle at Bus 21 for a 5-min simulation example.

Before estimating the auto-spectrum, the frequency components above 2-Hz are filtered out from the measurements. Figure 5-5 shows the results of the auto-spectrum estimation for all 10 generators. From Figure 5-5, two interarea oscillation modes can be clearly identified around 0.4-Hz and 0.68-Hz because two peaks can be observed at those frequencies.

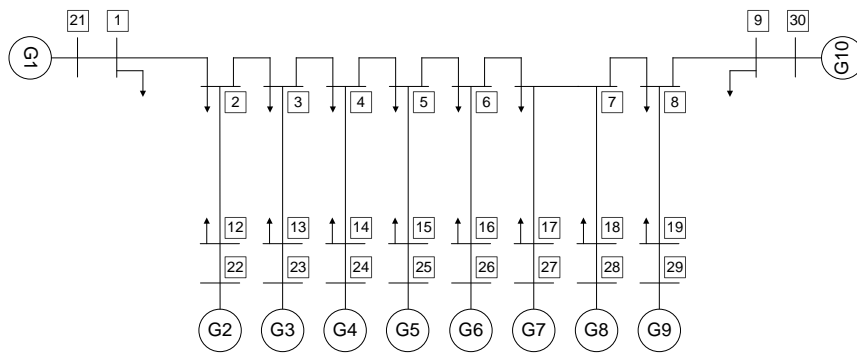


Figure 5-2. Western Japan 10-machine (West-10) example system

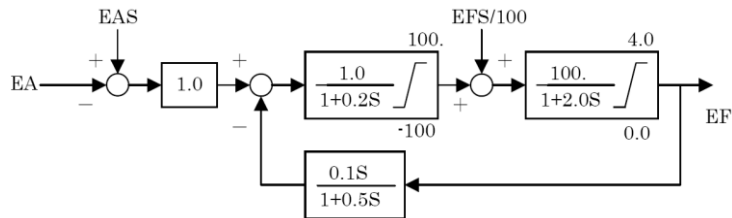


Figure 5-3. Exciter model for West10 system

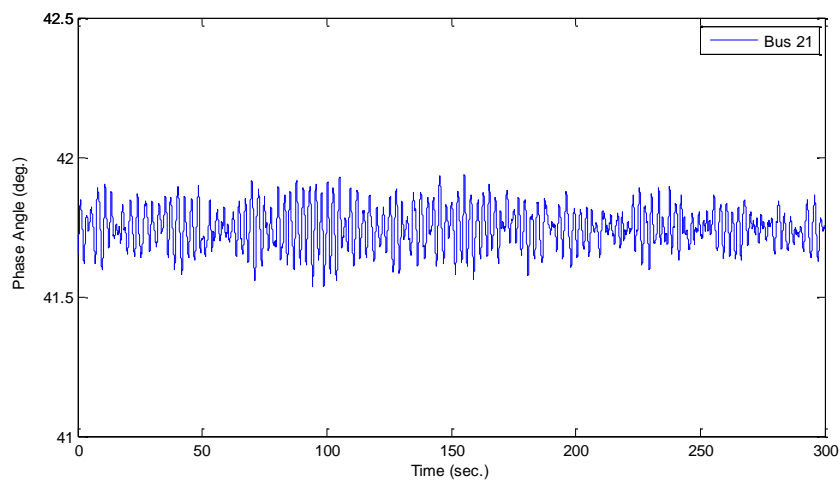


Figure 5-4. Bus 21 phase angle under random load excitation

Since this is a simulation example, the interarea oscillation modes for this test system can also be identified through modal analysis using simulation tool. Table 5-1 shows the identified modes by conducting a linear eigen-analysis of the system's small-signal model under simulated operating condition. As seen in Table 5-1 and Figure 5-5,

the peaks in the auto-spectrum accurately estimate the frequency of interarea oscillation modes.

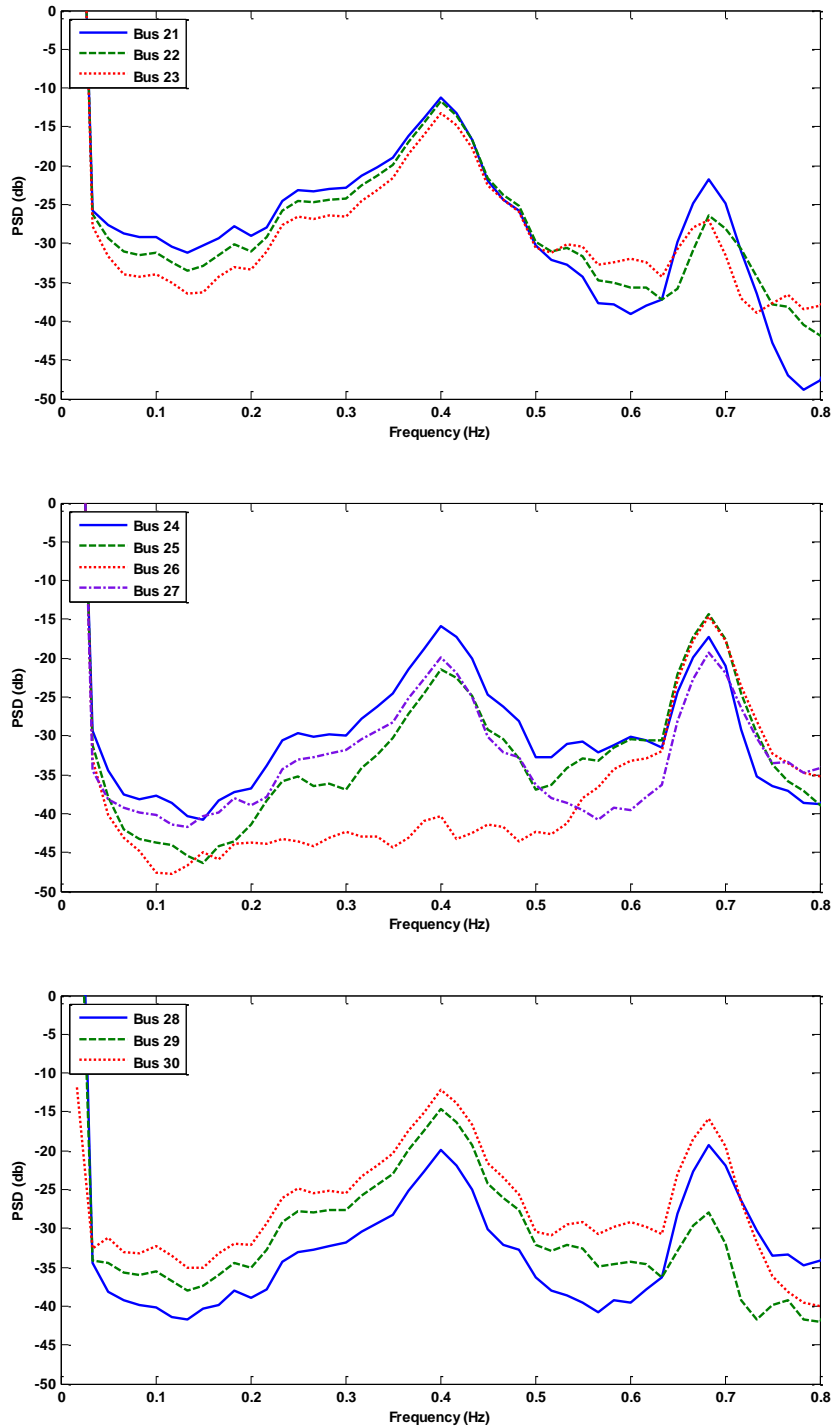


Figure 5-5. Auto-spectrum estimation for West-10 system

Table 5-1. Interarea modes of West-10 system

Mode	Frequency	Damping Ratio
1	0.409 Hz	4.94 %
2	0.693 Hz	0.92 %

Based on the estimated auto-spectrum results, the participation weight for 10 generators in two interarea modes are normalized and summarized in Figure 5-6. For near 0.4-Hz mode, generators 1, 2, 3 on the left side of example system and generators 9, 10 on the right side of example system have significant participation. For near 0.68-Hz mode, generators 5, 6 at center of example system and generators 10 on the right side of example system have significant participation.

For comparison, the normalized participation factor of 10 generators' rotor angle in these two interarea modes are calculated by conducting modal analysis. The results are shown in Figure 5-7. It can be observed that participation weight indicates coincident information with participation factor calculated from modal analysis.

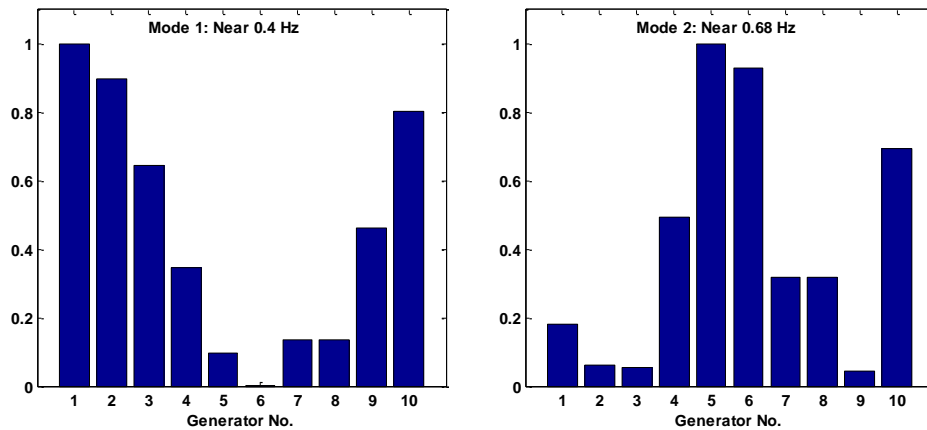


Figure 5-6. Participation weight for West-10 system

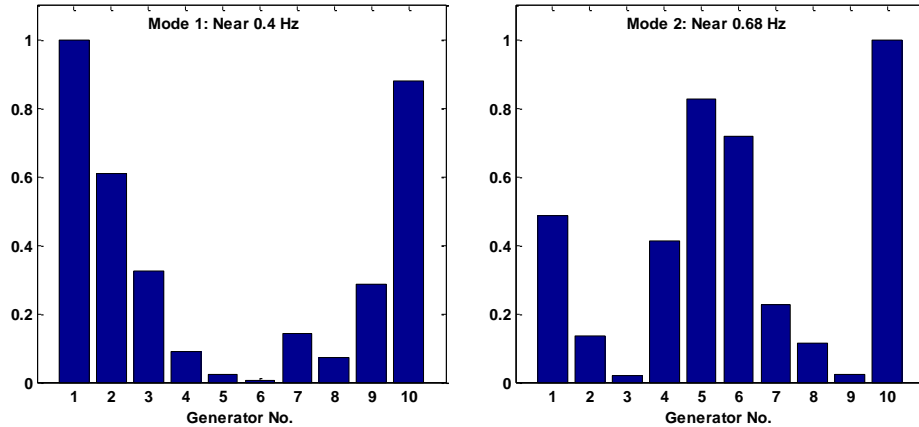


Figure 5-7. Participation factor for West-10 system

5.5.2 Western Japan 30-Machine System Study

Second test system is a 30-machine simulation model of western Japan 60-Hz power system. Network diagram and all other detailed information are also presented in [52]. The system consists of 30 generators and 115 buses. Each generator is represented using a 5-th order transient model equipped with a voltage regulator, and a turbine governor. The model of exciter and turbine governor are identical to previous example. PMU is assumed to be installed at terminal bus of every generator. Similarly, for the following examples, small stationary white noise signals are added to excite the system under simulated operating condition. The parameter settings for the participation weight estimation are same as in the first example. Table 5-2 shows the identified interarea modes with first three lowest frequencies by eigen-analysis under simulated operating condition. Figure 5-8 shows the results of the auto-spectrum estimation for four selected generators. The significant peaks in the auto-spectrum around 0.32-Hz, 0.61-Hz and 0.63-Hz clearly indicate that there are three interarea oscillation modes at those frequencies.

Table 5-2. Interarea modes of West-30 system

Mode	Frequency	Damping Ratio
1	0.322 Hz	5.28 %
2	0.657 Hz	0.15 %
3	0.658 Hz	0.18 %

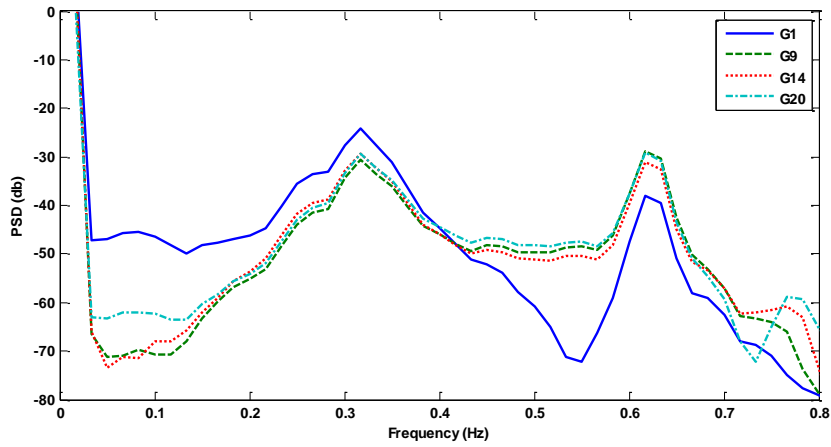


Figure 5-8. Auto-spectrum estimation for West-30 system

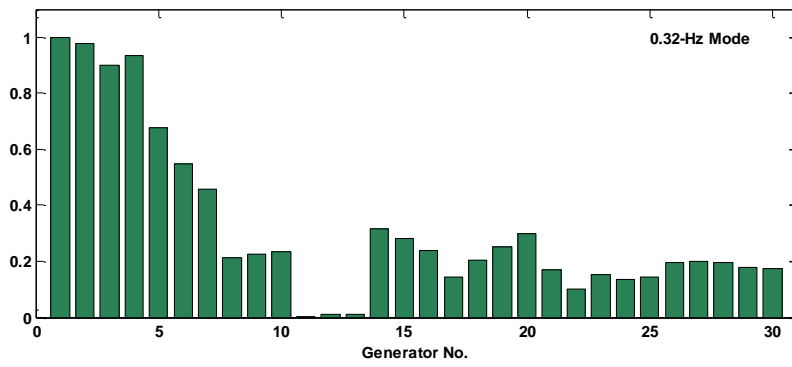


Figure 5-9. Participation weights for West-30 system

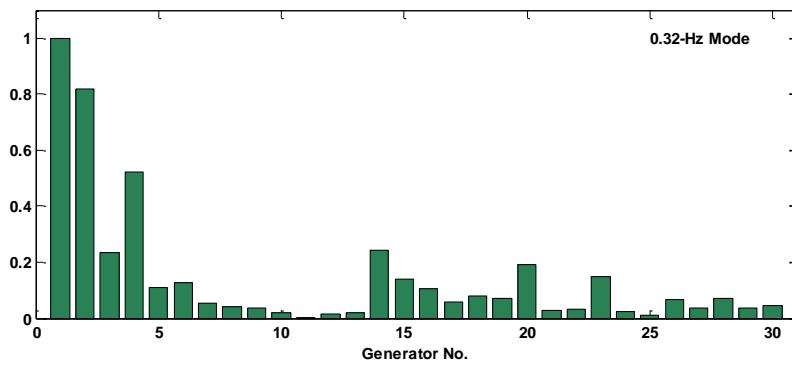


Figure 5-10. Participation factors for West-30 system

For demonstration purpose, the estimated participation weights of all 30 generators in the 0.32-Hz mode are summarized in Figure 5-9 based on the estimated auto-spectrum results. The normalized participation factors of 30 generators' rotor angle in the 0.32-Hz mode are shown in Figure 5-10. It can be observed that the estimated participation weights correctly indicate the generators with the most significant participation as well as relative participation level for most generators.

5.6 Application to CampusWAMS Measurements

According to [47], it is known that two interarea modes can be identified in western Japan 60-Hz power system: one is around 0.4-Hz (Mode 1), and another is around 0.55-Hz (Mode 2). For reference, the frequencies and damping ratios of these two interarea modes are estimated using single-mode-oriented method proposed in the previous chapter. The results are shown in Table 5-3.

Assume 8 PMUs are installed at terminal bus of 8 hypothetical generators which equivalently represents western Japan 60-Hz power system. The bus frequency of each equivalent generator is chosen to estimate the participation weights of 8 generators in the above-mentioned two modes. In practice, the bus frequency is calculated from the phase angle of voltage phasor measurements. As for data length, 10 minutes with 1/30s resampling interval is selected based on experiments.

Table 5-3. Interarea modes of western Japan 60-Hz power system

Mode	Frequency	Damping Ratio
1	0.370 Hz	3.92 %
2	0.527 Hz	5.55 %

As an example, the estimated auto-spectrum for three locations PMU 1, 5 and 8, which are representative locations of longitudinal network of western Japan 60-Hz system, are shown in Figure 5-11. The peaks near 0.37-Hz for PMU 1 and 8 indicate that these two locations significantly participate in Mode 1, while the fact that there is no peak for PMU 5 near 0.37-Hz implies that the center part of the system has no participation in Mode 1. On the other hand, the peaks near 0.53-Hz for all three PMUs indicate they all significantly participate in Mode 2. Moreover, compared to Table 5-3, it can be found that the peaks of auto-spectrum in Figure 5-11 correctly identify these two interarea oscillation modes and corresponding frequencies.

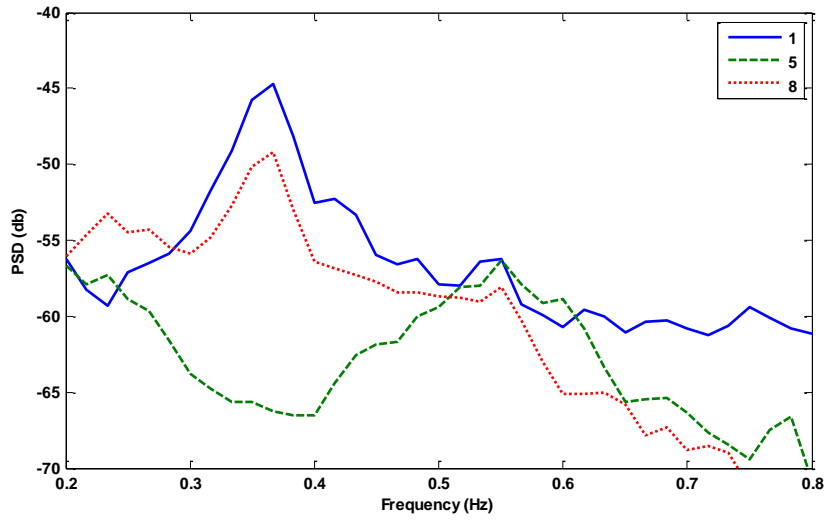


Figure 5-11. Auto-spectrum estimation for the CampusWAMS

The participation weights for all 8 PMU locations in Mode 1 and Mode 2 are normalized and summarized in Figure 5-12 based on the estimated auto-spectrum results. It can be seen that two ends have higher participation in Mode 1 than the center part, which implies that the phasor measurements of two ends, for example, 1 and 8, should be used in order to estimate the eigenvalue of Mode 1 using the method proposed in Chapter 4. On the other hand, both ends and the center part show strong participation for Mode 2.

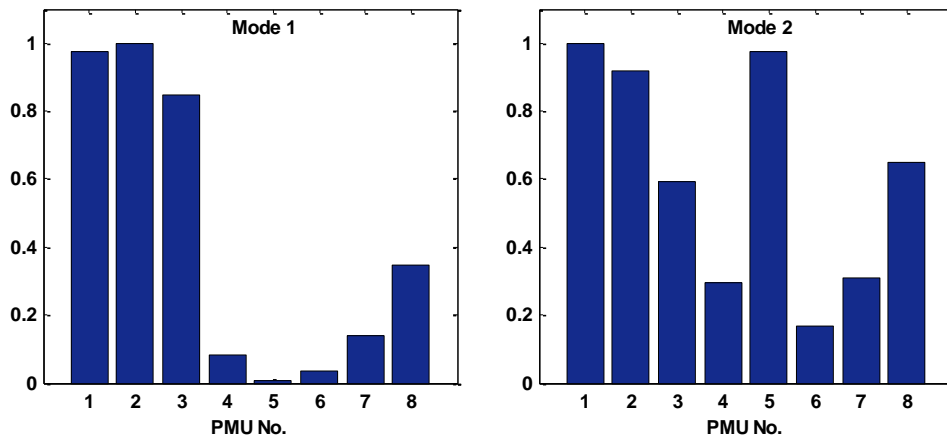


Figure 5-12. Participation weight for the CampusWAMS

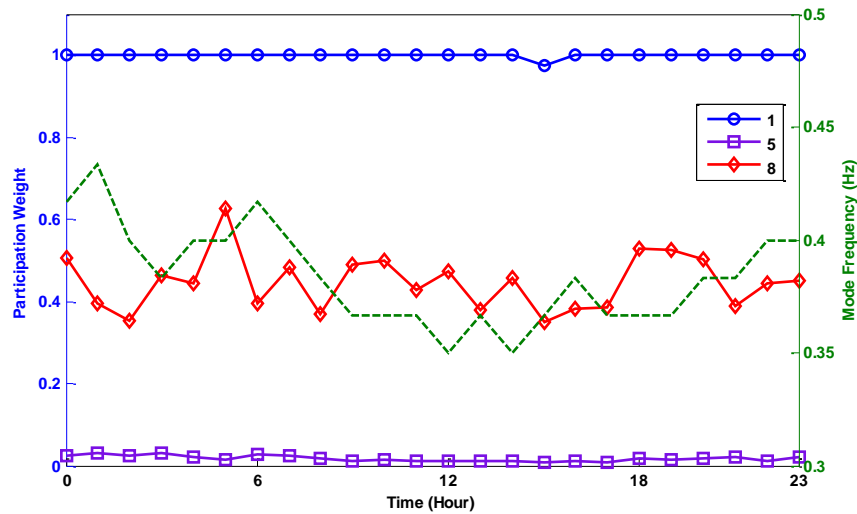


Figure 5-13. Participation weights in Mode 1 for the CampusWAMS

Based on the fact that the estimation of participation weight only needs phasor measurements, the analysis can be conducted at the time when new incoming measurements with selected length are available. Periodically online updating of the estimation of participation weight in a mode of interest can be realized. Figure 5-13 illustrates such an example. In Figure 5-13, 10-min measurements from the start of every hour of one day are employed to estimate participation weights of 8 PMU locations in Mode 1. The results of every hour are normalized with respect to the maximum participation weight of that hour. Only the results for 3 typical locations (PMU 1, 5 and 8) are shown in Figure 5-13. Moreover, the one day variation in mode frequency is also included in dash line corresponding to right Y axis. It is observed that although the identified frequency of Mode 1 varies during different time due to varying power demands, the participation weights of 3 typical locations in Mode 1 show no significant change.

5.7 Discussion and Summary

As the fundamental concept and the estimation procedure of participation weight are built on two basic assumptions which is made in Section 3.3.2, any violation of these assumptions could cause deterioration or loss of accuracy of estimation.

For example, the assumption of white noise excitation input with stationarity is sometimes difficult to satisfy, especially for actual system situation. For simulation examples, the ideal random input can be generated using some mathematical algorithms. The auto-spectrum can be adjusted to make it as flat as possible so that the generated signal is very close to a white noise. For practical system situation, the characteristics of

random load variations in power system cannot be exactly acquired or easily controlled.

In addition, the parameter settings of various algorithms for estimating auto-spectrum, such as data length for estimation, data length for FFT calculation, etc, have certain influence on estimation accuracy. Usually, there are no concrete formulas or settled policies to determine these parameter settings. Trial and error would be a general way to find satisfactory parameter settings for every different case studied. For example, 10 minutes measurements with 1/30s re-sampling interval are found to be enough to give good estimation results for practical system example in this work.

Suppose the random input to an assumed constant-parameter linear system is white noise signal, the auto-spectrum of output signal represents the scaled square of the gain factor of the system frequency response function. Accordingly, the peaks in the system gain factor, which represent the modes contained in the system, can be observed from the auto-spectrum of the system output.

In the chapter, the amplitude of a peak in the auto-spectrum of the system output signal is defined as participation weight which is used to indicate the relative participation of the system in the mode corresponding to the peak. Compared to participation factor from traditional model-based modal analysis, the participation weight is an output- and measurement-only-based index

The approach to estimating the participation weight based on synchronized phasor measurements (SPM) is proposed. Examples using data from simulation and practical measurements from the CampusWAMS are explored to demonstrate the proposed approach. The estimation results show that the participation weight can be an effective indicator of relative participation of multiple generators in an interarea mode of interest. Accordingly, it can be envisaged that it should be technically feasible to implement the proposed estimation scheme and integrate it into the existing SPM-based applications to achieve a completely SPM-based system for monitoring and controlling the interarea oscillations in a large power system.

Chapter 6.

Modeling of Two-Area HVDC-Connected-System for Load Frequency Control Based on Application of the CampusWAMS

6.1 Introduction

Basically, there are indirect and direct ways to take advantage of phasor data for measurement-based power system dynamic monitoring and stability control. For most situations, phasor measurements are directly adopted to realize the power system dynamic monitoring or stability controller design. For example, the single-mode-oriented oscillation data extraction and eigenvalue estimation method and the method of estimating the participation level of generators in one concerned interarea oscillation mode are proposed directly based on wide-area phasor measurements and auto-spectrum analysis in previous two chapters.

For indirect situation, phasor measurements are used to enhance the traditional model-based approach for power system dynamic analysis. In particular, phasor measurements can be utilized to estimate a traditional dynamic model of power system when the base-line information of the concerned system is no available or to validate an existing system dynamic model when the base-line data is available. The general concept is to take the real phasor measurements as standard or so-called reference signal to estimate or validate a simulation model so that the simulation model with estimated or validated parameters can produce the identical responses as the practical measurements.

In this chapter, a method of modeling a HVDC-only-interconnected two-area power system for describing the dynamic of its load frequency control is practiced based on

wide-area phasor measurements. In particular, without knowledge of the detailed base-line data of the studied system, the system model parameters that relates to two-area load frequency control are optimally estimated using phasor measurements during the period of an identifiable system disturbance event.

6.2 Overview of Kita-Hon HVDC Link

The Kita-Hon HVDC Link (full name called Hokkaido-Honshu HVDC Link) is a 193-km long, bipolar 250kV, rated 600MW DC transmission line for the interconnection of the AC grids of Hokkaido and Honshu; both belong to Eastern Japan 50-Hz power system. There are three power companies operating inside Eastern Japan 50-Hz power system; they are HEPCO, TOHOKU-EPCO and TEPCO, respectively. Figure 6-1 illustrates the interconnection of three power companies in the 50-Hz area. According to official website information, the generation capacity is 6500MW for HEPCO, 17140MW for TOHOKU-EPCO and 66000MW for TEPCO, respectively, by March 2007.

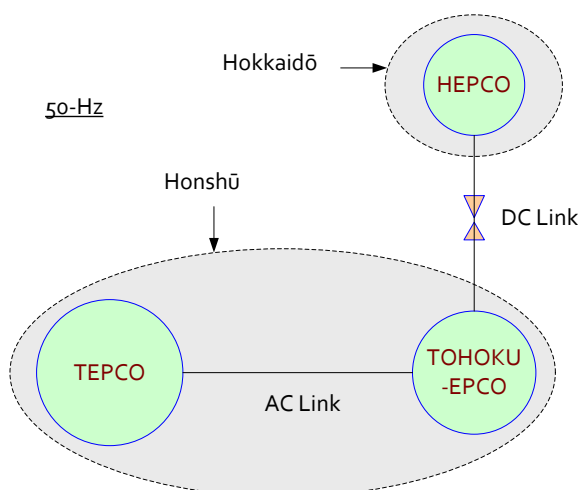


Figure 6-1. Interconnection inside Eastern Japan 50-Hz power system

As introduced in Section 2.4, the CampusWAMS for Eastern Japan 50-Hz power system consists of three PMUs which are placed at Hokkaido University (Sapporo), Hachinohe Institute of Technology and Yokohama National University respectively as shown in Figure 6-2. All 3 PMUs cover typical power supply area of three electric power companies in Eastern Japan 50-Hz power system. Based on the original phasor measurements from the CampusWAMS, the frequency deviation of each area of Eastern Japan 50-Hz system can be easily computed and used for load frequency control analysis.

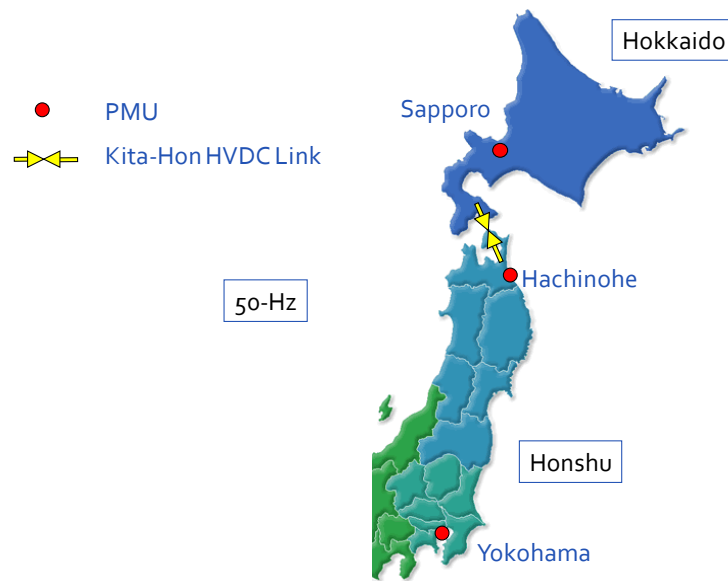


Figure 6-2. CampusWAMS for Eastern Japan 50-Hz power system

6.3 Analysis of Kita-Hon HVDC Link for Load Frequency Control

One of main functions of Kita-Hon HVDC link is to support load frequency control of connected two areas under normal operation condition and emergency situation by modulating amount and direction of DC power flow. In practice, Kita-Hon HVDC Link is equipped with an automatic frequency controller which is designed based on multivariable control theory [53]. Taking the frequency signals from both sides as its input, the controller modulates the transmitted DC power to suppress the system frequency deviations for both sides that is caused by load variations or system disturbances. Accordingly, it can be expected that Kita-Hon HVDC Link has certain effects on the load frequency control of both sides.

As an example, Figure 6-3 shows the computed frequency deviation of Honshu side and Hokkaido side during 00:50-01:10 on January 1st 2008 based on the phasor measurements at Hachinohe and Sapporo respectively. It can be visually found that the change trends of frequency deviation of both sides are very similar with each other. In order to further observe the correlation between two signals, the wavelet transformation is used at first to separate two signals into different frequency bands, and the coefficient of determination between two frequency deviation signals is then calculated over each separated frequency band.

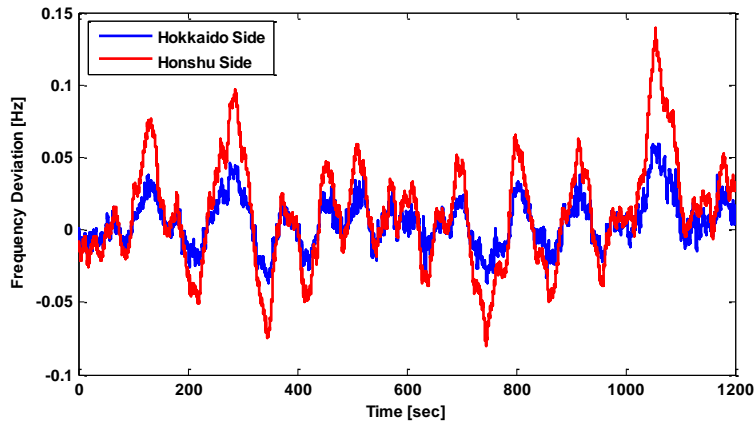


Figure 6-3. Frequency deviation signals of Honshu and Hokkaido

The coefficient of determination, often referred to as R^2 , is a measure of the correlation between a dependent variable and an independent variable. Essentially, the coefficient of determination quantitatively indicates the degree to which two sets of data vary together; for example, the frequency variation in one signal that is explained by the frequency variation in another signal. The coefficient of determination is the square of the correlation coefficient and therefore is always between 0 and 1.

The results shown in Figure 6-4 are the hour average of the coefficient of determination for different frequency bands, which are computed based on the phasor measurements from April 1st to April 7th in 2007. It verifies that the frequency deviations in Hokkaido side and Honshu side hold significant linear correlation with each other in the range of below 0.04 Hz. This strong correlation can be considered as the effect of Kita-Hon HVDC Link on the load frequency control of both sides.

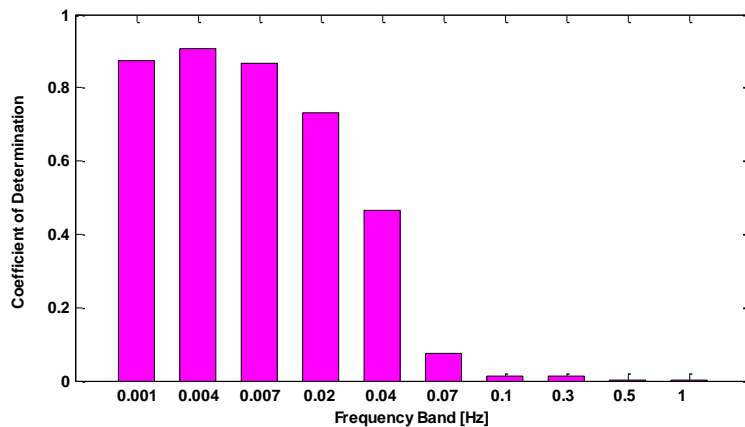


Figure 6-4. Coefficient of determination

6.4 Modeling of Kita-Hon HVDC Link for Load Frequency Control

In order to effectively analyze the effects of Kita-Hon HVDC Link on load frequency control of Eastern Japan 50-Hz power systems, it is useful to construct a simulation model which can represent the main effect on load frequency control and can reproduce as similar dynamic features as observed from practical phasor measurements of the CampusWAMS.

6.4.1 Simulation Model Construction

In this chapter, the well-known MABLAB/Simulink tools are adopted to construct a simplified load frequency control model for Eastern Japan 50-Hz power system. The constructed simulation model is shown as Figure 6-5. The upper part is Hokkaido side and the lower part is Honshu side. First of all, the system of TOHOKU-EPCO and the system of TEPCO are merged into one system to reduce the model complexity. The frequency deviations of these two areas are always identically changing due to load variations. Therefore, such simplification is acceptable. Secondly each system is simulated by an equivalent generator model. Both the load damping effect and generator governor speed regulation effect are included [7]. Although the blocks of governor and turbine are also included, the parameters of these two blocks are fixed for the consideration of simplification.

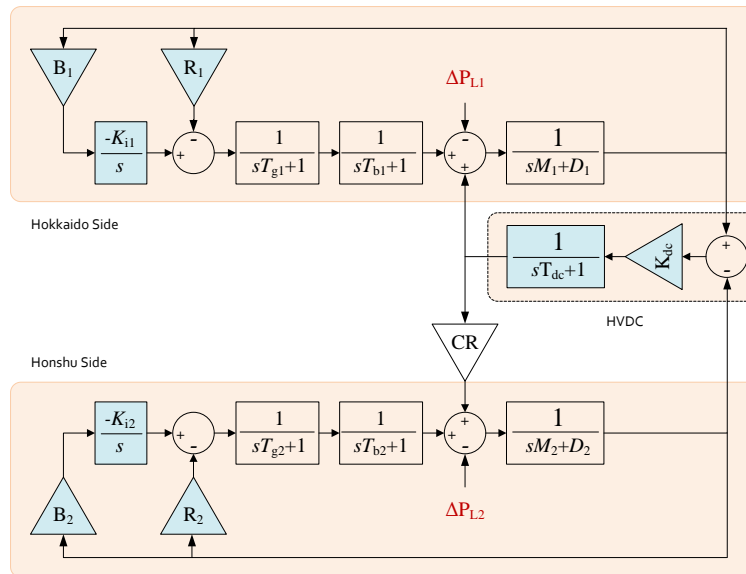


Figure 6-5. Simulation model for load frequency control analysis

According to [54], for area load frequency control scheme, Hokkaido side is using Flat Frequency Control (FFC), while Honshu side is using Flat Frequency Control (FFC) for TEPCO and Tie Line Bias Control (TBC) for TOHOKU-EPCO. Since Honshu side is regarded as a whole, it is reasonable to use FFC for Honshu side based on above analysis.

For simplification, HVDC model for representing the control effect of HVDC link on the load frequency control is represented by a proportional gain block and a first order block. The input signal of HVDC controller is the difference of frequency deviation of two sides.

6.4.2 Unknown Model Parameter Estimation

All parameters used in this simulation model are listed in Table 6-1. The parameters (with an asterisk mark) that play significant role in the area load frequency control are selected to be determined for this simulation model. The parameter "CR₁₂" is used to address the issue of different inertia constant in two sides so as to use same inertia constant for each side in the simulation model. The assumed known parameters are adopted from [55].

Table 6-1. All Model Parameters

Parameter Meaning	Symbol	Value
Inertial constant [p.u. MWs/Hz]	M_1, M_2	0.2
Load damping coefficient [p.u. MW/Hz]	D_1, D_2	0.008
Area Capacity ratio	CR_{12}	0.08
Time constant for governor [s]	T_{g1}, T_{g2}	0.2
Time constant for turbine [s]	T_{b1}, T_{b2}	0.3
Regulation ratio [Hz/p.u. MW]	R_1, R_2	*
FFC controller gain	B_1, B_2	*
FFC controller integration constant [s]	K_{i1}, K_{i2}	*
DC controller gain	K_{dc}	*
DC controller integration constant [s]	T_{dc}	*

The parameter estimation method is illustrated in Figure 6-6. The load variation

with known amount is imposed to either Hokkaido side or Honshu side. The frequency deviation can be simulated by using an initial set of unknown parameters. Then the simulated output of frequency deviation is compared to the reference frequency deviation, which is computed from the real measurement. The error between these two frequency deviation signals is utilized to optimally adjust unknown parameters, that is to say, an optimal set of unknown parameters will be finally determined so that the simulated output will approach the reference signal to make the error signal reaching its minimum. Mathematically, the proposed method turns to be a nonlinear optimization problem.

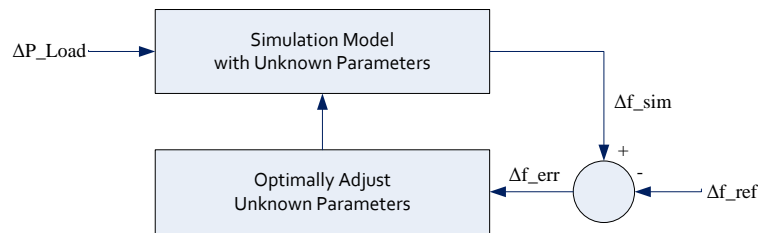


Figure 6-6. Unknown parameter estimation method

6.4.3 Load Input Identification from CampusWAMS Measurements

The remaining problem is to determine the known input load variation. It was reported that on Monday (July 16) 10:13, 2007, an earthquake shook the prefecture of Niigata on the main island of Honshu side. The epicenter was situated at a distance of approximately 10km from the Kashiwazaki-Kariwa nuclear power plant which belongs to TEPCO. According to TEPCO's release, three generators in this power plant tripped automatically after earthquake, and the total loss of generation capacity is about 4655MW. It indicates that the load increases about 4655MW at Honshu, which will cause significant frequency drop at entire Eastern Japan 50-Hz system. Figure 6-7 shows the observed frequency drops based on phasor measurements from the CampusWAMS.

Consequently, this equivalent load increase occurred at Honshu side can be regarded as a known load input to the simulation model to perform parameters estimation. The computed frequency deviations shown in Figure 6-7 are used as reference signal of estimation process. Some information and assumptions used in estimation are as follows:

- The amount of input signal is about 0.08pu based on the total load capacity of Honshu side of that time.
- The input signal increases up to 0.08pu in a ramp manner in 10 seconds.
- The measured frequency deviations of both sides are used as reference signal.

- Only the frequency deviation data from 190s to 540s (total 350s) in Figure 6-7 are used as reference signal.
- All other load variations during this 350s are neglected.

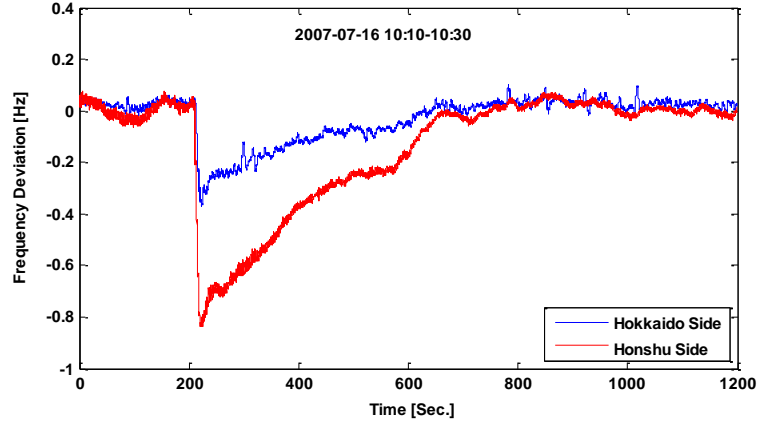


Figure 6-7. Measured frequency deviation due to earthquake

6.4.4 Model Estimation and Evaluation Results

The nonlinear least-squares data-fitting algorithm in MATLAB Optimization Toolbox is adopted to solve the optimal problem [67]. The result is listed in Table 6-2.

Table 6-2. Parameter estimation result

Symbol	Search Range	Final Value
R_1	[1, 15]	8.21
R_2		9.89
B_1	[0.1, 1]	0.26
B_2		0.16
K_{i1}	[0.001, 0.1]	0.001
K_{i2}		0.002
K_{dc}	[0.1, 10]	0.1
T_{dc}	[0.1, 10]	0.3

Figure 6-8 shows the comparison between the simulation results using searched set of unknown parameters and the real frequency deviation of both sides. It can be seen that the simulation results match well with the measured results from the CampusWAMS. Some minor deviations observed in Honshu side can be explained by above simplifications and assumptions made for the construction of simulation model. Another influential factor can be the precision of computation of input load increase amount.

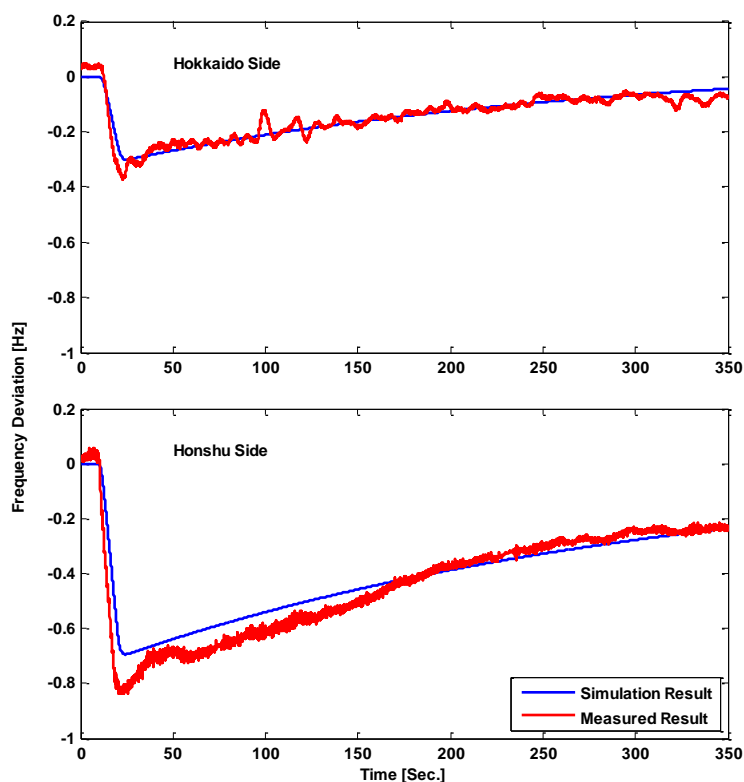


Figure 6-8. Comparison of simulated results and measured results

The effectiveness of the estimated model is checked by simulating normal operating condition when both sides are subject to the uncorrelated, small, random load variations. According to the press release, it is known that a project for retrofitting Kita-Hon HVDC Link system started on January 5th, 2008 and finished on April 25th, 2008. Over this period, Kita-Hon HVDC Link was out of service.

When Kita-Hon HVDC Link is out of operation, the frequency deviation for each side is only caused by the load variations in that side. Therefore, the load variations for each side during that period can be derived from the measured frequency deviation signals. For the simulation model shown in Figure 6-5, when HVDC controller is out of service, the transfer function between frequency deviation (input signal) and load

variation (output signal) can be derived as Equation (6.1), which holds for both Hokkaido side and Honshu side.

$$\frac{\Delta P}{\Delta f} = -(Ms + D) - \left(\frac{K_i}{s} \cdot B + \frac{1}{R} \right) \cdot \frac{1}{(T_g s + 1) \cdot (T_b s + 1)} \quad (6.1)$$

Figure 6-9 shows the simulated results when the constructed simulation model is excited by the derived load variations during 13:50-14:10 on February 25th, 2008. The coefficient of determination over different frequency bands between the frequency deviation signals of two sides is shown in Figure 6-10. It can be observed that the constructed simulation model can represent the effect of Kita-Hon HVDC Link on load frequency control, that is, with Kita-Hon HVDC Link in operation, the frequency deviation of Hokkaido side and Honshu side exhibit significant linear correlation.

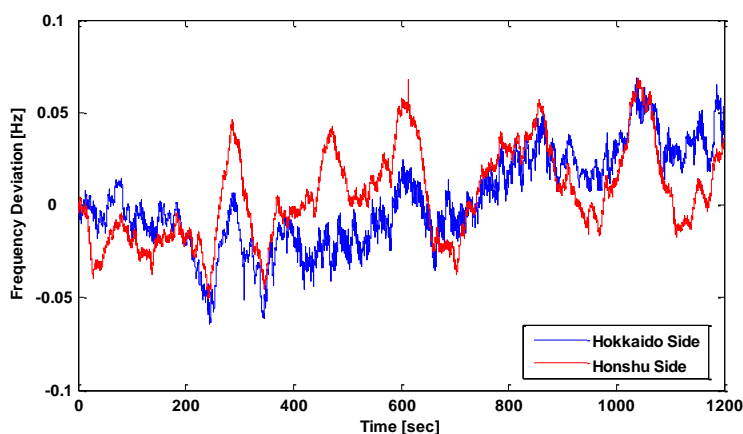


Figure 6-9. Simulated results using derived load variations

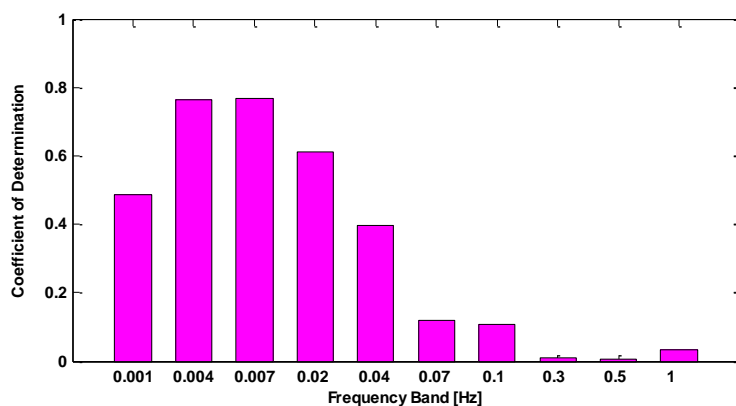


Figure 6-10. Coefficient of determination for simulated results

6.5 Summary

For the first time, phasor measurements are utilized to analyze and model Kita-Hon HVDC Link in this chapter. From the analysis results, it is found that the frequency deviation of Hokkaido side and Honshu side exhibit significant linear correlation when Kita-Hon HVDC Link is in service.

Furthermore, a simplified simulation model is constructed to represent the observed effect of Kita-Hon HVDC Link on load frequency control. Without knowledge of detailed base-line data of Kita-Hon HVDC Link, the unknown parameters that relate to two-area load frequency control are optimally estimated using phasor measurements during the period of an identifiable system disturbance event. The estimated model is verified by imposing uncorrelated random load variations which are derived from practical frequency deviation signals.

The analysis results in the paper demonstrate that phasor measurements have great potential for understanding of system characteristic, system model construction and parameter estimation.

Chapter 7.

Controller Design for Power Oscillation Damping Improvement Based on Phasor Measurements

7.1 Introduction

Based on experiences and investigations of previous power system blackouts or failures, it has been learned that the system-wide interarea oscillations, which are initially inconspicuous and considered as in the acceptable range, could gradually develop into the source of wide-area cascading events. Therefore, to detect, monitor and control dominant interarea oscillations under frequently changing operating conditions is important to power system safety and stability.

Phasor Measurement Unit (PMU) has ability to directly record bus voltage phasor and line current phasor which contain both the amplitude and angle information. An important feature of these phasor measurements is they are all time-synchronized with high accuracy, which means phasor angle measurements from multiple locations, even geographically distant, can be directly compared and processed. Consequently, phasor measurements with time-synchronization are practically opening an unprecedented way to online detection, monitoring and control of power system interarea oscillations.

Basically, there are two main reasons that result in the evolvement of interarea oscillations into system disasters: failure in timely detecting the existence or the occurrence of one interarea oscillation, and failure in properly controlling the endangering evolvement of one interarea oscillation. In Chapter 4, a single-mode-oriented phasor measurements-based method has been proposed to realize the effective detection of one dominant interarea oscillation mode as well as the estimation of its characteristics such

as damping, frequency and participation weight. In order to address the second reason mentioned above, this chapter proposes an online scheme for designing a supplementary damping controller and discusses the online self-tuning strategy of controller parameter based on synchronized phasor measurements.

For conventional way to design a supplementary damping controller, it is essential to build dynamic model of both system and controller based on knowledge of system configuration and parameters of all components beforehand. Furthermore, the parameter settings of the conventional damping controller are usually fixed at a certain set of values which correspond to a particular operating point. These factors possibly diminish or reverse damping effects after it is practically operated. This is an unavoidable problem of traditional model-based approach. In this chapter, a fully phasor measurement-based design scheme of supplementary damping controller, which takes advantage of various techniques described piously, is proposed.

7.2 Controller Structure and Damping Specification

Without loss of generality, the structure for supplementary controller is in a form of two-stage lead/lag compensator plus a gain block as shown in Figure 7-1.

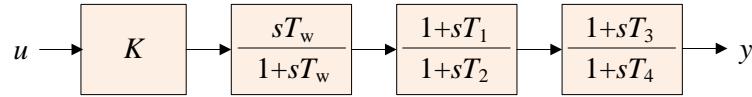


Figure 7-1. General structure of supplementary damping controller

In this structure, K is controller gain; T_w is washout time constant; T_1 to T_4 are time constants of compensator. All time constants are in unit seconds. The input signal and output signal for controller, u and y , are dependent damping provider, such as PSS, HVDC and energy storage device. In order to achieve specified damping performance, the controller gain K and the time constants T_1 to T_4 are needed to be determined optimally to meet the following requirement:

$$\zeta_{estimated} = -\frac{\text{Re}(\lambda)}{\sqrt{\text{Re}(\lambda)^2 + \text{Im}(\lambda)^2}} \geq \zeta_{specified} \quad (7.1)$$

where λ represents the estimated eigenvalue of the concerned interarea oscillation mode based on practical phasor measurements using method proposed in Chapter 4 and $\text{Re}(\lambda)$ and $\text{Im}(\lambda)$ represent the real part and imaginary part respectively.

Accordingly, comparing the estimated damping ratio to specified damping ratio can lead to the tuning of controller parameters. For power system stability control problem, it is well-recognized practice to maintain +5% damping ratio.

7.3 Design of HVDC Supplementary Damping Controller

Consider a simplified but typical AC/DC parallel system illustrated in Figure 7-2. Two big systems, S1 and S2, each containing many generators, are interconnected by an AC tie-line as well as a HVDC link. It is assumed that an interarea oscillation mode occurs between two studied systems under normal operating condition. One already known effect of HVDC link to its adjacent AC system is to improve the damping of that inter-area oscillation mode by means of supplementary controller. The supplementary controller generally takes active power variations of targeted tie-line or frequency deviations between two AC parts as its input signal to modulate the current order at rectifier side, and thereby rapidly adjusts power flow in the parallel tie-line. Not following the conventional way to conduct the design of such controller based on system small-signal model, the target of this work is to design the controller and further to determine its parameters only based on measurements.

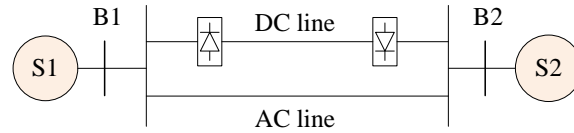


Figure 7-2. A simplified AC/DC parallel system

The input signal for controller, u , is frequency difference between AC systems at two sides in Figure 7-2. The controller output, y , is applied to the rectifier pole control to modulate current order. In order to achieve specified damping performance, the controller gain K and the time constants T_1 to T_4 are needed to be determined optimally.

As described in previous section, the objective of supplementary controller is to enhance the damping of interarea mode of interest. More specifically, it is to enhance the damping to a specified level so as to guarantee the small-signal stability of corresponding oscillation mode. To achieve this objective, three steps need to be done. First step is to construct an oscillation model to detect and estimate the interarea oscillation mode. Second step is to integrate the model of HVDC supplementary controller into the oscillation model in first step to reflect the control effect on oscillation mode. Third step is to adjust the controller parameters, i.e. gain and the time constants T_1 to T_4 , to find

an optimal set of these parameters for a specified damping level.

In short, the control objective can be expressed as follows: given a model estimated from phasor measurements which can describe both the characteristic of oscillation mode and the effect of HVDC supplementary controller, the control objective turns to be an optimization problem in (7.2) [56][57].

$$\begin{aligned}
& \zeta_{estimated} = f(K, T_1, T_2, T_3, T_4) \\
\text{obj.} & \quad \min |\zeta_{estimated} - \zeta_{specified}| \\
\text{cons.} & \quad K_{min} \leq K \leq K_{max} \\
& \quad T_{imin} \leq T_i \leq T_{imax} \quad i = 1, 2, 3, 4
\end{aligned} \tag{7.2}$$

7.3.1 Extended Oscillation Model

Firstly, the block representation of HVDC supplementary controller shown in Figure 7-1 can be converted to the state-space representation as follow [56][57]:

$$\begin{aligned}
\begin{bmatrix} \dot{x}_1 \\ \dot{x}_2 \\ \dot{x}_3 \\ \dot{x}_4 \end{bmatrix} &= \begin{bmatrix} -\frac{1}{T_0} & -\frac{T_1 T_3}{T_w T_2 T_4} & \frac{T_3}{T_2 T_4} \left(1 - \frac{T_1}{T_2}\right) & \frac{1}{T_4} \left(1 - \frac{T_3}{T_4}\right) \\ 0 & -\frac{1}{T_w} & 0 & 0 \\ 0 & -\frac{1}{T_w} & -\frac{1}{T_2} & 0 \\ 0 & -\frac{T_1}{T_w T_2} & \frac{1}{T_2} \left(1 - \frac{T_1}{T_2}\right) & -\frac{1}{T_4} \end{bmatrix} \begin{bmatrix} x_1 \\ x_2 \\ x_3 \\ x_4 \end{bmatrix} \\
& + K \cdot \begin{bmatrix} T_1 T_3 \\ T_2 T_4 \end{bmatrix} \begin{bmatrix} 1 & 1 \\ T_1 \\ T_2 \end{bmatrix}^T \cdot \Delta u
\end{aligned} \tag{7.3}$$

$$\Delta y = x_1 \tag{7.4}$$

where $x_i, i = 1, 2, 3, 4$ are internal state variables and T means matrix transpose.

Considering the output of HVDC supplementary controller will be applied to rectifier pole control and will finally result in variation of bus angle and bus frequency, model (4.7) can be expanded to include this effect as follow:

$$\begin{bmatrix} \Delta \dot{\delta}_{12} \\ \Delta \dot{\omega}_{12} \end{bmatrix} = \begin{bmatrix} 0 & 1 \\ \alpha_1 & \alpha_2 \end{bmatrix} \begin{bmatrix} \Delta \delta_{12} \\ \Delta \omega_{12} \end{bmatrix} + \begin{bmatrix} 0 \\ \alpha_3 \end{bmatrix} \Delta y \tag{7.5}$$

Furthermore, if Δu in (7.3) is taken as frequency difference $\Delta\omega_{12}$ in (7.5), then (7.3), (7.4) and (7.5) can be combined and become an extended model as follow:

$$\begin{bmatrix} \Delta\dot{\delta}_{12} \\ \Delta\dot{\omega}_{12} \\ \dot{x}_1 \\ \dot{x}_2 \\ \dot{x}_3 \\ \dot{x}_4 \end{bmatrix} = \begin{bmatrix} 0 & 1 & 0 & 0 & 0 & 0 \\ \alpha_1 & \alpha_2 & \alpha_3 & 0 & 0 & 0 \\ 0 & K\frac{T_1T_3}{T_2T_4} & -\frac{1}{T_0} & -\frac{T_1T_3}{T_wT_2T_4} & \frac{T_3}{T_2T_4}\left(1-\frac{T_1}{T_2}\right) & \frac{1}{T_4}\left(1-\frac{T_3}{T_4}\right) \\ 0 & K & 0 & -\frac{1}{T_w} & 0 & 0 \\ 0 & K & 0 & -\frac{1}{T_w} & -\frac{1}{T_2} & 0 \\ 0 & K\frac{T_1}{T_2} & 0 & -\frac{T_1}{T_wT_2} & \frac{1}{T_2}\left(1-\frac{T_1}{T_2}\right) & -\frac{1}{T_4} \end{bmatrix} \begin{bmatrix} \Delta\delta_{12} \\ \Delta\omega_{12} \\ x_1 \\ x_2 \\ x_3 \\ x_4 \end{bmatrix} \quad (7.6)$$

Apparently, the extended state matrix of model (7.6) integrally embodies both the characteristic of extracted oscillation mode and the effect of HVDC supplementary controller. In particular, the eigenvalue of extend oscillation model will be affected by parameters of HVDC supplementary controller.

The unknown elements α_1 , α_2 and α_3 can be estimated from model (7.5) based on the measurements of bus angle and output of the controller. Therefore, the extended state matrix of model (7.6) can be initially determined using initial selection of controller parameters and its eigenvalue can be calculated. To achieve the specified damping performance regulated by (7.2), global optimization is suggested for finding an optimal combination of all five relevant parameters. The effectiveness of searched parameters can be investigated by applying these new setting to the controller and then observing new system response. Therefore, this parameter tuning process can be repeatedly performed, each time starting from obtaining new measurements after applying the new set of parameters found in last time.

7.3.2 Controller Parameter Searching

Recently, search and optimal foraging of bacteria have been proposed for solving optimization problems [58][59]. The foraging behavior of *E. coli*, which is a common type of bacteria, can be simulated to mimic the searching process for an optimization problem. The driving force of bacteria foraging algorithm (BFA) is chemotaxis phenomenon in which bacteria direct their movements according to certain chemicals in their environment. The movement patterns of *E. coli* include tumbling and swimming by means of its six rigid spinning flagella. In brief, the result of chemotactic actions of the

bacteria is that the bacteria can move along positive nutrient gradient and finally climb up nutrient hills and at the same time avoid noxious substances. Obviously, this process is very similar to search a minimal objective function value for an optimal problem if objective function is regarded as distribution of nutrient. In addition to the movement of individual bacterium, the interaction effect among a swarm of bacteria as well as other behaviors, like reproduction and elimination-dispersal, can be modeled to enhance the search speed and accuracy.

In BFA, first suppose that θ is the position of a bacterium and then $J(\theta)$ represents nutrient level at that location. For the optimization problem defined in (7.2), θ actually represents one set of unknown parameters and $J(\theta)$ will be value of the objective function corresponding to that θ . Bacteria foraging process is completely equivalent to the process that the object function is continuously and stochastically evaluated using different set of unknown parameters. The algorithm to search optimal values of parameters is referred to [58].

7.3.3 Simulation Study

The example system shown in Figure 7-3 is used to illustrate the application of proposed design scheme and parameters search algorithm. This two-area-four-machine system with one additional HVDC link is adopted from [7].

For the following simulations, all generators are simulated using detailed 6-order sub-transient model equipped with static exciter model and turbine governor model. It is assumed that no PSS is applied so that the effect of HVDC supplementary controller can be easily examined. The whole system operates under normal load condition without any big disturbance. In addition to normal load at bus 4 and bus 14, another two small active load, independently and randomly, are injected at these two buses respectively to excite the oscillation in the test system.

The rectifier operates under constant current control mode and the inverter operates under constant extinction angle mode. Figure 7-4 shows rectifier and inverter model used for simulation. The HVDC supplementary controller only applies to the rectifier side to modulate its current order. The initial for controller parameters are listed in Table 7-1. Under such settings, the eigenvalue of interested interarea oscillation mode is $-0.11 \pm j3.86$, showing a light positive damping ratio of 2.85%.

For the estimation of unknown coefficients in model (7.5), 100 seconds data of phasor measurements are used. Δf is set to 0.05Hz when applying FFT filter. For optimal controller parameters search, following values are adopted for BSA parameters: $N = 5$, $S = 50$, $N_c = 50$, $N_s = 4$, $N_{re} = 4$, $S_r = 0.5$, $N_{ed} = 3$, $P_{ed} = 0.25$. The search range is set as

$1 \leq K \leq 5$ and $0.02 \leq T_i \leq 4, i = 1,2,3,4$. In order to avoid big shift in system characteristic caused by sudden parameter change, the search objective is set to +6% damping ratio.

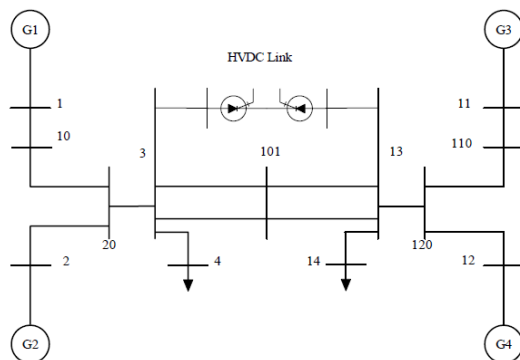


Figure 7-3. Two-area-four-generator system with HVDC link

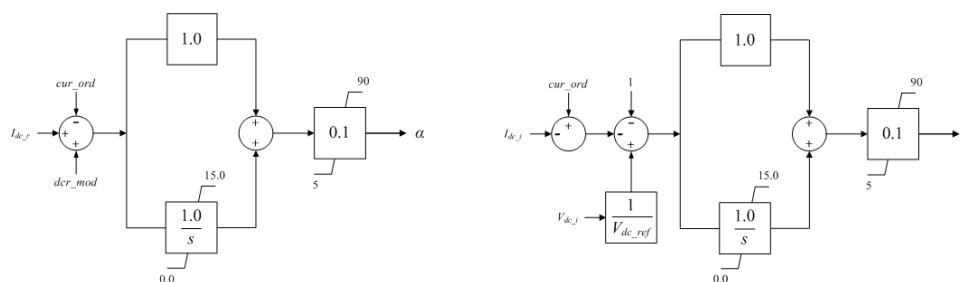


Figure 7-4. Simulation model for rectifier (left) and inverter (right)

Table 7-1. BSA Searched controller parameters

	K	T_1	T_2	T_3	T_4
Initial	1.0	0.04	0.10	0.04	0.10
Searched	3.0	0.24	0.45	1.87	1.05

The search result using BFA is also listed in Table 7-1. The eigenvalue of concerned mode using searched set of parameters is $-0.23 \pm j3.75$, showing a damping ratio of 6.15%. Figure 7-5 compares the system response signals to small random load variations after applying two difference sets of parameters: initial set and searched set. It can be seen that searched set of parameters provides more damping on the interested mode.

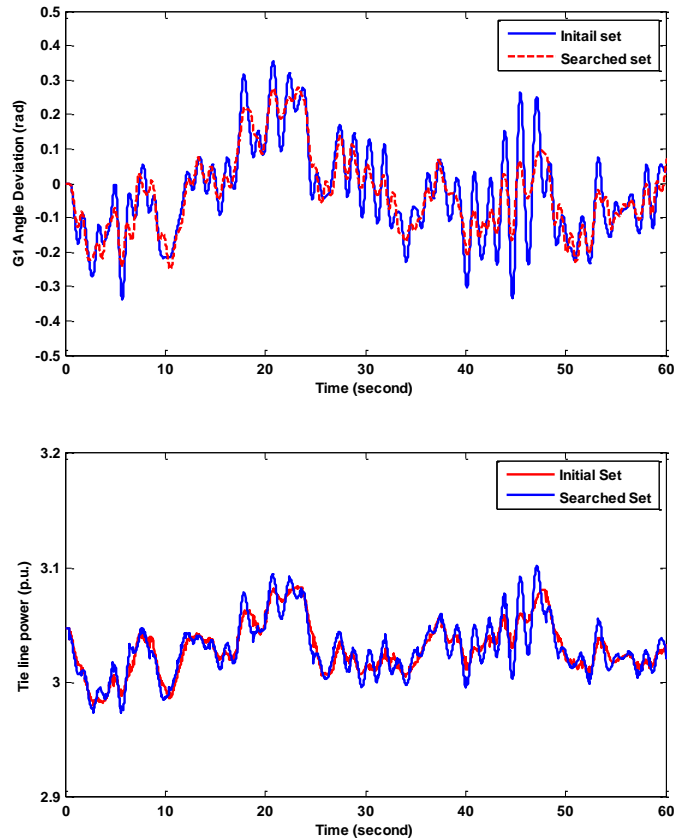


Figure 7-5. Responses to small random load changes

7.4 Online Parameter Self-Tuning Control Strategy

Non-adaptive controllers usually have fixed structure and fixed value of parameters setting. Although the controller is determined carefully to achieve desired control objective, it is not unusual that its control effect deteriorates or even reverses under certain conditions which are different from the designed conditions. Adaptive control systems exhibit application potential for this kind of problem.

As a strict control strategy, adaptive pole placement control has been studied over the years on the design of power system stabilizer [60]-[62] and other available control device, such as static VAR compensator to enhance power system dynamic performance [63]. Most of results in these studies are primarily based on single machine system and non-synchronized data. On the other hand, non-strict, i.e. measurements-based heuristic adaptive strategy was studied using HVDC as supplementary damping controller [64]. However, Prony analysis usually shows to some extent degraded efficiency in estimation of online model when system is under normal operation conditions.

In this sub-section, an adaptive parameter tuning controller design scheme based on synchronized phasor measurement is proposed. The objective of the designed controller is to maintain the sufficient damping of concerned interarea oscillation mode when power system is operated under normal but frequently changing conditions.

7.4.1 Online Oscillation Model Estimation

Traditionally, recursive least squares (RLS) or weighted recursive least squares (WRLS) are common choices in strict adaptive control design for the estimation of system to be controlled. The reason of using recursive algorithms is it can reduce the computational complexity which is often regarded as the main problem of non-iterative batch/block least squares (LS) algorithm. For an online application, however, RLS algorithms could suffer from several shortcomings, such as numerical instability due to round-off error caused by its recursive operations, and sensitivity on the initial setting of algorithm parameters. Moreover, parameters of strict adaptive controller could experience fast fluctuation based on strict adaptive law and online system model estimated using RLS algorithms when the system to be controlled is operated under frequently changing conditions.

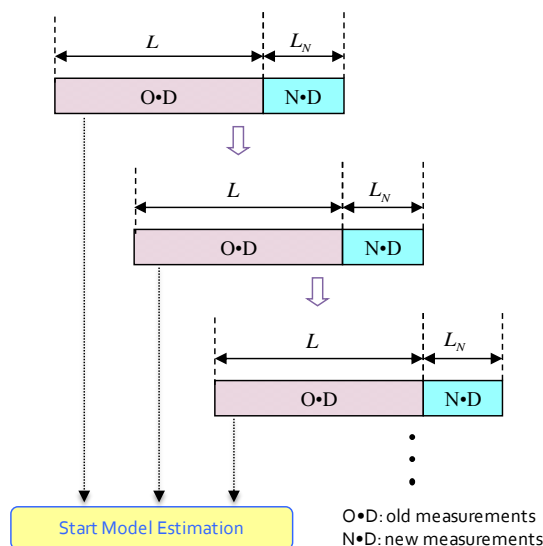


Figure 7-6. Online process of oscillation model estimation

In fact, benefiting from rapid advance in modern computer technology, the computational complexity of LS becomes much less an issue. For system with fewer parameters to be estimated, the computational power of existing DSP-based micro-computers is adequate for block LS. Research has shown that by simply extending the

block least squares to blockwise least squares (BLS), the classical LS algorithms can be applicable to on-line applications [65]. In this work, BLS, which uses measurements within fixed length window instead of entire available data, is adopted for online identification of oscillation model. Furthermore, the sliding window techniques can be utilized to improve the tracking capability of BLS algorithm when applied to an online application for a time-variant system. Using sliding window ensures updating estimate timely when new phasor measurements corresponding to current operating condition are available. The online process of oscillation model identification can be illustrated as Figure 7-6.

The identification performance is dependent on the length of the sliding window. Theoretically, the longer the window length is, the higher the estimation accuracy is. The window length should vary with different systems or different oscillation modes. For each case, an appropriate window length can be determined so as to guarantee the sufficient estimation accuracy and to discard effectively out-of-date information from the past measurements on the other hand.

7.4.2 Self-Tuning Control Strategy

First strategy is to simply tune the value of gain K while time constants of compensator blocks unchanged. With well-designed initial parameters, the desired damping ratio can be achieved by only adjusting the gain K . the adjustment direction and amount can be determined based on prior experiences or preset rules or even heuristic trial and error. It is usual to finally achieve specified damping ratio by multiple steps of gain adjustment. It should be noted that here this online gain tuning is different with conventional gain scheduling control, in which the scheduled gains are determined by offline design process.

Second strategy is to tune gain K and four time constants separately, i.e. not at the same time. Similarly, the adjusting order and adjusting value can be based on prior experiences or preset rules or even heuristic trial and error. More effectively, the approximate linear sensitivity functions of damping ratio with respect to each control parameter can be constructed in advance by offline design efforts to guide the online adjustment of parameters. The adjusting process can stop once desired damping ratio is achieved.

Third strategy is to tune all parameters simultaneously. For this approach, the parameter tuning problem usually turns to be an optimization problem – in a finite parameter space, using various optimization algorithms to find a set of parameters that can produce the desired damping ratio. Since this kind of searching process usually involves the multi-dimension parameter space and lacks of the gradient information of

optimization objective function, the global stochastic search algorithms are more preferable. Available algorithms includes genetic algorithm, particle swarm optimization, bacteria foraging algorithms, etc.

Fourth strategy is also to tune all related parameters simultaneously. For this strategy, the nonlinear mapping between all parameters and damping ratio under various corresponding operating condition can be constructed in advance based on artificial neural network, fuzzy logic or other self-learning mechanism. Thereby, according to the online estimated damping ratio and the corresponding operating conditions, the optimal setting for the controller parameters can be determined.

7.4.3 Simulation Study

As a demonstration, power system stabilizer (PSS) for damping interarea oscillation is considered in this section. Similar as previous section, the structure of PSS is in a form of two-stage lead/lag compensator plus gain block as shown in Figure 7-1. Five relevant parameters, controller gain K and time constants T_1 to T_4 are all tunable. The input signal for PSS in this paper is selected to be the difference between two bus frequency signals from generators which participate the same oscillation mode. The controller output is applied to the generator exciter control to provide positive damping.

The simulation system is the same 2A4G system used in Section 4.1.2 as shown in Figure 4-2. The simulation model for generator, governor and exciter are also same as those used in Section 4.1.2. The system parameters are the same with example 12.6 in [7] and the initial load flow setting are set as shown in Table 7-2. Traditional small-signal analysis indicates that under initial operating condition, there is an interarea oscillation mode between Area 1 (G1 and G2) and Area 2 (G3 and G4) around 0.6Hz.

Table 7-2. Initial load flow setting of 2A4G system

Component	P (MW)	Q (MVar)	V (p.u.)	θ (degree)
G1	700	-	1.03	-
G2	700	-	1.01	-
G3	-	-	1.03	-6.8
G4	700	-	1.01	-
L3	1167	100	-	-
L13	1567	100	-	-

For power system modeling, Dymola 6.1 with power system component library called ObjectStab is used [68]. Dymola provides the interface with MATLAB so that the Dymola module can be simulated in the Simulink environment. Therefore, the model estimation algorithm, sliding estimation process and parameters tuning logic can be implemented in MATLAB/Simulink environment. The designed PSS is assumed to be installed with G1. It is assumed that PMU is installed at each generator terminal bus. The bus frequency between bus 1 and bus 11 is used as the input signal for PSS. The initial parameter setting is listed in Table 7-3.

Table 7-3. Initial parameter for PSS

K	T_1	T_2	T_3	T_4
10	0.05	0.03	3.00	5.40

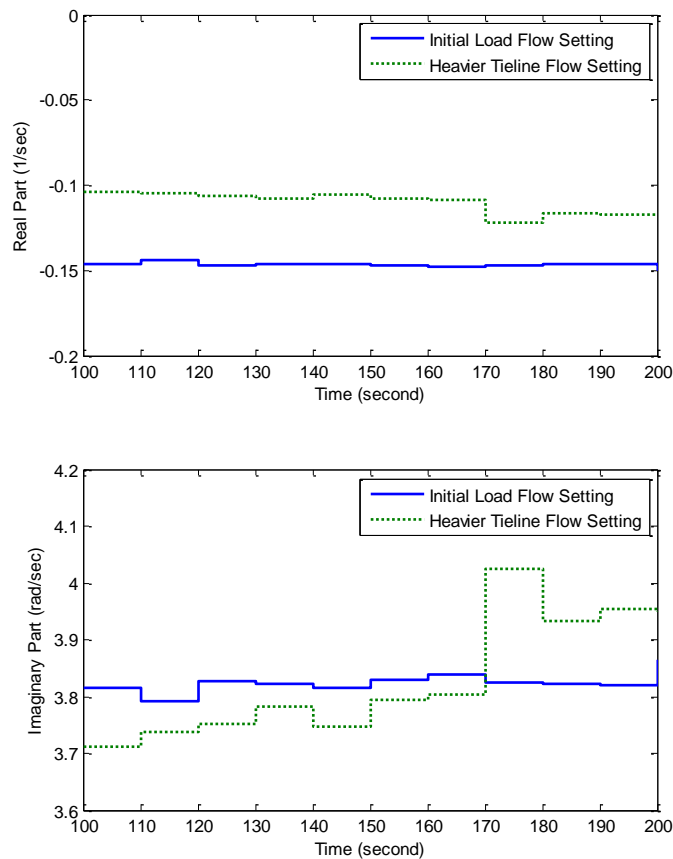


Figure 7-7. Estimated eigenvalues using online sliding window technique

Firstly, to evaluate the performance of online oscillation model estimation under

different operating conditions, the following two scenarios are simulated: first is the initial setting and second is with 100MW increase in L13 active load and 100MW decrease in L3 active load compared to the initial setting. Besides, during simulation, a small random active load variation is added at L13. In this evaluation, the parameter self-tuning mechanism is not active. Therefore, the power flow on the tie-lines becomes heavier and it can be expected that the damping of interarea mode changes. The sliding window length is set to be 100s and the new measurements window length is 10s. Figure 7-7 shows the estimated results which correctly reflect the change of damping of corresponding oscillation mode under different operating conditions.

Next, the system with load flow setting as $L3 = 967\text{MW}$ and $L13 = 1767\text{MW}$ are simulated and the parameter self-tuning function is activated. For demonstration, the first tuning strategy discussed in Section 7.4.2, i.e. with only adjustment of gain K is used for this simulation. The sliding window length is 100s and the new measurements window length is 50s. The simulation results are shown in Figure 7-8, which is comparison of angle difference between G1 and G3. This oscillation in angle difference also indicates the oscillation in tie-line power flow. It can be seen that without self-tuning controller, the concerned interarea oscillation is relatively bigger than that when self-tuning mechanism is activated.

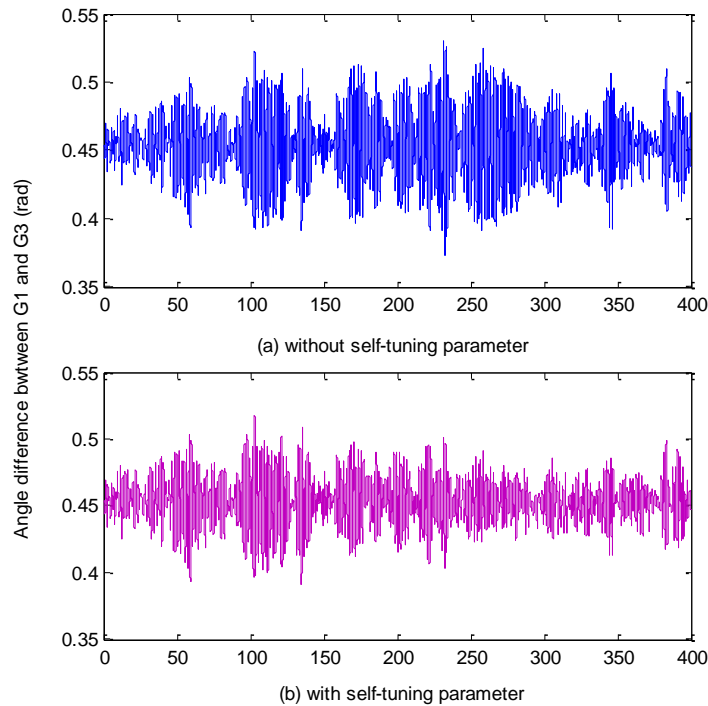


Figure 7-8. Comparison of angle difference with and without self-tuning strategy

7.5 Summary

In this chapter, a damping controller design scheme which takes advantages of phasor measurements and a new global searching algorithm – bacterial foraging algorithm – is proposed and demonstrated by designing a HVDC supplementary damping controller. In this scheme, the key point is to identify a extend oscillation model which can describe both the dynamic of oscillation mode and controller effect and then the controller design problem turns to be an optimization problem.

Furthermore, a phasor measurement-only-based design scheme for adaptive damping controller is proposed. Several strategies for online controller parameter self-tuning are discussed and evaluated by simulation study. The ultimate objective of the designed controller is to online estimate the concerned interarea oscillation mode in a wide-area power system and provide sufficient damping by automatically adjust its parameters when the power system is operated under normal but frequently changing conditions. The single-mode-oriented simplified oscillation model can be identified based on successive phasor measurements using the sliding window blockwise estimation technique. The evaluation results using a two-area-four-machine system show the effectiveness of the proposed scheme.

Chapter 8.

Conclusions

8.1 Contributions

The nature of the measurement-based analysis methods is to estimate an instantaneous system model in some forms based on the online measurements of system inputs and/or outputs by means of various available analysis techniques. Based on wide-area synchronized phasor measurements, this thesis concentrates on the study of power system small-signal dynamic monitoring and stability control problems on the basis of the concept of the measurement-based approach. The main contributions from this research can be summarized as follows.

- Previous methods for oscillation parameter estimation are principally oriented to multiple modes which always face the difficulty to determine the suitable model order. A single-mode-oriented concept is proposed here to tackle this difficulty. In order to guarantee the performance of single mode estimation, it is important to accurately extract the oscillation data that corresponding to the concerned mode. The auto-spectrum analysis is proposed in this thesis to automatically and accurately determine the center frequency of the concerned mode which is then be used to determine the frequency range of the extraction. It is shown that the proposed method is easier to implement and computationally more efficient, and thus should be useful for on-line monitoring applications in power systems.
- Currently participation factor index used for the determination of relative participation of generators in one concerned oscillation mode is based on off-line analyses, which rely on approximate DAE models and system data. The proposed new participation weight is an on-line index, based only on the phasor

measurements of system output, which allows for the determination of relative level of generators participating in a concerned oscillation mode in practice and therefore can be easily integrated into other online phasor-based applications.

- The measurement-based approach can be used to improve the model-based approach by estimating or validating a traditional dynamic model based on the phasor measurements of real power system. A hybrid simulation concept is practiced based on the real phasor measurements and a simulation model for describing load frequency control effect of a two-area HVDC-connected system. The phasor measurements during the period of an identifiable system disturbance are proposed to help to estimate the unknown model parameters that relate to two-area load frequency control, when the knowledge of detailed base-line data is not available.
- A damping controller design scheme which takes advantages of phasor measurements and a new global searching algorithm – bacterial foraging algorithm – is proposed and demonstrated by designing a HVDC supplementary damping controller. Furthermore, several strategies for online controller parameter self-tuning are discussed and evaluated by simulation study. It is shown that this entire control design scheme succeeds in online maintaining the sufficient damping of the concerned interarea oscillation mode when power system is operated under normal but frequently changing conditions.

The proposed methods and corresponding results presented in this thesis have been published in [69]-[74].

8.2 Considerations for Future Work

In order to apply the methods proposed in this thesis to the real power system, two fundamental assumptions are inevitable: loads continuously vary as a stationary white noise and system is linear time-variant around a concerned operating point. Unfortunately, the real power system is practically non-linear, high order and time-varying and on the other hand the characteristic of practical load variations can never be recognized. Therefore, two main considerations can be practiced and evaluated in future work:

- Admit the fact of non-linearity of real power system and non-stationarity of practical load variations, to analyze the small-signal stability using non-linear analysis techniques such as Hilbert spectral analysis or HHT (Huang-Hilbert Transformation).

- Since power system is primarily stochastic in nature, every estimate of modal properties is actually a sample estimate of its true value. Hence, it might be better not try to give just one single estimate but try to give a statistical estimation of the model properties of the concerned oscillation mode.

In addition, to apply online self-tuning parameter control strategy, it is a true challenge to realize a quick and accurate tracking of the change of eigen-parameter of the concerned oscillation mode.

Finally, even measurement-based methods have shown some advantages in some aspects, it probably still cannot completely replace the role of the traditional model-based method. Maybe the best way to make use of the advantages of both methods is to use them complementarily in practice to realize successful dynamic monitoring and stability control of power system small-signal problem.

Currently, PMUs-based WAMS is designed to improve power system operators' situational awareness of the realtime status of a wide-area power system. From this point of view, WAMS is functioning as an "Early Warning System". In my perspective of WAMS in a future "Smart Grid", it should function not only as an "Early Warning System", but also as an "Early Response System". Specifically speaking, future WAMS should be capable of reacting smartly to any potentially dangerous disturbance so as to get rid of the possibility of large area blackout; and should be capable of predicting realtime stability status so as to maintain a stable system by advance control ahead of its going out of control.

References

- [1]. US-Canada Power System Outage Task Force, “Final report on the August 14th 2003 Blackout in the United States and Canada,” April 2004, available at <https://reports.energy.gov/BlackoutFinal-Web.pdf>.
- [2]. “Report on the events of September 28th, 2003 culminating in the separation of the Italian power system from the other UCTE networks”, April 2004, available at <http://www.autorita.energia.it/docs/04/061-04all.pdf>.
- [3]. Ekraft, “Power failure in Eastern Denmark and Southern Sweden on 23.09.03 – Final report on the course of events”, Nov. 2004, available at http://www.geocities.jp/ps_dictionary/blackout/Final_report_uk-web.pdf.
- [4]. “Technical summary of the Athens and Southern Greece Blackout of July 12, 2004”, Aug. 2004, available at <http://www.pserc.wisc.edu>.
- [5]. Prabha S. Kundur, “Tutorial Course - Blackouts and Blackout Prevention”, in Proceeding CD of 16th Power System Computer Conference, Glasgow, 2008.
- [6]. Antonio Gomez-Exposito, Antonio J. Conejo, Claudio Canizares, “Electric Energy Systems: Analysis and Operation”, CRC Press, 1st Edition, July 2008.
- [7]. Prabha S. Kundur, “Power System Stability and Control”, McGraw-Hill, Jan. 1994.
- [8]. A. G. Phadke. and J.S. Thorp, “Computer relaying for power systems”, Research Studies Press, Somerset, England, 1988.
- [9]. A. G. Phadke, “Synchronized phasor measurements in power systems”, IEEE Computer Applications in Power, Vol.6, No.2, pp.10-15, 1993.
- [10]. A. G. Phadke, J. S. Thorp and M. G. Adamiak, “A new measurement technique for tracking voltage phasors, local system frequency and rate of change of frequency”, IEEE Trans. Power Apparatus and Systems, Vol.102, No.5, pp.1025-1038, 1983.
- [11]. IEEE Power Engineering Society, “IEEE Std C37.118: IEEE Standard for Synchrophasors for Power Systems”, Mar. 2006.
- [12]. CIGRE WG C4.601 Report, “Wide Area Monitoring and Control for Transmission Capability Enhancement”, 2007.
- [13]. A.G. Phadke, H. Volskis, R.M. de Moraes, Tianshu Bi, etc., “The wide world of wide-area measurement”, IEEE Power and Energy Magazine, Vol.5, No.5, pp.52-65, 2008.

- [14]. Tianshu Bi, “WAMS Implementation in China Part I: Current status”, available at http://www.naspi.org/meetings/workgroup/2010june/presentations/session'03/bi_north_china_wams_20100608.pdf
- [15]. Mitani Y, Saeki O, Hojo M, Ukai H. “Online monitoring system for Japan Western 60 Hz power system based on multiple synchronized phasor measurements”. Papers of Technical Meeting on Power Engineering and Power System Engineering, IEE Japan, PE-02-60, PSE-02-70, 2002. (in Japanese)
- [16]. R. Tsukui, P. Beaumont, T. Tanaka, and K. Sekiguchi, “Intranet-based protection and control”, IEEE Computer Applications in Power, Vol.14, No.2, pp.14-17, Apr. 2001.
- [17]. IEEE-CIGRE Joint Task Force on Stability Terms and Definitions, “Definition and classification of power system stability”, IEEE Trans. Power Systems, Vol.19, No.3, pp.1387–1401, August 2004.
- [18]. Julius S. Bendat and Allan G. Piersol, “Random Data: Analysis and Measurement Procedures”, Wiley, 1st edition, 1971.
- [19]. Samuel D. Stearns, “Digital Signal Processing with Examples in MATLAB”, CRC Press, August 2002.
- [20]. S.Lawrence Marple, “Digital Spectral Analysis with Applications”, Prentice Hall PTR, March 1987.
- [21]. Francis Castanie, “Spectral Analysis: Parametric and Non-parametric Digital Methods”, Wiley-ISTE, June 2006.
- [22]. L. Ljung, “System Identification: Theory for the User”, Prentice Hall, 2nd edition, January 1999.
- [23]. T. Soderstrom and P. Stoica, “System Identification”, Prentice-Hall, 1989.
- [24]. Jorge Nocedal Stephen J. Wright, “Numerical Optimization”, Springer, 2006
- [25]. K. Y. Lee and Mohamed A. El-Sharkawi, “Modern Heuristic Optimization Techniques - Theory and Applications to Power Systems”, Wiley-IEEE Press, February, 2008.
- [26]. J. F. Hauer, C. J. Demeure, and L. L. Scharf, “Initial results in prony analysis of power system response signals,” IEEE Trans. Power Systems, Vol.5, No.1, pp.80-89. February 1990.
- [27]. J. F. Hauer, “Application of prony analysis to the determination of modal content and equivalent models for measured power system response”, IEEE Trans. Power System, Vol.6, No.3, pp.1062-1068, Aug. 1991.

- [28]. D.J. Trudnowski, J.M. Johnson, J.F. Hauer, "Making Prony analysis more accurate using multiple signals", *IEEE Trans. Power System*, Vol,14, No.1, pp.226-231, 1999.
- [29]. J.J. Sanchez-Gasca, J.H. Chow, "Performance comparison of three identification methods for the analysis of electromechanical oscillation", *IEEE Trans. Power System*, Vol.14, No.3, pp.995-1002, 1999.
- [30]. J. Xiao, X. Xie, Y. Han, and J. Wu, "Dynamic tracking of low-frequency oscillations with improved prony method in wide-area measurement system", in *Proc. IEEE Power Eng. Soc. General Meeting*, 2004, pp.1104-1109, Jun. 2004.
- [31]. B.A. Archer, U.D. Annakkage, "Monitoring and predicting power system behavior by tracking dominant modes of oscillation", in *Proceedings of the IEEE PES General Meeting*, Vol.2, pp.1475-1482, 2005.
- [32]. Shuqing Zhang, Xiaorong Xie, Jingtao Wu, "WAMS-based detection and early-warning of low-frequency oscillations in large-scale power systems", *Electric Power Systems Research*, Vol.78, No.5, pp.897-906, May 2008.
- [33]. J. W. Pierre, D. J. Trudnowski, M. K. Donnelly, "Initial results in electromechanical mode identification from ambient data", *IEEE Trans. Power Systems*, Vol.12, No.3, pp.1245-1251, Aug. 1997.
- [34]. R. W. Wies, J. W. Pierre, D. J. Trudnowski, "Use of ARMA block processing for estimating stationary low-frequency electromechanical modes of power systems", *IEEE Trans. Power Systems*, Vol.18, No.1, pp.167-173, Feb. 2003.
- [35]. M. G. Anderson, N. Zhou, J. W. Pierre, R. W. Wies, "Bootstrap-based confidence interval estimates for electromechanical modes from multiple output analysis of measured ambient data", *IEEE Trans. Power Systems*, Vol.20, No.2, pp.943-950, May 2005.
- [36]. R. W. Wies, A. Balasubramanian, and J. W. Pierre, "Combining least mean adaptive filter and auto regressive block processing techniques for estimating the low-frequency electromechanical modes in power systems", in *Proc. IEEE Power Eng. Soc. General Meeting*, Montreal, QC, Canada, 2006.
- [37]. N. Zhou, J. W. Pierre, D. J. Trudnowski, and R. T. Guttromson, "Robust RLS methods for online estimation of power system electromechanical modes", *IEEE Trans. Power Systems*, Vol.22, No.3, pp.1240-1249, Aug. 2007.
- [38]. N. Zhou, D. Trudnowski, J. Pierre, W. Mittelstadt, "Electromechanical mode on-line estimation using regularized robust RLS methods", *IEEE Trans. Power Systems*, Vol.23, No.4, pp.1670-1680, Nov. 2008.
- [39]. N. Zhou, J. W. Pierre, and J. F. Hauer, "Initial results in power system identification from injected probing signals using a subspace method", *IEEE Trans.*

Power Systems, Vol.21, No.3, pp.1296-1302, Aug. 2006.

- [40]. D. Trudnowski, J. Pierre, N. Zhou, J. Hauer, and M. Parashar, "Performance of three mode-meter block-processing algorithms for automated dynamic stability assessment", *IEEE Trans. Power Systems*, Vol.23, No.2, pp.680-690, May 2008.
- [41]. D.J. Trudnowski, J.W. Pierre, "Overview of algorithms for estimating swing modes from measured responses", in *Proceedings of the IEEE PES General Meeting*, July 2009.
- [42]. I. Kamwa, J. Beland, G. Trudel, R. Grondin, C. Lafond and D. McNabb, "Wide-area monitoring and control at Hydro- Quebec: past, present and future", *IEEE PES General Meeting*, 2006.
- [43]. K.E.Martin, "Phasor measurement systems in the WECC", *Proc. IEEE PES General Meeting*, 2006.
- [44]. Jingtao Wu, "New implementations of wide area monitoring system in power grid of china", *IEEE/PES Transmission and Distribution Conference and Exhibition: Asia and Pacific*, 2005.
- [45]. X. Xie, Y. Xin, J. Xiao, J. Wu, Y. Han, "WAMS applications in Chinese power systems", *IEEE Power & Energy Magazine*, Vol.4, No.1, pp. 54-63, 2006.
- [46]. J. Rasmussen and P. Jorgensen, "Synchronized phasor measurements of a power system event in eastern Denmark", *IEEE Trans. Power System*, vol.21, no.1, pp.278-284, Feb. 2006.
- [47]. T. Hashiguchi, M. Watanabe, A. Matsushita, Y. Mitani, O. Saeki, K. Tsuji, M. Hojo, and H. Ukai, "Identification of characterization factor for power system oscillation based on multiple synchronized phasor measurements", *IEEEJ Trans. on Power and Energy*, Vol.125, No.4, pp.417-425, 2005. (in Japanese)
- [48]. I.J. Perez-Arriaga, G.C. Verghese, F.C. Schweppe: "Selective modal analysis with applications to electric power systems, PART I: heuristic introduction", *IEEE Trans. Power Apparatus and Systems*, Vol.101, No.9, pp.3117-3125, 1982.
- [49]. M. Watanabe, T. Hashiguchi, T. Izumi, and Y. Mitani, "Power system stabilization control based on the wide area phasor measurement", *IEEEJ Trans. PE*, Vol.126, No.12, pp.1199-1206 (2006) (in Japanese)
- [50]. D. J. Trudnowski, "Estimating electromechanical mode shape from synchro-phasor measurements", *IEEE Trans. Power System*, Vol.23, No.3, pp.1188-1195, 2008.
- [51]. D.R. Ostojic, "Identification of Optimum Site for Power System Stabilizer Applications", *Generation, Transmission and Distribution, IEE Proceedings C*, Vol.135, Issue 5, pp.416-419, 1988.

- [52]. IEEJ, “Electrical power system standard models”, Technical Report No.754, 1999. (in Japanese)
- [53]. M. Sanpei, A. Kakehi, H. Takeda, “Application of multi-variable control for automatic frequency controller of HVDC transmission system”, IEEE Trans. Power Delivery, Vol.9, No.2, pp.1063-1068, 1994.
- [54]. IEEJ, “Load frequency control for power system under normal and emergency condition”, Technical Report No.869, 2002. (in Japanese)
- [55]. Y. Okada, Y. Mitani, M. Watanabe, ”Dynamic characteristic analysis of HVDC based on multiple synchronized phasor measurements”, Proc. CD-ROM of the 2008 Annual Conference of IEE Japan, No.6-119, 2008. (in Japanese)
- [56]. M. Watanabe, T. Hashiguchi, T. Izumi, Y. Mitani, “Power system stabilization control based on the wide area phasor measurement”, IEEJ Trans. on Power and Energy, Vol.126, No.12, pp.1199-1206, 2006. (in Japanese)
- [57]. S. Dechanupaprittha, K. Hongesombut, M. Watanabe, Y. Mitani, and I. Ngamroo, “A heuristic-based design of robust SMES controller taking system uncertainties into consideration”, IEEJ Trans. on Electrical and Electronic Engineering, Vol.1, No.3, pp.255-267, 2006.
- [58]. K.M. Passino, “Biomimicry of bacterial foraging for distributed optimization and control”, IEEE Control Systems Magazine, Vol. 22, pp.52-67, Jun. 2002.
- [59]. B. Sumanbabu, S. Mishra, B.K. Panigrahi, and G.K. Venayagamoorthy, “Robust tuning of modern power system stabilizers using Bacterial Foraging Algorithm”, IEEE Congress on Evolutionary Computation, pp.2317-2324, Sept. 2007.
- [60]. G.P. Chen, O.P. Malik, G.S. Hope, Y.H. Qin, G.Y. Xu, “An adaptive power system stabilizer based on the self-optimizing pole shifting control strategy”, IEEE Trans. Energy Conversion, Vol.8, No.4, pp.639-645, Dec. 1993.
- [61]. Ghosh, A., G. Ledwich, O.P. Malik and G.S. Hope, “Power system stabilizer based on adaptive control techniques”, IEEE Trans. on Power Apparatus and Systems, Vol.PAS-103, pp.1983-1986, 1984.
- [62]. S.J. Cheng, O.P. Malik and G.S. Hope, “Damping of multi-modal oscillations in power systems using a dual-rate adaptive stabilizer”, IEEE Trans. on Power Systems, Vol.PWRS-3, No.1, pp.101-108, 1998.
- [63]. A.H.M.A. Rahim, E.P. Nowicki, and O.P. Malik, “Enhancement of power system dynamic performance through an on-line self-tuning adaptive SVC controller”, Electric Power System Research, Vol.76, pp.801-807, 2006.
- [64]. Jingbo He, Chao Lu, Xiaochen Wu, Jingtao Wu and Tishu Bi, ”Design and

experiment of heuristic adaptive HVDC supplementary damping controller based on online prony analysis”, Power Engineering Society General Meeting, IEEE, Tampa, Florida, 2007.

- [65]. Jin Jiang, and Youmin Zhang, ”A revisit to block and recursive least squares for parameter estimation”, Computer and Electrical Engineering, Vol.30, pp.403-416, 2004.
- [66]. Mathworks, “Signal Processing Toolbox User’s Guide”, online available at <http://www.mathworks.com>.
- [67]. Mathworks, “Optimization Toolbox User’s Guide”, online available at <http://www.mathworks.com>.
- [68]. Mats Larsson, “ObjectStab-An Educational Tool for Power System Stability Studies”, IEEE Trans. Power System, Vol.19, No.1, pp.56-63, 2004.
- [69]. Li Changsong, Watanabe Masayuki, Mitani Yasunori, Okubo Masatoshi, and Kosaku Yokota, “Estimation of global steady state stability based on phasor measurement with auto spectrum-based FFT filter”, Proceedings CD of the International Conference on Electrical Engineering 2008, Okinawa, Japan, July, 2008. (5 pages)
- [70]. C. Li, K. Higuma, M. Watanabe, and Y. Mitani, “Monitoring and Estimation of Interarea Power Oscillation Mode Based on Application of CampusWAMS”, Proceeding CD of the 16th Power System Computation Conference, Glasgow, 2008.
- [71]. C. Li, M. Watanabe, and Y. Mitani, “HVDC controller design for damping of interarea oscillation using synchronized phasor measurements and bacteria foraging algorithm”, Proceedings CD of the International Conference on Electrical Engineering 2009, Shenyang, China, July, 2009.
- [72]. C. Li, M. Watanabe, Y. Mitani, and B. Monchusi “Participation weight estimation in power oscillation mode based on synchronized phasor measurements and auto-spectrum analysis”, IEEJ Trans. on Power and Energy, Vol.129, No.12, pp.1449-1456, 2009.
- [73]. C. Li, Y. Okada, M. Watanabe, and Y. Mitani, “Modeling Kita-Hon HVDC link for load frequency control of Eastern Japan 50-Hz power system based on application of the CampusWAMS”, Proceedings CD of the IEEE International Symposium on Circuits and Systems, Paris, France, May, 2010.
- [74]. C. Li, M. Watanabe, and Y. Mitani, “Design of adaptive parameter tuning controller for interarea oscillation damping improvement based on synchronized phasor measurements”, Proceedings CD of the International Conference on Electrical Engineering 2010, Busan, Korea, July, 2010.

Biography of the Author



Li Changsong received his B.Eng. and M.Sc. degrees in Electrical Engineering from Chengdu University of Science and Technology¹, Sichuan Union University², China, in 1994 and 1998, respectively. From July 1994 to July 1998, he worked as an instructor of undergraduate student in Sichuan University. Since July 1998, he is a lecturer at Department of Electrical Engineering in Sichuan University. He was a PhD student with the Japanese government scholarship at MITANI Lab, Department of Electrical and Electronic Engineering, Graduate School of Engineering, Kyushu Institute of Technology (KIT). With this thesis, he has completed his PhD degree in Electrical Engineering from KIT in September, 2010. His research interests are in applications of synchronized phasor measurements to the monitoring and control of power system dynamics and stability, and applications of advanced digital signal processing techniques to power systems. He is a member of the Institute of Electrical Engineers of Japan (IEEJ) and the IEEE.

¹ Merged into Sichuan Union University in April 1994

² Changed its name to Sichuan University in 1998